

UNCLASSIFIED

AD 415362

DEFENSE DOCUMENTATION CENTER

FOR

SCIENTIFIC AND TECHNICAL INFORMATION

CAMERON STATION, ALEXANDRIA, VIRGINIA



UNCLASSIFIED

NOTICE: When government or other drawings, specifications or other data are used for any purpose other than in connection with a definitely related government procurement operation, the U. S. Government thereby incurs no responsibility, nor any obligation whatsoever; and the fact that the Government may have formulated, furnished, or in any way supplied the said drawings, specifications, or other data is not to be regarded by implication or otherwise as in any manner licensing the holder or any other person or corporation, or conveying any rights or permission to manufacture, use or sell any patented invention that may in any way be related thereto.

63-4-5

RTD-TDR-63-3021

RTD
TDR
63-3021

CATALOGED BY DDC
AS AD No. 415362

INTERACTION OF PLANE ELASTIC WAVES WITH A
CYLINDRICAL CAVITY

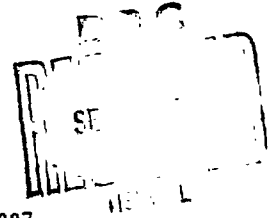
June 1963

TECHNICAL DOCUMENTARY REPORT NO. RTD TDR-63-3021

Research and Technology Division
AIR FORCE WEAPONS LABORATORY
Air Force Systems Command
Kirtland Air Force Base
New Mexico

This research has been funded by the
Defense Atomic Support Agency under WEB No. 13,148

Project No. 1080, Task No. 108001



(Prepared under Contract AF 29(601)-5007
by Stanley L. Paul and Arthur R. Robinson,
University of Illinois, Urbana, Illinois)

Best Available Copy

Research and Technology Division
Air Force Systems Command
AIR FORCE WEAPONS LABORATORY
Kirtland Air Force Base
New Mexico

When Government drawings, specifications, or other data are used for any purpose other than in connection with a definitely related Government procurement operation, the United States Government thereby incurs no responsibility nor any obligation whatsoever; and the fact that the Government may have formulated, furnished, or in any way supplied the said drawings, specifications, or other data, is not to be regarded by implication or otherwise as in any manner licensing the holder or any other person or corporation, or conveying any rights or permission to manufacture, use, or sell any patented invention that may in any way be related thereto.

This report is made available for study upon the understanding that the Government's proprietary interests in and relating thereto shall not be impaired. In case of apparent conflict between the Government's proprietary interests and those of others, notify the Staff Judge Advocate, Air Force Systems Command, Andrews AF Base, Washington 25, DC.

This report is published for the exchange and stimulation of ideas; it does not necessarily express the intent or policy of any higher headquarters.

Qualified requesters may obtain copies of this report from DDC. Orders will be expedited if placed through the librarian or other staff member designated to request and receive documents from DDC.

RTD TDR-63-3021

FOREWORD

This report is based upon a doctoral dissertation by S. L. Paul in partial fulfillment of the requirements for the degree of Doctor of Philosophy in Engineering at the University of Illinois. The research was partially supported by the Air Force Special Weapons Center, Kirtland Air Force Base, New Mexico, under Contract AF 29(601)-5007.

The authors wish to express their gratitude to Dr. N. M. Newmark, Head, Department of Civil Engineering, and to Dr. J. L. Merritt, Associate Professor of Civil Engineering, for their advice and suggestions.

Special thanks are due the staff of the Digital Computer Laboratory at the University of Illinois for their cooperation.

ABSTRACT

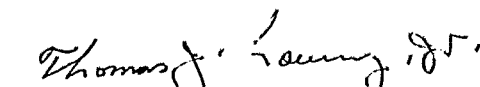
A method is presented for computing stresses in the vicinity of a long cylindrical cavity in an infinite, elastic, isotropic, homogenous medium when the cavity is enveloped by a plane stress wave traveling in a direction perpendicular to its axis. Hoop stresses around the cavity boundary were computed for the passage of a wave of dilation and a wave of pure shear; the stresses in the medium away from the boundary were computed for a wave of dilation. Initially the stress behind the incident wave front was considered to be constant. The effect of a stress decay behind the front was then computed by using the Duhamel integral for the case of an incident wave of dilation.

The method of solution of the problem involves superposition of the stress field of an incoming plane step wave and a stress field corresponding to waves which diverge from a line source.

PUBLICATION REVIEW

This report has been reviewed and is approved.


JOE E. JOHNSON
Lt USAF
Project Officer


THOMAS J. LOWRY, JR.
Colonel USAF
Chief, Structures Branch

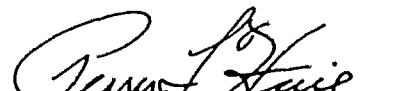

PERRY L. HUIE
Colonel USAF
Chief, Research Division

TABLE OF CONTENTS

	Page
I. DESCRIPTION OF THE PROBLEM	1
II. METHOD OF ANALYSIS	4
III. DERIVATION OF EQUATIONS.	7
3.1 Fourier Analysis of Incident Wave of Dilatation	7
3.2 Fourier Analysis of Incident Shear Waves.	10
3.3 Derivation of Equations for the Diverging Wave (Incident Dilatational Wave).	12
3.4 Derivation of Equations for the Diverging Wave (Incident Shear Wave)	20
3.5 Boundary Conditions	21
IV. MODIFICATION OF EQUATIONS FOR COMPUTER SOLUTION.	25
4.1 Equations for Incident Wave of Dilatation	25
4.2 Equations for Incident Shear Waves.	38
4.3 Equations for Stress in the Medium.	43
V. DERIVATION OF THE SHORT TIME SOLUTION.	48
5.1 Short Time Solution for Hoop Stress at the Boundary	48
5.2 Short Time Solution for Stresses in the Medium.	56
VI. RESULTS AND INTERPRETATION	61
6.1 Incident Wave of Dilatation	61
6.2 Incident Shear Wave	67
6.3 Use in Protective Construction.	69
VII. CONCLUSIONS.	71
BIBLIOGRAPHY	73
APPENDIX A. DERIVATION OF THE INTEGRATION FORMULA	74
APPENDIX B. SOME PROPERTIES OF THE DISPLACEMENT POTENTIALS.	77
B.1 General Solution of the Scalar Wave Equations in Cylindrical Coordinates.	77
B.2 General Form of ϕ and ψ for Arbitrary n	80
APPENDIX C. DESCRIPTION OF THE COMPUTER PROGRAM	84
FIGURES.	87

LIST OF FIGURES

Number		Page
3.1	Sign convention for stresses at a point.	87
3.2	Geometry of envelopment of a cylindrical boundary by a plane wave of dilatation	87
3.3	Variation with time of the Fourier coefficients for stress on a cylindrical boundary during envelopment by an incident wave of dilatation, $\bar{\nu} = 1/3$	88
3.4	Comparison of actual stress on the boundary during envelopment by the incident plane wave of dilatation with the Fourier representation, $\bar{\nu} = 1/3$	89
3.5	Geometry of envelopment of a cylindrical boundary by an incident shear wave.	90
3.6	Coordinate system and point-source waves reaching point p at time t.	90
4.1	Results of the numerical solution for $F'''(\eta_1)$ and $G'''(\eta_2)$ in the case $n = 1$ ($\bar{\nu} = 0$ and $\bar{\nu} = 1/3$).	91
4.2	Results of the computer solution for hoop stress in modes 0, 1 and 2 due to an incident wave of dilatation ($\bar{\nu} = 0$).	92
4.3	Results of the computer solution for hoop stress in modes 0, 1 and 2 due to an incident wave of dilatation ($\bar{\nu} = 1/3$).	93
4.4	Results of the computer solution for hoop stress in modes 0, 1 and 2 due to an incident shear wave ($\bar{\nu} = 0$ and $1/3$).	94
4.5	Geometry associated with computation of stress in the medium	95
5.1	Comparison of the short-time and the computer solutions for total modewise hoop stress at the boundary in an incident wave of dilatation. The short time solution is also shown for modes $n = 3$ and 4.	96
5.2	Comparison of the short-time and the computer solutions for hoop stress at the boundary in the diverging wave due to an incident shear wave.	97
5.3	Comparison of the short-time and the computer solutions for hoop stress at $r/a = 1.25$ due to an incident wave of dilatation ($n = 1$, $\bar{\nu} = 1/3$, $\theta = 0^\circ$).	98

LIST OF FIGURES (CONT'D)

Number		Page
6.1	Hoop stress at the boundary due to an incident wave of dilatation using $n = 0, 1, 2$ ($\bar{\nu} = 0$)	99
6.2	Hoop stress at the boundary due to an incident wave of dilatation using $n = 0, 1, 2$ ($\bar{\nu} = 1/3$)	100
6.3	Comparison of the present computations with those of Refs. (3) and (4) for hoop stress at $\theta = 0^\circ$ due to an incident wave of dilatation ($\bar{\nu} = 1/3$)	101
6.4	Comparison of the present computations with those of Refs. (3) and (4) for hoop stress at $\theta = 90^\circ$ due to an incident wave of dilatation ($\bar{\nu} = 1/3$)	102
6.5	Radial stress vs. time at various radii due to an incident wave of dilatation ($\bar{\nu} = 0, \theta = 0^\circ$)	103
6.6	Hoop stress vs. time at various radii due to an incident wave of dilatation ($\bar{\nu} = 0, \theta = 90^\circ$)	104
6.7	Radial stress vs. time at various radii due to an incident wave of dilatation ($\bar{\nu} = 1/3, \theta = 0^\circ$)	105
6.8	Hoop stress vs. time at various radii due to an incident wave of dilatation ($\bar{\nu} = 1/3, \theta = 90^\circ$)	106
6.9	Stress vs. radius at several times due to an incident wave of dilatation ($\bar{\nu} = 1/3$)	107
6.10	Hoop stress at the boundary vs. time due to an incident wave of dilatation with 4000 psi at the front and various rates of decay behind the front ($\bar{\nu} = 1/3, \theta = 0^\circ$)	108
6.11	Hoop stress at the boundary vs. time due to an incident wave of dilatation with 4000 psi at the front and various rates of decay behind the front ($\bar{\nu} = 1/3, \theta = 90^\circ$)	109
6.12	Hoop stress at the boundary due to an incident shear wave using $n = 0, 1, 2$ ($\bar{\nu} = 0$)	110
6.13	Hoop stress at the boundary due to an incident shear wave using $n = 0, 1, 2$ ($\bar{\nu} = 1/3$), (also the hoop stress from Ref. (3) is shown for the same conditions)	111

I. DESCRIPTION OF THE PROBLEM

The purpose of this investigation is to determine the stresses in the region of a cylindrical cavity in an infinite, elastic, isotropic, homogeneous medium when the cavity is enveloped by a plane stress wave traveling in a direction perpendicular to its axis. Stresses due to incoming dilatational waves and to incoming shear waves were considered. Initially the stress behind the incident wave front is considered to be constant, but some consideration is given to the effect of pressure decay behind a shock front through the use of the Duhamel integral. The problem is one of plane strain; that is, each section perpendicular to the axis of the cavity is in the same state of stress, there is no displacement in the direction of the cavity axis, and only three stress components must be computed. Some consideration is given to the variation of the parameters which define the properties of the medium.

The practical problem corresponding to the dynamic elasticity problem described above concerns the effect of stress waves initiated by nuclear explosions on underground protective installations. Although any practical problem of this type cannot exactly reproduce the conditions of the theoretical problem, it may be reasoned that under certain conditions, particularly under those for which such protective construction is likely to be built, fairly good agreement may be expected. For example, rock is neither isotropic nor homogeneous, but a protective structure would be constructed at a site where the rock is as sound and unstriated as possible. The assumption of an infinite medium is more reasonable than it might at first appear. For, in this case a protective structure would surely be several diameters

below the ground surface, and since the maximum hoop stress is reached at about four to five transit times after the wave reaches the opening, reflections from the surface will not interfere with the peak stress. Probably the most severe restriction is that of linear elasticity. However, many rocks approach this property in the lower range of their stress-strain diagrams. The actual opening is not likely to be a perfect cylinder; nevertheless, current mining procedures can produce an opening which approximates a cylindrical shape quite well.

The importance of this problem has been recognized by several earlier investigators. In Ref. (1) a study was made of the stresses in the medium using a "high frequency" approximation similar to the approach used in geometrical optics. This method does not allow the solution to be carried out for sufficient time to obtain the maximum stresses. Reference (2) considered the stresses around a hole in a thin plate when enveloped by a plane stress wave of harmonic variation in time and space behind the wave front, i.e. the plane stress problem corresponding to the plane strain problem treated herein. Reference (3) presented a solution to the problem investigated in the present report obtained by using an integral transform in time of the displacement potentials. The resulting equations were then solved in terms of Hankel functions. Considerable difficulty is encountered in this method in the computation of the inverse transform. In the present work an entirely different method of solving the partial differential equations, which has several advantages over the previous method, is presented. The results of the two analyses will be compared in Chapter VI. In Ref. (4) the method of Ref. (3) was used to solve the same problem again and was extended to include stresses away from the boundary. Also possible failure

mechanisms based solely on the elastic stress state were discussed. Results were presented in the form of contour maps of principal stresses at each time interval. The angle of minimum principal stresses and angles of possible failure planes are also presented. In Ref. (5) the solution to the same problem was formally carried out by a method quite similar to that used in Refs. (3) and (4). The theoretical derivation of the equations was reported in Ref. (5), but numerical results had not yet been obtained.

The problem has also been considered experimentally. In Ref. (6) a combination of photoelasticity and grid analysis was used to determine the stress distribution on the boundary of holes in a plate of low modulus material. The shape of the holes and duration of stress wave were varied. The method results in a stress field of both dilatational and shear waves with a rather long rise time at the front of the wave. Reference (7) contains the results of a large number of experiments made by detonating an explosive charge at the surface of blocks of brittle material which contained openings of various shapes. The medium, shape of opening and distance from a free surface to the opening were varied. These experiments are useful in predicting the type of failure to be expected.

II. METHOD OF ANALYSIS

The basic method of solution of the problem involves superposition of the stress field of an incoming plane step wave and the stress field corresponding to waves which diverge from a line source. The diverging waves are chosen so that the radial and shear stresses due to the two waves combine to produce a traction-free cylindrical boundary centered on the line source. This cylindrical boundary is then the boundary of the cavity.

A solution to the scalar wave equations corresponding to a cylindrical wave diverging from a line source may be found in Refs. (8) and (9). This solution can be applied to the dynamic elasticity problem by considering the displacement potentials to be represented by Fourier series expanded in θ , with the coefficients written as functions of radial distance and time. These series are substituted into the wave equations, resulting in hyperbolic partial differential equations in two independent variables which must be satisfied by the coefficients of each term of the series. The general solution of these differential equations is then written in integral form; therefore, the boundary conditions result in integral equations.

In order to satisfy the boundary conditions, the sum of the stresses due to the diverging wave and the incident stresses expanded in Fourier series were set equal to zero at a fixed radius from the line source. In general this results in two linear integral equations, one from the radial stress condition and one from the shear stress condition, which must be solved simultaneously for two unknown functions appearing in the integrands of the integrals mentioned above. The integral equations were solved numerically in order to determine these unknown functions.

A program for solving the simultaneous integral equations and computing the various stresses at the boundary and in the medium away from the boundary was written in Fortran language for solution on a CDC 1604 digital computer. This program will be described in Appendix C.

In order to check the results obtained from the computer, the same basic equations were solved by another method. Each of the Fourier coefficients of the displacement potentials for the diverging wave and the incident stresses was expanded in a Taylor series about zero time. By considering only the first few terms of the series, it was feasible to carry out the computations by hand. The results thus obtained are only valid when the variable in the Taylor expansions, time, is small. For this reason the method is called the short-time solution. This additional solution is useful as a check on the computer solution at early time and also gives the initial values of the unknown functions in the integral equations, which are needed in the machine solution. As a further check on the computer solution, the static stresses on the boundaries and in the medium were compared with those obtained from the machine solution at very long time.

This general method of solution was applied to the problems of an incident wave of dilatation and an incident wave of pure shear. Further details of the representation of the incoming stress field and of the stress field diverging from a line source are described in Sections 3.1 to 3.4. The equations resulting from the combination of these two waves to obtain the boundary equations are derived in a form suitable for use in a computer in Sections 4.1 and 4.2.

The diverging wave which has been determined at the boundary, of course, continues to travel outward and becomes the reflected and diffracted waves. To find the stress in the medium away from the boundary the same superposition procedure may be used, except that the effect of change of radial distance of the diverging wave must be considered. The computer solution for stress in the medium due to a plane wave of dilatation is presented in Section 4.3.

III. DERIVATION OF EQUATIONS

3.1 Fourier Analysis of Incident Wave of Dilatation

First consider a plane step wave of dilatation traveling in the negative x direction, with a stress σ_x in the direction of wave propagation. It may be shown that the stresses in the y and z direction are

$$\sigma_y = \frac{\nu}{(1-\nu)} \sigma_x$$

$$\sigma_z = \frac{\nu}{(1-\nu)} \sigma_x$$

where ν is Poisson's ratio. For convenience $\bar{\nu}$ will be used as defined by

$$\bar{\nu} = \frac{\nu}{(1-\nu)} \quad 3.1$$

In the following work tensile stresses will be considered positive

Consider the stresses on a circle of radius a (in cylindrical coordinates) being enveloped by the wave front described above, with $r_x = a$, and with no cavity in the medium. Referring to Fig. 3.1 the radial stress σ_{rr} , shear stress $\tau_{r\theta}$, and hoop stress $\sigma_{\theta\theta}$ behind the front may be written using the general rules of transformation of stress,

$$\begin{aligned} \sigma_{rr} &= \sigma (\cos^2 \theta + \bar{\nu} \sin^2 \theta) \\ \sigma_{r\theta} &= -\sigma \frac{(1-\bar{\nu})}{2} \sin 2\theta \\ \sigma_{\theta\theta} &= \sigma (\sin^2 \theta + \bar{\nu} \cos^2 \theta) \end{aligned} \quad 3.2$$

Since σ_{rr} and $\sigma_{\theta\theta}$ are even in θ while $\sigma_{r\theta}$ is odd in θ , the Fourier series corresponding to these expressions can be written:

$$\left. \begin{aligned}
 \sigma_{rr} &= \frac{a_0(t)}{2} + \sum_{n=1}^{\infty} a_n(t) \cos n\theta \\
 \sigma_{r\theta} &= \sum_{n=1}^{\infty} b_n(t) \sin n\theta \\
 \sigma_{\theta\theta} &= \frac{d_0(t)}{2} + \sum_{n=1}^{\infty} d_n(t) \cos n\theta
 \end{aligned} \right\} 3.3$$

The coefficients in these series may be evaluated from the following integrals where θ_1 defines the extent to which the wave has enveloped the circular boundary as shown in Fig. 3.2, and therefore is a function of time

$$\left. \begin{aligned}
 a_n(t) &= \frac{2}{\pi} \int_0^{\theta_1} \sigma_{rr}(\theta) \cos n\theta \, d\theta \\
 b_n(t) &= \frac{2}{\pi} \int_0^{\theta_1} \sigma_{r\theta}(\theta) \sin n\theta \, d\theta \\
 d_n(t) &= \frac{2}{\pi} \int_0^{\theta_1} \sigma_{\theta\theta}(\theta) \cos n\theta \, d\theta
 \end{aligned} \right\} 3.4$$

If time is measured from the instant that the wave touches the boundary, the plane dilatational wave with a velocity of propagation C_1 will travel in the time t

$$C_1 t = a (1 - \cos \theta_1)$$

from which

$$\theta_1 = \cos^{-1} (1 - tC_1/a) \quad 3.5$$

$$\text{for } 0 \leq tC_1/a \leq 2$$

$$\text{and } \theta_1 = \pi$$

$$\text{for } tC_1/a \geq 2$$

Carrying out the integrations in Eqs. 3.4, one obtains the following expressions for the Fourier coefficients as a function of time:

For $t \leq 2a/C_1$

$$\frac{a_0(t)}{2} = \frac{\sigma}{\pi} \left[\theta_1 \frac{(1+\bar{v})}{2} + \frac{(1-\bar{v})}{4} \sin 2\theta_1 \right] \quad 3.6$$

$$a_n(t) = \frac{\sigma}{2\pi} \left[(1-\bar{v}) \left(\frac{\sin(2-n)\theta_1}{(2-n)} + \frac{\sin(2+n)\theta_1}{(2+n)} \right) + 2(1+\bar{v}) \frac{\sin n\theta_1}{n} \right] \quad 3.7$$

$$b_n(t) = -\frac{\sigma}{2\pi} (1-\bar{v}) \left[\frac{\sin(2-n)\theta_1}{(2-n)} - \frac{\sin(2+n)\theta_1}{(2+n)} \right] \quad 3.8$$

$$\frac{d_0(t)}{2} = \frac{\sigma}{2\pi} \left[(1+\bar{v})\theta_1 + \frac{(\bar{v}-1)}{2} \sin 2\theta_1 \right]$$

$$d_n(t) = \frac{\sigma}{\pi} \left[(1+\bar{v}) \frac{\sin n\theta_1}{n} - \frac{(1-\bar{v})}{2} \left(\frac{\sin(2+n)\theta_1}{(2+n)} + \frac{\sin(2-n)\theta_1}{(2-n)} \right) \right] \quad 3.9$$

For $t \geq 2a/C_1$

$$\frac{a_0(t)}{2} = \frac{\sigma(1+\bar{v})}{2}$$

$$a_n(t) = 0, \quad n \neq 2, \quad a_2(t) = \frac{\sigma(1-\bar{v})}{2}$$

$$b_n(t) = 0, \quad n \neq 2, \quad b_2(t) = -\frac{\sigma(1-\bar{v})}{2} \quad 3.10$$

$$\frac{d_0(t)}{2} = \frac{\sigma(1+\bar{v})}{2}$$

$$d_n(t) = 0, \quad n \neq 2, \quad d_2(t) = -\frac{\sigma(1-\bar{v})}{2}$$

Equations 3.3 and 3.4 combined with Eqs. 3.6 to 3.10 give the time dependence of the free field incident stresses on a cylindrical boundary with radius a . The variation of the first three of these coefficients with time is shown in Fig. 3.3 for a value of $\bar{v} = 1/3$ and with $\sigma = 1.0$. The accuracy with which the first three terms of a Fourier series represent the

stress variation with angle around the opening at two times may be observed in Fig. 3.4. In this figure the variation of σ_{rr} , $\sigma_{r\theta}$, and $\sigma_{\theta\theta}$ with angle is shown for the times $tC_1/a = 0.5$ and 1.0 . Also shown on this figure is the actual variation of these stresses for comparison. It may be observed from these curves that the representation is not as good for the earlier time as the later, as would be expected. For this reason the method presented is not applicable for early stress computations unless a larger number of terms is used in the Fourier series. The representation for the incoming wave is exact, however, for all times after the wave has enveloped the boundary. Also it may be seen that the representation is much better for σ_{rr} and $\sigma_{r\theta}$ than it is for $\sigma_{\theta\theta}$. Since the diverging wave form is determined by the incident boundary stresses σ_{rr} and $\sigma_{r\theta}$, the determination of the diverging wave should be fairly accurate.

3.2 Fourier Analysis of Incident Shear Wave

Consider the case of a plane step wave of pure shear with magnitude of stress $\tilde{\tau}$ traveling in the negative x direction. Stresses on a cylindrical boundary behind the front may be written,

$$\begin{aligned}\tilde{\sigma}_{rr} &= \tilde{\tau} \sin 2\theta \\ \tilde{\sigma}_{r\theta} &= \tilde{\tau} \cos 2\theta \\ \tilde{\sigma}_{\theta\theta} &= -\tilde{\tau} \sin 2\theta\end{aligned}\tag{3.11}$$

where positive shear is defined in Fig. 3.5. A tilde will be placed over those quantities associated with an incident shear wave in order to distinguish them from the corresponding quantities associated with an incident wave of dilatation. The Fourier series corresponding to these expressions are,

$$\begin{aligned}
\bar{\sigma}_{rr} &= \sum_{n=1}^{\infty} \tilde{b}_n(t) \sin n\theta \\
\bar{\sigma}_{r\theta} &= \frac{\tilde{a}_0(t)}{2} + \sum_{n=1}^{\infty} \tilde{a}_n(t) \cos n\theta \\
\bar{\sigma}_{\theta\theta} &= \sum_{n=1}^{\infty} \tilde{d}_n(t) \sin n\theta
\end{aligned} \tag{3.12}$$

The Fourier coefficients, found in the same manner as for waves of dilatation, are

for $t \leq 2a/C_2$

$$\begin{aligned}
\tilde{b}_n(t) &= \frac{\tilde{\tau}}{\pi} \left[\frac{\sin(2-n)\theta_2}{(2-n)} - \frac{\sin(2+n)\theta_2}{(2+n)} \right] \\
\tilde{a}_n(t) &= \frac{\tilde{\tau}}{\pi} \left[\frac{\sin(2-n)\theta_2}{(2-n)} + \frac{\sin(2+n)\theta_2}{(2+n)} \right] \\
\tilde{d}_n(t) &= -\frac{\tilde{\tau}}{\pi} \left[\frac{\sin(2-n)\theta_2}{(2-n)} - \frac{\sin(2+n)\theta_2}{(2+n)} \right],
\end{aligned} \tag{3.13}$$

for $t \geq 2a/C_2$

$$\begin{aligned}
\tilde{b}_n(t) &= 0, \quad n \neq 2, \quad \tilde{b}_2(t) = \tilde{\tau} \\
\tilde{a}_n(t) &= 0, \quad n \neq 2, \quad \tilde{a}_2(t) = \tilde{\tau} \\
\tilde{d}_n(t) &= 0, \quad n \neq 2, \quad \tilde{d}_2(t) = -\tilde{\tau}
\end{aligned} \tag{3.14}$$

where C_2 is the velocity of propagation of a shear wave. The angle θ_2 may be written as follows by referring to Fig. 3.5

$$\theta_2 = \cos^{-1} (1 - tC_2/a)$$

for $0 \leq tC_2/a \leq 2.0$

and $\theta_2 = \pi$

for $tC_2/a \geq 2.0$.

3.3 Derivation of Equations for Diverging Wave (Incident Dilatational Wave)

The equilibrium equations may be expressed in the following form for an elastic medium

$$\begin{aligned} (\lambda + \mu) \frac{\partial \Delta}{\partial x} + \mu \nabla^2 u - \rho \ddot{u} &= 0 \\ (\lambda + \mu) \frac{\partial \Delta}{\partial y} + \mu \nabla^2 v - \rho \ddot{v} &= 0 \\ (\lambda + \mu) \frac{\partial \Delta}{\partial z} + \mu \nabla^2 w - \rho \ddot{w} &= 0 \end{aligned} \quad 3.15$$

where Δ is the dilatation given by

$$\Delta = \frac{\partial u}{\partial x} + \frac{\partial v}{\partial y} + \frac{\partial w}{\partial z}$$

and u , v , and w are displacements in the x , y and z directions. It is convenient to introduce the following representation for the displacement vector $\ddot{\mathbf{u}}$ in terms of a scalar potential ϕ and a vector potential $\bar{\Psi}$

$$\ddot{\mathbf{u}} = \text{grad } \phi + \text{curl } \bar{\Psi}.$$

Then $\text{grad } \phi$ represents the irrotational part of the displacement and $\text{curl } \bar{\Psi}$ represents a displacement corresponding to no dilatation. Observing from the physical problem that there is no variation in displacement with z along the cavity axis and that there is, therefore, only rotation about the z axis, one may write the following simplified expressions

$$\begin{aligned} \text{grad } \phi &= \frac{\partial \phi}{\partial x} \hat{i} + \frac{\partial \phi}{\partial y} \hat{j} \\ \text{Curl } \bar{\Psi} &= \frac{\partial \bar{\Psi}_z}{\partial y} \hat{i} - \frac{\partial \bar{\Psi}_z}{\partial x} \hat{j}. \end{aligned}$$

Therefore

$$\bar{u} = \left(\frac{\partial \phi}{\partial x} + \frac{\partial \psi}{\partial y} \right) \hat{i} + \left(\frac{\partial \phi}{\partial y} - \frac{\partial \psi}{\partial x} \right) \hat{j}$$

setting $\bar{v}_z = \psi$.

The displacements u , v , and w may be written then

$$\begin{aligned} u &= \frac{\partial \phi}{\partial x} + \frac{\partial \psi}{\partial y} \\ v &= \frac{\partial \phi}{\partial y} - \frac{\partial \psi}{\partial x} \\ w &= 0 \end{aligned} \tag{3.16}$$

The equations of motion (Eqs. 3.15) will be satisfied if the potentials ϕ and ψ satisfy the following two wave equations,

$$\begin{aligned} c_1^2 \nabla^2 \phi &= \ddot{\phi} \\ c_2^2 \nabla^2 \psi &= \ddot{\psi}, \end{aligned} \tag{3.17}$$

where the velocities of the dilatational and shear waves are given by

$$c_1^2 = \frac{\lambda + 2\mu}{\rho} \quad \text{and} \quad c_2^2 = \frac{\mu}{\rho}. \tag{3.18}$$

In polar coordinates the displacement components of Eqs. 3.16 are given by

$$\begin{aligned} u_r &= \frac{\partial \phi}{\partial r} + \frac{1}{r} \frac{\partial \psi}{\partial \theta} \\ u_\theta &= \frac{1}{r} \frac{\partial \phi}{\partial \theta} - \frac{\partial \psi}{\partial r} \\ u_z &= 0 \end{aligned} \tag{3.19}$$

where u_r is taken positive in the direction of increasing r and u_θ is positive in the direction of increasing θ

In Ref. (8) the following general solution to equations of the type represented by Eqs. 3.17 is given. First the potential (displacement potentials in this case), ϕ and ψ , are taken in the following form:

$$\begin{aligned}\phi &= \sum_{n=1}^{\infty} r^n f_n(r,t) \cos n\theta \\ \psi &= \sum_{n=1}^{\infty} r^n g_n(r,t) \sin n\theta .\end{aligned}\tag{3.20}$$

These particular forms for the displacement potentials were chosen because they satisfy $\nabla^2 \phi = 0$ and $\nabla^2 \psi = 0$, a "homogeneous" part of the differential equations if $f_n(r,t)$ and $g_n(r,t)$ are assumed constant. These functions of r and t must be chosen so that the equations with $\ddot{\phi}$ and $\ddot{\psi}$ on the right are satisfied. Since the displacements u_r caused by the incident wave of dilatation are even in θ while the displacements u_θ are odd in the θ , ϕ is chosen even and ψ odd so that Eqs. 3.19 will result in displacements of the same form when ϕ and ψ are substituted into them. Therefore this form for representing the diverging wave is only suitable for use with an incident wave of dilatation.

Substitution of Eqs. 3.20 into Eqs. 3.17 gives the following differential equations to be satisfied by the Fourier coefficients,

$$\begin{aligned}C_1^2 \left(\frac{\partial^2 f_n}{\partial r^2} + \frac{2n+1}{r} \frac{\partial f_n}{\partial r} \right) &= f_n \\ C_2^2 \left(\frac{\partial^2 g_n}{\partial r^2} + \frac{2n+1}{r} \frac{\partial g_n}{\partial r} \right) &= g_n .\end{aligned}\tag{3.21}$$

The solution to these equations may be written in terms of the solution for $n = 0$ as

$$f_n = \left(\frac{1}{r} \frac{\partial}{\partial r}\right)^n f_0 \quad \text{and} \quad g_n = \left(\frac{1}{r} \frac{\partial}{\partial r}\right)^n g_0. \quad 3.22$$

In Section B.1 of Appendix B it is shown that Eqs. 3.22 do indeed satisfy Eqs. 3.21. The next step is to find f_0 and g_0 . This may be done in the following way. Consider the first of Eqs. 3.21 with $n = 0$.

$$c_1^2 \left(\frac{\partial^2 f_0}{\partial r^2} + \frac{1}{r} \frac{\partial f_0}{\partial r} \right) = f_0 \quad 3.23$$

This is recognized as the wave equation in cylindrical coordinates for the case of symmetry about the z axis. The form of f_0 which satisfies Eq. 3.23 may be obtained through the following reasoning. It is known that the form of the displacement potential for a spherically symmetrical point source wave is

$$f_s = \frac{1}{\rho} f \left(t - \frac{\rho}{c_1} \right).$$

The displacement potential for a line source may be found by integrating the displacement potentials for all point sources uniformly distributed along the z axis from $z = -\infty$ to $z = +\infty$, each point source having the same variation with time. Then the symmetrical line source displacement potential may be written

$$f_0 = \int_{-\infty}^{+\infty} \frac{1}{\rho} f \left(t - \frac{\rho}{c_1} \right) dz. \quad 3.24$$

This same form of displacement potential is used in Ref. 9 in the investigations of supersonic fluid flow around a long wing.

In Fig. 3.6 the coordinate system is shown. From this figure it may be seen that ρ is equal to $\sqrt{r^2 + z^2}$. Therefore, Eq. 3.24 may be written in the following form

$$f_o = \int_{-\infty}^{+\infty} f\left(t - \frac{\sqrt{r^2 + z^2}}{c_1}\right) \frac{dz}{\sqrt{r^2 + z^2}}. \quad 3.25$$

At this point the variable u is introduced such that

$$r \cosh u = \sqrt{r^2 + z^2} = \rho$$

or

$$u = \cosh^{-1} \left(\frac{1}{r} \sqrt{r^2 + z^2} \right).$$

Taking the derivative of both sides gives

$$du = \frac{dz}{\sqrt{r^2 + z^2}}.$$

By introducing the above identities, Eq. 3.25 may be rewritten in the following form,

$$f_o = 2 \int_{u=0}^{u=+\infty} f\left(t - \frac{r}{c_1} \cosh u\right) du = \int_0^{\infty} F\left(t - \frac{r}{c_1} \cosh u\right) du. \quad 3.26$$

In a similar manner the displacement potential for a symmetrical shear wave becomes

$$g_o = \int_{u=0}^{u=+\infty} G\left(t - \frac{r}{c_2} \cosh u\right) du. \quad 3.27$$

Combining Eqs. 3.26 and 3.27 with 3.22 one obtains

$$\begin{aligned} f_n &= \left(\frac{1}{r} \frac{\partial}{\partial r}\right)^n \int_0^{\infty} F\left(t - \frac{r}{c_1} \cosh u\right) du \\ g_n &= \left(\frac{1}{r} \frac{\partial}{\partial r}\right)^n \int_0^{\infty} G\left(t - \frac{r}{c_2} \cosh u\right) du \end{aligned} \quad 3.28$$

From Eqs. 3.28 and Eqs. 3.20,

$$\begin{aligned}\varphi &= \sum_{n=0}^{\infty} r^n \left(\frac{1}{r} \frac{\partial}{\partial r}\right)^n \int_0^{+\infty} F\left(t - \frac{r}{c_1} \cosh u\right) du \cos n\theta \\ \psi &= \sum_{n=0}^{\infty} r^n \left(\frac{1}{r} \frac{\partial}{\partial r}\right)^n \int_0^{+\infty} G\left(t - \frac{r}{c_2} \cosh u\right) du \sin n\theta.\end{aligned}\quad 3.29$$

Considerable simplification can be effected in the solution by noting that Eqs. 3.29 can be written in the following form

$$\begin{aligned}\varphi &= \left[\sum_{n=0}^{\infty} \frac{(-1)^n}{c_1^n} \int_0^{+\infty} F^n\left(t - \frac{r}{c_1} \cosh u\right) \cosh nu \, du \right] \cos n\theta \\ \psi &= \left[\sum_{n=0}^{\infty} \frac{(-1)^n}{c_2^n} \int_0^{+\infty} G^n\left(t - \frac{r}{c_2} \cosh u\right) \cosh nu \, du \right] \sin n\theta,\end{aligned}\quad 3.30$$

where the superscripts on F and G indicate the order of the derivative.

The proof of the conversion from Eqs. 3.29 to 3.30 is shown in Section B.2 of Appendix B.

In terms of displacements, the stresses at any point in the medium may be expressed as follows:

$$\begin{aligned}\sigma_{rr} &= \lambda \Delta + 2\mu \frac{\partial u_r}{\partial r} \\ \sigma_{r\theta} &= \mu \gamma_{r\theta} \\ \sigma_{\theta\theta} &= \lambda \Delta + \frac{2\mu}{r} \left(\frac{\partial u_\theta}{\partial \theta} + u_r \right)\end{aligned}\quad 3.31$$

where

$$\begin{aligned}\Delta &= \frac{\partial u_r}{\partial r} + \frac{u_r}{r} + \frac{\partial u_\theta}{\partial \theta} \\ \gamma_{r\theta} &= \frac{\partial u_\theta}{\partial r} + \frac{1}{r} \frac{\partial u_r}{\partial \theta} - \frac{u_\theta}{r}.\end{aligned}$$

By substituting into these equations the displacements given by Eqs. 3.19, one obtains the stresses in terms of displacement potentials.

$$\begin{aligned}
 \sigma_{rr} &= (\lambda + 2\mu) \frac{\partial^2 \Phi}{\partial r^2} + \frac{\lambda}{r} \frac{\partial \Phi}{\partial r} + \frac{\lambda}{r^2} \frac{\partial^2 \Phi}{\partial \theta^2} + \frac{2\mu}{r} \frac{\partial^2 \Psi}{\partial r \partial \theta} - \frac{2\mu}{r^2} \frac{\partial \Psi}{\partial \theta} \\
 \sigma_{r\theta} &= \mu \left(\frac{2}{r} \frac{\partial^2 \Phi}{\partial r \partial \theta} - \frac{2}{r^2} \frac{\partial \Phi}{\partial \theta} - \frac{\partial^2 \Psi}{\partial r^2} + \frac{1}{r^2} \frac{\partial^2 \Psi}{\partial \theta^2} + \frac{1}{r} \frac{\partial \Psi}{\partial r} \right) \\
 \sigma_{\theta\theta} &= \lambda \frac{\partial^2 \Phi}{\partial r^2} + \frac{(\lambda + 2\mu)}{r} \frac{\partial \Phi}{\partial r} + \frac{(\lambda + 2\mu)}{r^2} \frac{\partial^2 \Phi}{\partial \theta^2} - \frac{2\mu}{r} \frac{\partial^2 \Psi}{\partial r \partial \theta} + \frac{2\mu}{r^2} \frac{\partial \Psi}{\partial \theta}.
 \end{aligned} \tag{3.32}$$

Substitution of the general expressions for Φ and Ψ (Eqs. 3.30) into Eqs. 3.32 gives the general expressions for stress in the diverging wave.

$$\begin{aligned}
 \sigma_{rr} &= \sum_{n=0}^{\infty} \left[\frac{(-1)^n}{c_1^{n+2}} \int_0^{u_1} F^{n+2}(\eta_1) [(2\mu \cosh^2 u + \lambda) \cosh nu] du \right. \\
 &\quad \left. - \frac{(-1)^n}{c_2^{n+2}} \int_0^{u_2} G^{n+2}(\eta_2) [\mu \sinh 2u \sinh nu] du \right] \cos n\theta
 \end{aligned} \tag{3.33}$$

$$\begin{aligned}
 \sigma_{r\theta} &= \sum_{n=0}^{\infty} \left[\frac{(-1)^n}{c_1^{n+2}} \int_0^{u_1} F^{n+2}(\eta_1) [\mu \sinh 2u \sinh nu] du \right. \\
 &\quad \left. - \frac{(-1)^n}{c_2^{n+2}} \int_0^{u_2} G^{n+2}(\eta_2) [\mu \cosh 2u \cosh nu] du \right] \sin n\theta
 \end{aligned} \tag{3.34}$$

$$\begin{aligned}
 \sigma_{\theta\theta} &= \sum_{n=0}^{\infty} \left[\frac{(-1)^n}{c_1^{n+2}} \int_0^{u_1} F^{n+2}(\eta_1) [(\lambda - 2\mu \sinh^2 u) \cosh nu] du \right. \\
 &\quad \left. + \frac{(-1)^n}{c_2^{n+2}} \int_0^{u_2} G^{n+2}(\eta_2) [\mu \sinh 2u \sinh nu] du \right] \cos n\theta
 \end{aligned} \tag{3.35}$$

where

$$\eta_1 = (t - \frac{r}{c_1} \cosh u) \quad \text{and} \quad \eta_2 = (t - \frac{r}{c_2} \cosh u). \tag{3.36}$$

The integration limits on Eqs. 3.24 and therefore on Eqs. 3.30 extend to $+\infty$ since there are point sources all along the z axis. The wave emanating from each point source is considered to have the same variation in time. Therefore, at any finite time only the point source waves out to a finite value of z have reached the point in question provided they all started at the same finite time. For a finite time the integration in u need only extend to the value corresponding to this value of z .

By substituting Eqs. 3.30 into Eqs. 3.19, the general expressions for displacements may also be found.

$$u_r = \sum_{n=0}^{\infty} \left[-\frac{(-1)^n r}{c_1^{n+2}} \int_0^{u_1} F^{n+2}(\eta_1) \left[\frac{\sinh(1+n)u}{2(1+n)} + \frac{\sinh(1-n)u}{2(1-n)} \right] \sinh u \, du \right. \\ \left. + \frac{(-1)^n r}{c_2^{n+2}} \int_0^{u_2} G^{n+2}(\eta_2) \left[\frac{\sinh(1+n)u}{2(1+n)} - \frac{\sinh(1-n)u}{2(1-n)} \right] \sinh u \, du \right] \cos n\theta$$

3.37

$$u_\theta = \sum_{n=0}^{\infty} \left[-\frac{(-1)^n r}{c_1^{n+2}} \int_0^{u_1} F^{n+2}(\eta_1) \left[\frac{\sinh(1+n)u}{2(1+n)} - \frac{\sinh(1-n)u}{2(1-n)} \right] \sinh u \, du \right. \\ \left. + \frac{(-1)^n r}{c_2^{n+2}} \int_0^{u_2} G^{n+2}(\eta_2) \left[\frac{\sinh(1+n)u}{2(1+n)} + \frac{\sinh(1-n)u}{2(1-n)} \right] \sinh u \, du \right] \sin n\theta .$$

These expressions for stress and displacement in a wave diverging from a line source are only suitable for elimination of the boundary stresses due to an incident wave of dilatation since the variation in θ has the same form in the two cases.

3.4 Derivation of Equations for the Diverging Wave (Incident Shear Wave)

The displacements in the medium caused by a plane incident shear wave with a constant state of stress behind the front are odd in θ in the radial direction and even in the θ direction. In order that the displacements caused by the diverging wave (Eqs. 3.19) might have this same variation $\tilde{\phi}$ should be odd and $\tilde{\psi}$ even in θ . The displacement potentials in this case are then the same as for an incident wave of dilatation except for the variation in θ , and may be written as follows by analogy with Eq. 3.29:

$$\begin{aligned}\tilde{\phi} &= \sum_{n=0}^{\infty} r^n \left(\frac{1}{r} \frac{\partial}{\partial r} \right)^n \int_0^{+\infty} F(\eta_1) du \sin n\theta \\ \tilde{\psi} &= \sum_{n=0}^{\infty} r^n \left(\frac{1}{r} \frac{\partial}{\partial r} \right)^n \int_0^{+\infty} G(\eta_2) du \cos n\theta.\end{aligned}$$

These expressions may be written by analogy with Eq. 3.30

$$\begin{aligned}\tilde{\phi} &= \sum_{n=0}^{\infty} \left[\frac{(-1)^n}{c_1^n} \int_0^{+\infty} F^n(\eta_1) \cosh nu du \right] \sin n\theta \\ \tilde{\psi} &= \sum_{n=0}^{\infty} \left[\frac{(-1)^n}{c_2^n} \int_0^{+\infty} G^n(\eta_2) \cosh nu du \right] \cos n\theta.\end{aligned}\tag{3.38}$$

Substitution of Eqs. 3.38 into the general expressions for stress in terms of displacement potentials (Eq. 3.32) gives,

$$\begin{aligned}\sigma_{rr} &= \sum_{n=0}^{\infty} \left[\frac{(-1)^n}{c_1^{n+2}} \int_0^{u_1} F^{n+2}(\eta_1) [(2\mu \cosh^2 u + \lambda) \cosh nu] du \right. \\ &\quad \left. + \frac{(-1)^n}{c_2^{n+2}} \int_0^{u_2} G^{n+2}(\eta_2) [\mu \sinh 2u \sinh nu] du \right] \sin n\theta\end{aligned}$$

The two equations resulting from these boundary conditions are to be solved for the functions $F^{n+2}(\eta_1)$ and $G^{n+2}(\eta_2)$.

For an incident wave of dilatation the boundary equations may be found by combining the first two of Eqs. 3.3 with Eqs. 3.33 and 3.34 and applying the resulting conditions at the radius $r = a$.

$$0 = \frac{a_0(t)}{2} + \sum_{n=1}^{\infty} a_n(t) \cos n\theta + \sum_{n=0}^{\infty} \left[\frac{(-1)^n}{c_1^{n+2}} \int_0^{u_1} F^{n+2}(\eta_1) [(2\mu \cosh^2 u + \lambda) \cosh nu] du \right. \\ \left. - \frac{(-1)^n}{c_2^{n+2}} \int_0^{u_2} G^{n+2}(\eta_2) [\mu \sinh 2u \sinh nu] du \right] \cos n\theta \quad 3.41$$

$$0 = \sum_{n=1}^{\infty} b_n(t) \sin n\theta + \sum_{n=0}^{\infty} \left[\frac{(-1)^n}{c_1^{n+2}} \int_0^{u_1} F^{n+2}(\eta_1) [\mu \sinh 2u \sinh nu] du \right. \\ \left. - \frac{(-1)^n}{c_2^{n+2}} \int_0^{u_2} G^{n+2}(\eta_2) [\mu \cosh 2u \cosh nu] du \right] \sin n\theta$$

In a similar manner the boundary equations for an incident shear wave may be found by combining the first two of Eqs. 3.12 with the first two of Eqs. 3.39.

$$0 = \sum_{n=0}^{\infty} \tilde{b}_n(t) \sin n\theta + \sum_{n=1}^{\infty} \left[\frac{(-1)^n}{c_1^{n+2}} \int_0^{u_1} F^{n+2}(\eta_1) [2\mu \cosh^2 u + \lambda] \cosh nu du \right. \\ \left. + \frac{(-1)^n}{c_2^{n+2}} \int_0^{u_2} G^{n+2}(\eta_2) [\mu \sinh 2u \sinh nu] du \right] \sin n\theta \quad 3.42$$

$$0 = \frac{\tilde{a}_0(t)}{2} + \sum_{n=1}^{\infty} \tilde{a}_n(t) \cos n\theta + \sum_{n=0}^{\infty} \left[\frac{(-1)^n}{c_1^{n+2}} \int_0^{u_1} F^{n+2}(\eta_1) [-\mu \sinh 2u \sinh nu] du \right. \\ \left. - \frac{(-1)^n}{c_2^{n+2}} \int_0^{u_2} G^{n+2}(\eta_2) [\mu \cosh 2u \cosh nu] du \right] \cos n\theta$$

The two equations resulting from these boundary conditions are to be solved for the functions $F^{n+2}(\eta_1)$ and $G^{n+2}(\eta_2)$.

For an incident wave of dilatation the boundary equations may be found by combining the first two of Eqs. 3.3 with Eqs. 3.33 and 3.34 and applying the resulting conditions at the radius $r = a$.

$$0 = \frac{a_0(t)}{2} + \sum_{n=1}^{\infty} a_n(t) \cos n\theta + \sum_{n=0}^{\infty} \left[\frac{(-1)^n}{C_1^{n+2}} \int_0^{u_1} F^{n+2}(\eta_1) [(2\mu \cosh^2 u + \lambda) \cosh nu] du - \frac{(-1)^n}{C_2^{n+2}} \int_0^{u_2} G^{n+2}(\eta_2) [\mu \sinh 2u \sinh nu] du \right] \cos n\theta$$

3.41

$$0 = \sum_{n=1}^{\infty} b_n(t) \sin n\theta + \sum_{n=0}^{\infty} \left[\frac{(-1)^n}{C_1^{n+2}} \int_0^{u_1} F^{n+2}(\eta_1) [\mu \sinh 2u \sinh nu] du - \frac{(-1)^n}{C_2^{n+2}} \int_0^{u_2} G^{n+2}(\eta_2) [\mu \cosh 2u \cosh nu] du \right] \sin n\theta$$

In a similar manner the boundary equations for an incident shear wave may be found by combining the first two of Eqs. 3.12 with the first two of Eqs. 3.39.

$$0 = \sum_{n=0}^{\infty} \tilde{b}_n(t) \sin n\theta + \sum_{n=1}^{\infty} \left[\frac{(-1)^n}{C_1^{n+2}} \int_0^{u_1} F^{n+2}(\eta_1) [2\mu \cosh^2 u + \lambda) \cosh nu] du + \frac{(-1)^n}{C_2^{n+2}} \int_0^{u_2} G^{n+2}(\eta_2) [\mu \sinh 2u \sinh nu] du \right] \sin n\theta$$

3.42

$$0 = \frac{\tilde{a}_0(t)}{2} + \sum_{n=1}^{\infty} \tilde{a}_n(t) \cos n\theta + \sum_{n=0}^{\infty} \left[\frac{(-1)^n}{C_1^{n+2}} \int_0^{u_1} F^{n+2}(\eta_1) [-\mu \sinh 2u \sinh nu] du - \frac{(-1)^n}{C_2^{n+2}} \int_0^{u_2} G^{n+2}(\eta_2) [\mu \cosh 2u \cosh nu] du \right] \cos n\theta$$

The number of parameters involved in the solution of the problem may be found from Eqs. 3.41. The last two terms in each equation, which give the stresses in the outgoing wave, contain only λ and μ as parameters. But λ may be expressed as

$$\lambda = \mu \frac{2\nu}{1-2\nu} .$$

By making this substitution for λ , one may factor μ out of both terms, leaving ν as the only parameter that cannot be factored out. The actual form of $a_n(t)$, $b_n(t)$, and $d_n(t)$ may be seen by referring to Eqs. 3.6-3.10, where it is found that the only parameter within each term is $\bar{\nu}$, σ , the incident stress, being a common factor of each term. Since $\bar{\nu}$ is a function of ν (Eq. 3.1), Poisson's ratio is also the only parameter which cannot be factored out of these terms. In the actual machine computations all terms were divided by μ and the ratio $\frac{\sigma}{\mu}$ set equal to unity, i.e. μ was taken as the unit of stress. Then a single parameter appears in the solution, ν . In the derivation of equations which follows, λ and μ are retained in the equations so that it is clear to what extent the variation of these constants alters the solution of the problem.

All the constants mentioned thus far occur in the equations for hoop stress and equations for the stress in the medium in precisely the same way as mentioned above. Therefore, the same comments may be made concerning the parameters involved in these computations.

The same observations may be made concerning Eqs. 3.42 for an incident shear wave, except that $\bar{\tau}$ is a common factor in each term for stress due to the incident wave (Eqs. 3.13 and 3.14) and $\bar{\nu}$ does not appear.

The last two terms of each equation are the same as before and again, μ may be factored out leaving v as the only parameter that cannot be factored out. In the computer solution \tilde{v}/μ was set equal to unity in this case.

In the numerical solution of the problem, the fundamental unit of length was taken as a , of velocity C_1 (C_2 for incident shear wave), and of stress μ . These three units completely determine all the other units required. In Eqs. 3.41 the value of C_1 is unity while the value of C_2 is α . Where α is defined to be the ratio $\frac{C_2}{C_1}$. C_1 and C_2 are nevertheless carried through the derivation.

IV. MODIFICATION OF EQUATIONS FOR COMPUTER SOLUTION

4.1 Equations for an Incident Wave of Dilatation

Consider the numerical solution of the boundary equations given by Eqs. 3.41 for an incident wave of dilatation. The first terms on the right involving $a_n(t)$ and $b_n(t)$ represent the stresses due to the incident plane wave. These terms are functions of time and may be evaluated by computing the time-dependent angle θ_1 from Eq. 3.5 and substituting this angle into the appropriate expression for the Fourier coefficients given by Eqs. 3.6 - 3.10.

The last summations in Eqs. 3.41 represent the stresses in the diverging wave and contain integrals which must be evaluated to obtain the stress. It is important to note that these integrals are of the convolution type and therefore the integrations must be performed anew for each value of time considered. At any time for which the stress in the diverging wave is to be evaluated the integration can be performed numerically provided all the previous values of $F^{n+2}(\eta_1)$ and $G^{n+2}(\eta_2)$ are known. It is these functions, however, which must be found from the boundary conditions. This is possible since Eq. 3.41 constitutes two equations with two unknowns.

In the numerical integration process it is convenient to take equal steps in the independent variable. However, if equal steps in u_1 and u_2 are taken, unequal steps in time and unequal steps in movement of the outgoing wave in space will result. To avoid this complication the variable of integration will be changed

Referring to Fig. 3.6 and the equation following Eq. 3.25 one may write the limits on the integrals, u_1 and u_2 for the time t ,

$$r \cosh u_1 = \rho_1 = r + tC_1$$

$$r \cosh u_2 = \rho_2 = r + tC_2.$$

Solve for $\cosh u_1$ and $\cosh u_2$

$$\cosh u_1 = 1 + \frac{tC_1}{r} = 1 + \bar{\zeta}_1 \quad 4.1$$

$$\cosh u_2 = 1 + \frac{tC_2}{r} = 1 + \bar{\zeta}_2.$$

Therefore Eq. 3.41 may be written, using the substitution

$$\cosh u = 1 + \zeta, \quad 4.2$$

with the limits $\bar{\zeta}_1$ on the integrals involving $F^{n+2}(\eta_1)$ and $\bar{\zeta}_2$ on those involving $G^{n+2}(\eta_2)$. These upper limits may be expressed as follows from Eq. 4.1 for the particular case $r = a$,

$$\bar{\zeta}_1 = \frac{tC_1}{a} \text{ and } \bar{\zeta}_2 = \frac{tC_2}{a}.$$

By using the substitution of Eq. 4.2, one may write the arguments of $F^{n+2}(\eta_1)$ and $G^{n+2}(\eta_2)$ given by Eq. 3.36

$$\eta_1 = t - \frac{r}{C_1} (1 + \zeta) \text{ and } \eta_2 = t - \frac{r}{C_2} (1 + \zeta). \quad 4.3$$

In performing the numerical integration it is convenient to have the limits on all the integrals the same. This will be accomplished by changing the upper limit on the integrals of $G^{n+2}(\eta_2)$ to agree with that for $F^{n+2}(\eta_1)$ i.e. both upper limits become $\bar{\zeta}_1$. To do this the variable of

integration for the integrals involving $G^{n+2}(\eta_2)$ must be multiplied by the ratio of the limits

$$\frac{\xi_2}{\xi_1} = \frac{C_2}{C_1} = \alpha. \quad 4.4$$

For simplicity the subscript on the upper limits will be dropped. Then the upper limits for all the integrals is

$$\xi = \frac{tC_1}{r} \quad 4.5$$

or, for the particular case $r = a$,

$$\xi = \frac{tC_1}{a}$$

and the variable of integration ξ for the integrals involving $G^{n+2}(\eta_2)$ will be replaced by $\alpha\xi$.

In the remaining explanation of the numerical solution of Eqs. 3.41 it is convenient to consider a particular value of n in order to simplify the equations involved. The case $n = 1$ will be considered, however, the derivations are quite similar for n equal to any other value except for certain simplifications when $n = 0$.

Consider the integral portions of Eqs. 3.41 representing stresses due to the diverging wave with $n = 1$ (these stresses are also given by Eq. 3.33 and 3.34)

$$\begin{aligned} \sigma_{rr} = & \left[\frac{-1}{C_1^2} \int_0^{u_1} F^{(1)}(\eta_1) [(2u \cosh^2 u + \lambda) \cosh u] du \right. \\ & \left. + \frac{1}{C_2^2} \int_0^k G^{(1)}(\eta_2) [u \sinh 2u \sinh u] du \right] \cos \theta \end{aligned}$$

$$\sigma_{r\theta} = \left[\frac{-1}{c_1^3} \int_0^{u_1} F'''(\eta_1) [\mu \sinh 2u \sinh u] du \right. \\ \left. + \frac{1}{c_2^3} \int_0^{u_2} G'''(\eta_2) [\mu \cosh 2u \cosh u] du \right] \sin \theta$$

Also the hoop stress in the diverging wave may be written by setting $n = 1$ in Eq. 3.35.

$$\sigma_{\theta\theta} = \left[\frac{-1}{c_1^3} \int_0^{u_1} F'''(\eta_1) [(\lambda - 2\mu \sinh^2 u) \cosh u] du \right. \\ \left. - \frac{1}{c_2^3} \int_0^{u_2} G'''(\eta_2) [\mu \sinh 2u \sinh u] du \right] \cos \theta$$

By using the substitution for $\cosh u$ in terms of t as given by Eq. 4.2 these equations for stress may be written with the same upper limits on all the integrals, ξ , as previously discussed.

$$\sigma_{rr} = \left[\frac{-1}{c_1^3} \int_0^{\xi} F'''(\eta_1) \left[\frac{(\lambda + 2\mu) + (\lambda + 6\mu)\xi + 6\mu\xi^2 + 2\mu\xi^3}{\sqrt{2\xi} \sqrt{1 + \xi/2}} \right] d\xi \right. \\ \left. + \frac{1}{c_2^3} \int_0^{\xi} G'''(\eta_2) \left[\frac{4\mu\alpha\xi(1+\alpha\xi)(1+\alpha\xi/2)}{\sqrt{2\alpha\xi} \sqrt{1 + \alpha\xi/2}} \right] \alpha d\xi \right] \cos \theta \quad 4.6$$

$$\sigma_{r\theta} = \left[\frac{-1}{c_1^3} \int_0^{\xi} F'''(\eta_1) \left[\frac{2\mu\xi(1+\xi)(1+\xi/2)}{\sqrt{2\xi} \sqrt{1 + \xi/2}} \right] d\xi \right. \\ \left. + \frac{1}{c_2^3} \int_0^{\xi} G'''(\eta_2) \left[\frac{\mu(1+\alpha\xi + \alpha^2\xi^2 + \alpha^3\xi^3)}{\sqrt{2\alpha\xi} \sqrt{1 + \alpha\xi/2}} \right] \alpha d\xi \right] \sin \theta \quad 4.7$$

$$\sigma_{\theta\theta} = \left[\frac{+1}{c_1^3} \int_0^{\xi} F'''(\eta_1) \left[\frac{-\lambda - (\lambda + 4\mu)\xi + 6\mu\xi^2 + 2\mu\xi^3}{\sqrt{2\xi} \sqrt{1 + \xi/2}} \right] d\xi \right. \\ \left. - \frac{1}{c_2^3} \int_0^{\xi} G'''(\eta_2) \left[\frac{4\mu\alpha\xi(1+\alpha\xi)(1+\alpha\xi/2)}{\sqrt{2\alpha\xi} \sqrt{1 + \alpha\xi/2}} \right] \alpha d\xi \right] \cos \theta \quad 4.8$$

Numerical integration of these equations is hindered by the fact that one term of each stress equation has an integrable singularity at ζ equal to zero. It is also necessary to assume the functions $F'''(\eta_1)$ and $G''(\eta_2)$ to be well behaved, however this assumption is justified for small t by the short time solution which will be discussed in Section 5.1. Also there is an integrable singularity in $F'''(\eta_1)$ at the value of the argument $\eta_1 = +a/C_1$, however it turns out that this does not affect the stresses obtained from the numerical integration. Consider as an example the numerical integration of the first term on the right of Eq. 4.6. The method of integration to be used assumes all of the integrand except $\zeta^{1/2}$ in the denominator to be linear between discrete values of ζ . Weighting factors consistent with a linear variation in ζ divided by $\zeta^{1/2}$ are computed and applied to the ordinates at each end of the interval in order to find the value of the integral in the interval. The derivation of the integration formula is shown in Appendix A. This method of treating integrals of the type encountered here is similar to a method derived in Ref (10). If ζ is divided into equal steps, $\Delta\zeta$, and the above idea applied, the value of the integral between $m\Delta\zeta$, and $(m+1)\Delta\zeta$, for the first term on the right of Eq. 4.6 may be written

$$\begin{aligned}
 &= \frac{1}{C_1^3} \int_{m\Delta\zeta}^{(m+1)\Delta\zeta} F'''(\eta_1) \left[\frac{(\lambda + 2\mu) + (\lambda + \mu)\zeta + \epsilon\mu\zeta^2 + 2\mu\zeta^3}{\sqrt{2\zeta} \sqrt{1 + \zeta/2}} \right] d\zeta \\
 &= \frac{\Delta\zeta}{C_1^3} \left[(F''(\eta_1))_m (R_{A1}^F)_m \left[\frac{2}{3} [(m+1)^{3/2} - m^{3/2}] - \frac{2}{3} [(m+1)^{1/2} - m^{1/2}] \right] \right. \\
 &\quad \left. + (F''(\eta_1))_{m+1} (R_{A1}^F)_{m+1} \left[\frac{2}{3} [(m+1)^{3/2} - m^{3/2}] - \frac{2}{3} [(m+1)^{1/2} - m^{1/2}] \right] \right] \quad + 9
 \end{aligned}$$

where R_{A1}^F on the right is equal to

$$R_{A1}^F = \frac{(\lambda+2\mu) + (\lambda+6\mu)\xi + 6\mu\xi^2 + 3\mu\xi^3}{c_1^3 \sqrt{2} \sqrt{1+\xi/2}} \quad 4.10$$

and m is the numbering of steps in $\Delta\xi$ starting with zero at $\xi = 0$. For brevity the following symbols are used for the weighting factors in Eq. 4.9.

$$\begin{aligned} A_m &= 2(1+m)[(m+1)^{1/2} - m^{1/2}] - \frac{2}{3} [(m+1)^{3/2} - m^{3/2}] \\ B_m &= \frac{2}{3} [(m+1)^{3/2} - m^{3/2}] - 2m[(m+1)^{1/2} - m^{1/2}] \end{aligned} \quad 4.11$$

It is shown in Appendix A that these weighting factors may be used for any of the integrals involved in the stress equations as long as the function to be integrated is well approximated by a linear relation in ξ divided by $\xi^{1/2}$ in any interval.

It would only be necessary to use the special integration scheme for the first few steps near $\xi = 0$; however, in the computer solution it is convenient to continue to use it throughout the range of integration. The total integral may be expressed as the summation of all the integrals in the interval $\Delta\xi$ as given by Eq. 4.9.

The following abbreviations for quantities in Eqs. 4.6 to 4.8 are used:

$$\begin{aligned} R_{A1}^G &= \left[\frac{\mu\alpha\xi(1+\alpha\xi)(1+\alpha\xi/2)}{\sqrt{2\alpha} \sqrt{1+\alpha\xi/2} \alpha^2 c_1^2} \right] \alpha \\ R_{B1}^F &= \left[\frac{-4\mu\xi(1+\xi)(1+\xi/2)}{\sqrt{2} \sqrt{1+\xi/2} c_1^3} \right] \\ R_{B1}^G &= \left[\frac{\mu(1+5\alpha\xi+6\alpha^2\xi^2+2\alpha^3\xi^3)}{\sqrt{2\alpha} \sqrt{1+\alpha\xi/2} \alpha^3 c_1^3} \right] \alpha \end{aligned} \quad 4.12$$

$$R_{D1}^F = \left[\frac{-\lambda - (\lambda + \mu) \xi + 6\mu\xi^2 + 2\mu\xi^3}{\sqrt{2} \sqrt{1+\xi/2} C_1^3} \right]$$

$$R_{D1}^G = \left[\frac{4\mu\alpha\xi(1+\alpha\xi)(1+\alpha\xi/2)}{\sqrt{2\alpha} \sqrt{1+\alpha\xi/2} \alpha^3 C_1^3} \right] \alpha$$

The stress equations given by Eqs. 4.6 - 4.8 may be written as follows for any time, $t = p\Delta t$, where $p = 0, 1, 2, \dots$, by using the summations of Eq. 4.9 for the integrals and the abbreviations of Eqs. 4.11 and 4.12

$$\begin{aligned} \sigma_{rr} = & \left[\sum_{m=0}^{p-1} \sqrt{\Delta\xi} \left[(F''''(\eta_1))_{p-m} (R_{A1}^F)_{m,m} + (F''''(\eta_1))_{p-m-1} (R_{A1}^F)_{m+1,m} \right] \right. \\ & \left. + \sum_{m=0}^{p-1} \sqrt{\Delta\xi} \left[(G''''(\eta_2))_{p-m} (R_{A1}^G)_{m,m} + (G''''(\eta_2))_{p-m-1} (R_{A1}^G)_{m+1,m} \right] \right] \cos \theta \end{aligned}$$

4.13

$$\begin{aligned} \sigma_{r\theta} = & \left[\sum_{m=0}^{p-1} \sqrt{\Delta\xi} \left[(F''''(\eta_1))_{p-m} (R_{B1}^F)_{m,m} + (F''''(\eta_1))_{p-m-1} (R_{B1}^F)_{m+1,m} \right] \right. \\ & \left. + \sum_{m=0}^{p-1} \sqrt{\Delta\xi} \left[(G''''(\eta_2))_{p-m} (R_{B1}^G)_{m,m} + (G''''(\eta_2))_{p-m-1} (R_{B1}^G)_{m+1,m} \right] \right] \sin \theta \end{aligned}$$

4.14

$$\begin{aligned} \sigma_{\theta\theta} = & \left[\sum_{m=0}^{p-1} \sqrt{\Delta\xi} \left[(F''''(\eta_1))_{p-m} (R_{D1}^F)_{m,m} + (F''''(\eta_1))_{p-m-1} (R_{D1}^F)_{m+1,m} \right] \right. \\ & \left. + \sum_{m=0}^{p-1} \sqrt{\Delta\xi} \left[(G''''(\eta_2))_{p-m} (R_{D1}^G)_{m,m} + (G''''(\eta_2))_{p-m-1} (R_{D1}^G)_{m+1,m} \right] \right] \cos \theta \end{aligned}$$

4.15

In order that the value of B may be computed once and used each time the integrations are performed, equal steps in time are chosen and steps $\Delta\xi$ are used as

given by

$$\Delta \xi = \Delta t \frac{c_1}{a}.$$

The use of Eqs. 4.13 and 4.14 in numerical form permits the boundary conditions given by Eqs. 3.41 to be rewritten as follows for the case $n = 1$. In these equations the unknown values, $(F'''(\eta_1))_p$ and $(G'''(\eta_2))_p$, are removed from the summations.

$$\begin{aligned} 0 = & (a_1(t))_p + \sqrt{\Delta \xi} \left[(F'''(\eta_1))_p (R_{A1}^F)_0 A_0 + (G'''(\eta_2))_p (R_{A1}^G)_0 A_0 \right] \\ & + \sum_{m=0}^{p-2} \sqrt{\Delta \xi} \left[(F'''(\eta_1))_{p-m-1} (R_{A1}^F)_{m+1} + (G'''(\eta_2))_{p-m-1} (R_{A1}^G)_{m+1} \right] (B_m + A_{m+1}) \\ & + \sqrt{\Delta \xi} \left[(F'''(\eta_1))_0 (R_{A1}^F)_p + (G'''(\eta_2))_0 (R_{A1}^G)_p \right] B_{p-1} \end{aligned} \quad 4.16$$

$$\begin{aligned} 0 = & (b_1(t))_p + \sqrt{\Delta \xi} \left[(F'''(\eta_1))_p (R_{B1}^F)_0 A_0 + (G'''(\eta_2))_p (R_{B1}^G)_0 A_0 \right] \\ & + \sum_{m=0}^{p-2} \sqrt{\Delta \xi} \left[(F'''(\eta_1))_{p-m-1} (R_{B1}^F)_{m+1} + (G'''(\eta_2))_{p-m-1} (R_{B1}^G)_{m+1} \right] (B_m + A_{m+1}) \\ & + \sqrt{\Delta \xi} \left[(F'''(\eta_1))_0 (R_{B1}^F)_p + (G'''(\eta_2))_0 (R_{B1}^G)_p \right] B_{p-1} \end{aligned} \quad 4.17$$

These equations are to be applied at $r = z$.

The stress caused by the incident wave, i.e., $a_1(t)$ and $b_1(t)$, is a known function of time and therefore may be evaluated at times $p\Delta t$. If all the previous values of $F'''(\eta_1)$ and $G'''(\eta_2)$ are known then the values of the summations are computed except for the terms involving $(F'''(\eta_1))_p$ and $(G'''(\eta_2))_p$. The values of these unknowns may then be found from the resulting equations. Since the first value of time that can be considered with these equations is $t = \Delta t$, it is necessary to find the values, $(F'''(\eta_1))_0$ and $(G'''(\eta_2))_0$, by some other means. Then the values at $t = \Delta t$ can be computed. Knowing the values of

the functions at $t = 0$ and $t = \Delta t$, those at $t = 2\Delta t$ may be computed, and so on.

The short time solution by which the initial values of $F'''(\eta_1)$ and $G'''(\eta_2)$ were found is discussed in Chapter V, where the values are given as

$$\begin{aligned}(F'''(\eta_1))_0 &= -2C_1^3\sigma/[\pi(\lambda+2\mu)] \\ (G'''(\eta_2))_0 &= 0.\end{aligned}\tag{4.18}$$

For machine solution Eqs. 4.16 and 4.17 may be written

$$\begin{aligned}(F'''(\eta_1))_p (R_{A1}^F)_0 A_0 + (G'''(\eta_2))_p (R_{A1}^G)_0 A_0 &= -\frac{(a_1(t))_p}{\sqrt{\Delta t}} - (S_{A1})_p \\ (F'''(\eta_1))_p (R_{B1}^F)_0 A_0 + (G'''(\eta_2))_p (R_{B1}^G)_0 A_0 &= -\frac{(b_1(t))_p}{\sqrt{\Delta t}} - (S_{B1})_p\end{aligned}\tag{4.19}$$

where

$$\begin{aligned}(S_{A1})_p &= \sum_{m=0}^{p-2} \left[(F'''(\eta_1))_{p-m-1} (R_{A1}^F)_{m+1} + (G'''(\eta_2))_{p-m-1} (R_{A1}^G)_{m+1} \right] (B_m + A_{m+1}) \\ &\quad + [(F'''(\eta_1))_0 (R_{A1}^F)_p + (G'''(\eta_2))_0 (R_{A1}^G)_p] B_{p-1} \\ (S_{B1})_p &= \sum_{m=0}^{p-2} \left[(F'''(\eta_1))_{p-m-1} (R_{B1}^F)_{m+1} + (G'''(\eta_2))_{p-m-1} (R_{B1}^G)_{m+1} \right] (B_m + A_{m+1}) \\ &\quad + [(F'''(\eta_1))_0 (R_{B1}^F)_p + (G'''(\eta_2))_0 (R_{B1}^G)_p] B_{p-1}\end{aligned}\tag{4.20}$$

Once all the values of $F'''(\eta_1)$ and $G'''(\eta_2)$ are known up to a given time, it is possible to find the hoop stress at this time. In order to perform the summations for $\sigma_{\theta\theta}$ along with the other summations it is necessary to write Eq. 4.15 for the stress due to the diverging wave in the same form that Eq. 4.13 and 4.14 were written, leaving the term involving $(F'''(\eta_1))_p$ and $(G'''(\eta_2))_p$ out of the summation. Once the unknowns are found, the term can be added to

the summation. Also the stress due to the incident wave, $(d_1(t))_p$, is added to that caused by the diverging wave.

$$\begin{aligned} \sigma_{\theta\theta} = & (d_1(t))_p + \sqrt{\Delta\zeta} [(F''''(\eta_1))_p (R_{D1}^F)_o A_o + (G''''(\eta_2))_p (R_{D1}^G)_o A_o] \\ & + \sqrt{\Delta\zeta} \sum_{m=0}^{p-2} [(F''''(\eta_1))_{p-m-1} (R_{D1}^F)_{m+1} + (G''''(\eta_2))_{p-m-1} (R_{D1}^G)_{m+1}] (B_m + A_{m+1}) \\ & + \sqrt{\Delta\zeta} [(F''''(\eta_1))_o (R_{D1}^F)_p + (G''''(\eta_2))_o (R_{D1}^G)_p] B_{p-1} \end{aligned} \quad 4.21$$

To compute the incident stresses at any time it is desirable to have the variable, t , in $a_1(t)$, $b_1(t)$, and $d_1(t)$ written in terms of $t = p\Delta t$. This may be done by dividing the time required for the wave to travel one radius into N steps and starting time when the plane wave first reaches the side of the opening. Then the ratio p/N is equal to tC_1/a where p is the step number corresponding to the time $t = p\Delta t$, until the wave reaches the back of the opening. Therefore, Eq. 3.5 may be written

$$\theta_1 = \cos^{-1} (1 - p/N). \quad 4.22$$

Once θ_1 is known Eqs. 3.6 through 3.10 may be evaluated. For the case $n = 1$ and $p \leq 2N$ these equations became

$$\begin{aligned} a_1(t) &= \frac{+\sigma}{2\pi} \left[(3 + \bar{v}) \sin \theta_1 + \frac{(1-\bar{v})}{3} \sin 3\theta_1 \right] \\ b_1(t) &= \frac{-\sigma}{2\pi} (1 - \bar{v}) \left[\sin \theta_1 - \frac{1}{3} \sin 3\theta_1 \right] \\ d_1(t) &= \frac{+\sigma}{2\pi} \left[(3\bar{v} - 1) \sin \theta_1 - \frac{(1-\bar{v})}{3} \sin 3\theta_1 \right], \end{aligned} \quad 4.23$$

and for $p \geq 2N$

$$a_1(t) = 0, \quad b_1(t) = 0, \quad d_1(t) = 0. \quad 4.24$$

The case $n = 0$ is considerably simplified by the absence of a shear wave throughout the computation. There is only one equation then to compute

$F''(\eta_1)$; $G''(\eta_2)$ does not appear. For the case $n = 2$ the derivation is completely similar to that for $n = 1$.

The equations for $n = 0$ are as follows:

$$(F''(\eta_1))_p (R_{A1}^F)_o A_o = - \left(\frac{a_o(t)}{2} \right)_p / \sqrt{\Delta \zeta} - (S_{Ao})_p \quad 4.25a$$

$$(S_{Ao})_p = \sum_{m=0}^{p-2} \left[(F''(\eta_1))_{p-m-1} (R_{Ao}^F)_{m+1} \right] (B_m + A_{m+1}) \\ + (F''(\eta_1))_o (R_{Ao}^F)_p B_{p-1} \quad 4.25b$$

$$\sigma_{\theta\theta} = \left(\frac{d_o(t)}{2} \right)_p + \sqrt{\Delta \zeta} \left[(F''(\eta_1))_p (R_{Do}^F)_o A_o \right] \\ + \sqrt{\Delta \zeta} \sum_{m=0}^{p-2} \left[(F''(\eta_1))_{p-m-1} (R_{Do}^F)_{m+1} \right] (B_m + A_{m+1}) \\ + \sqrt{\Delta \zeta} (F''(\eta_1))_o (R_{Do}^F)_p B_{p-1} \quad 4.25c$$

$$\left. \begin{aligned} R_{Ao}^F &= + \left[\frac{\lambda + 2\mu(1 + 2\zeta + \zeta^2)}{c_1^2 \sqrt{2} \sqrt{1+\zeta/2}} \right] \\ R_{Do}^F &= + \left[\frac{\lambda - 2\mu\zeta(1 + \zeta/2)}{c_1^2 \sqrt{2} \sqrt{1+\zeta/2}} \right] \end{aligned} \right\} \quad 4.25d$$

$$(F''(\eta_1))_o = \sigma_o^* \sigma / [(1+2\mu)\tau] \quad 4.25e$$

for $p \leq 2N$

$$\left. \begin{aligned} \frac{u_o(t)}{2} &= \frac{+\sigma}{2\pi} \left[(1 + \sqrt{\nu}) \tau_1 + \frac{(1-\sqrt{\nu})}{2} \sin 2\theta_1 \right] \\ \frac{v_o(t)}{2} &= \frac{+\sigma}{2\pi} \left[(1 + \sqrt{\nu}) \tau_1 - \frac{(1-\sqrt{\nu})}{2} \sin 2\theta_1 \right] \end{aligned} \right\} \quad 4.25f$$

for $p \geq 2N$

$$\frac{u_o(t)}{2} = \sigma (1+\sqrt{\nu}) \tau_1, \quad \frac{v_o(t)}{2} = \sigma (1+\sqrt{\nu}) \tau_1 \quad 4.25g$$

The equations for the case $n = 2$ are as follows:

$$\left. \begin{aligned} (F^{IV}(\eta_1))_F (R_{A2}^F)_O A_O + (G^{IV}(\eta_2))_P (R_{A2}^G)_O A_O &= - \frac{(a_2(t))_F}{\sqrt{\Delta\xi}} - (S_{A2}^F)_P \\ (F^{IV}(\eta_1))_P (R_{B2}^F)_O A_O + (G^{IV}(\eta_2))_P (R_{B2}^G)_O A_O &= - \frac{(b_2(t))_P}{\sqrt{\Delta\xi}} - (S_{B2}^F)_P \end{aligned} \right\} \quad 4.26a$$

$$\left. \begin{aligned} (S_{A2}^F)_P &= \sum_{m=0}^{F-2} \left[(F^{IV}(\eta_1))_{P-m-1} (R_{A2}^F)_{m+1} + (G^{IV}(\eta_2))_{P-m-1} (R_{A2}^G)_{m+1} \right] (B_m + A_{m+1}) \\ &\quad + \left[(F^{IV}(\eta_1))_O (R_{A2}^F)_F + (G^{IV}(\eta_2))_O (R_{A2}^G)_F \right] B_{P-1} \\ (S_{B2}^F)_F &= \sum_{m=0}^{F-2} \left[(F^{IV}(\eta_1))_{P-m-1} (R_{B2}^F)_{m+1} + (G^{IV}(\eta_2))_{P-m-1} (R_{B2}^G)_{m+1} \right] (B_m + A_{m+1}) \\ &\quad + \left[(F^{IV}(\eta_1))_O (R_{B2}^F)_F + (G^{IV}(\eta_2))_O (R_{B2}^G)_F \right] B_{F-1} \end{aligned} \right\} \quad 4.26b$$

$$\begin{aligned} \sigma_{\theta\theta} &= (a_2(t))_F + \sqrt{\Delta\xi} \left[(F^{IV}(\eta_1))_P (R_{D2}^F)_O A_O + (G^{IV}(\eta_2))_P (R_{D2}^G)_O A_O \right] \\ &\quad + \sqrt{\Delta\xi} \sum_{m=0}^{F-2} \left[(F^{IV}(\eta_1))_{P-m-1} (R_{D2}^F)_{m+1} + (G^{IV}(\eta_2))_{P-m-1} (R_{D2}^G)_{m+1} \right] (B_m + A_{m+1}) \\ &\quad + \sqrt{\Delta\xi} \left[(F^{IV}(\eta_1))_O (R_{D2}^F)_F + (G^{IV}(\eta_2))_O (R_{D2}^G)_F \right] B_{F-1} \end{aligned} \quad 4.26c$$

$$R_{A2}^F = + \left[\frac{(1+\xi+2\xi^2)(8\mu(1+\xi\xi^2)+1)}{C_1^4 \sqrt{2} \sqrt{1+\xi/2}} \right]$$

$$R_{A2}^G = - \left[\frac{8\mu\xi(1+\xi/2)^{1/2}(1+\xi\xi^2)}{\alpha^4 C_1^4 \sqrt{2} \sqrt{1+\xi/2}} \right] \alpha$$

$$R_{B2}^F = + \left[\frac{8\mu\xi(1+\xi/2)^{1/2}(1+\xi\xi^2)}{C_1^4 \sqrt{2}} \right]$$

$$R_{B2}^J = - \left[\frac{\mu(1+\alpha\zeta+\alpha\zeta^2)^2}{\alpha^4 C_1^+ \sqrt{2\alpha} \sqrt{1+\alpha\zeta/2}} \right] \alpha \quad 4.26d$$

$$R_{D2}^F = + \left[\frac{(1+\alpha\zeta+\alpha\zeta^2)(1-2\mu(2\zeta+\zeta^2))}{C_1^+ \sqrt{2} \sqrt{1+\zeta/2}} \right]$$

$$R_{D2}^G = + \left[\frac{8\mu\alpha\zeta(1+\alpha\zeta/2)^{1/2}(1+\alpha\zeta)^2}{\alpha^4 C_1^+ \sqrt{2\alpha}} \right] \alpha$$

$$(F^{IV}(\eta_1))_0 = +2C_1^+ \sigma / [(1+2\mu)\pi], \quad (G^{IV}(\eta_2))_0 = 0 \quad 4.26e$$

For $\bar{v} \leq 2\pi$

$$\left. \begin{aligned} u_2(\tau) &= \frac{+\sigma}{2\pi} [(1-\bar{v}) \sigma_1 + (1+\bar{v}) \sin 2\theta_1 + \frac{1}{4} (1-\bar{v}) \sin 4\theta_1] \\ t_2(\tau) &= - \frac{\sigma(1-\bar{v})}{2\pi} [\sigma_1 - \frac{1}{4} \sin 4\theta_1] \\ i_2(\tau) &= \frac{+\sigma}{2\pi} [(\bar{v}-1) \sigma_1 + (1+\bar{v}) \sin 2\theta_1 + \frac{1}{4} (\bar{v}-1) \sin 4\theta_1] \end{aligned} \right\} \quad 4.26f$$

For $\bar{v} \geq 2\pi$

$$u_2(\tau) = \sigma(1-\bar{v})/2, \quad t_2(\tau) = -\sigma(1-\bar{v})/2, \quad i_2(\tau) = -\sigma(1-\bar{v})/2 \quad 4.26g$$

Figure 4.1 shows the result of the solution of Eqs. 4.19 for $F^{IV}(\eta_1)$ and $G^{IV}(\eta_2)$ in the cases $\bar{v} = 0$ ($v=0$) and $\bar{v} = 1/3$ ($v=1/4$). At the time when the wave front reaches the opening $F^{IV}(\eta_1)$ jumps to its initial value, and soon thereafter the back of the opening a sharp drop occurs. The time steps Δt are rather short (0.001) in order to obtain an accurate numerical integration. However, if the time interval is much too short the time required for making the computations becomes quite lengthy (increasing roughly as $(1/\Delta t)^2$).

During the numerical computations the hoop stress in the flexing wave was calculated for each term of the Fourier representation ($n = 1, 2, 3, \dots$) was obtained. These stress components are shown in Fig. 4.2 for $\bar{v} = 0$ and in Fig. 4.3 for $\bar{v} = 1/3$. For the values greater than $n = 2$ the resultant stresses, σ_{rr} and $\sigma_{\theta\theta}$, in the

boundary are small and go to zero at one transit time. Since the stresses in the outgoing waves are determined by these incident stresses, it is reasonable to expect that they should also be small and die off quickly after one transit time similar to the stress for $n = 1$, which also goes to zero at the back of the opening. The final stresses computed by using the first three modes will be presented and discussed in Chapter VI.

4.2 Equations for Incident Shear Wave

The numerical solution of the boundary equations for an incident shear wave (Eqs. 3.42) is quite similar to the procedure discussed above for an incident wave of dilatation. It may be seen from Eqs. 3.13 and 3.14 that the incident stress on the cylindrical boundary does not depend on Poisson's ratio. It may be observed, however, from Eqs. 3.42 that the stresses caused by the waves which diverge from a line source do depend on Poisson's ratio since these equations contain both λ and μ .

It is again convenient to consider the solution for a particular value of n in order to simplify the explanation; the value $n = 1$ will be used. Also since the derivation is so similar to the case just considered, the discussion will be somewhat abbreviated.

Consider only the integral terms in Eqs. 3.42 which represent the stresses in the diverging wave, and let $n = 1$ (also given by the first two of Eqs. 3.39).

$$\begin{aligned} \tilde{\sigma}_{rr} = & \left[\frac{-1}{c_1^2} \int_0^{u_1} F''''(\eta_1) [(2\mu \cosh^2 u + \lambda) \cosh u] du \right. \\ & \left. - \frac{1}{c_2^2} \int_0^{u_2} G''''(\eta_2) [\mu \sinh 2u \sinh u] du \right] \sin \theta \end{aligned}$$

$$\begin{aligned} \tilde{\sigma}_{r\theta} = & \left[\frac{+1}{c_1^3} \int_0^{u_1} F'''(\eta_1) [\mu \sinh 2u \sinh u] du \right. \\ & \left. + \frac{1}{c_2^3} \int_0^{u_2} G'''(\eta_2) [\mu \cosh 2u \cosh u] du \right] \cos \theta \end{aligned} \quad 4.27$$

Also the hoop stress in the diverging wave may be written by setting $n = 1$ in the last of Eqs. 3.39.

$$\begin{aligned} \tilde{\sigma}_{\theta\theta} = & \left[\frac{-1}{c_1^3} \int_0^{u_1} F'''(\eta_1) [2\mu \sinh^2 u + \lambda] \cosh u] du \right. \\ & \left. + \frac{1}{c_2^3} \int_0^{u_2} G'''(\eta_2) [\mu \sinh 2u \sinh u] du \right] \sin \theta \end{aligned} \quad 4.28$$

Again the substitution for $\cosh u$ in terms of ξ as given by Eq. 4.2 will be used, and the upper limits on the $F'''(\eta_1)$ and $G'''(\eta_2)$ integrals become

$$\tilde{\xi}_1 = \frac{+C_1}{a} \quad \text{and} \quad \tilde{\xi}_2 = \frac{+C_2}{a} .$$

In this case it is convenient to have the upper limit on the integrals involving $F'''(\eta_1)$ agree with that on the integrals involving $G'''(\eta_2)$. In order to change the upper limit to $\tilde{\xi}_2$ on the $F'''(\eta_1)$ integrals, the variable of integration must be multiplied by the ratio of the old to the new limits,

$$\frac{\tilde{\xi}_1}{\tilde{\xi}_2} = \frac{C_1}{C_2} = \frac{1}{\alpha} = \gamma .$$

For simplicity the subscript will be dropped on the upper limit; then the limit for the integrals becomes

$$\tilde{\xi} = \frac{+C_2}{a} .$$

The above equations for stress may then be written as follows:

$$\begin{aligned}
\tilde{\sigma}_{rr} &= \left[\frac{-1}{C_1^3} \int_0^{\tilde{\zeta}} F'''(\eta_1) \left[\frac{(2\mu(1+\gamma\zeta)^2 + \lambda)(1+\gamma\zeta)}{\sqrt{2\gamma\zeta} \sqrt{1+\gamma\zeta/2}} \right] \gamma d\zeta \right. \\
&\quad \left. + \frac{1}{C_2^3} \int_0^{\tilde{\zeta}} G'''(\eta_2) \left[\frac{4\mu\zeta(1+\zeta/2)^{1/2}(1+\zeta)}{\sqrt{2\zeta}} \right] d\zeta \right] \sin \theta \\
\tilde{\sigma}_{r\theta} &= \left[\frac{+1}{C_1^3} \int_0^{\tilde{\zeta}} F'''(\eta_1) \left[\frac{4\mu\gamma\zeta(1+\gamma\zeta/2)^{1/2}(1+\gamma\zeta)}{\sqrt{2\gamma\zeta}} \right] \gamma d\zeta \right. \\
&\quad \left. + \frac{1}{C_2^3} \int_0^{\tilde{\zeta}} G'''(\eta_2) \left[\frac{\mu(1+\zeta)(1+4\zeta+2\zeta^2)}{\sqrt{2\zeta} \sqrt{1+\zeta/2}} \right] d\zeta \right] \cos \theta \\
\tilde{\sigma}_{\theta\theta} &= \left[\frac{-1}{C_1^3} \int_0^{\tilde{\zeta}} F'''(\eta_1) \left[\frac{(\lambda-4\mu\gamma\zeta(1+\gamma\zeta/2))(1+\gamma\zeta)}{\sqrt{2\gamma\zeta} \sqrt{1+\gamma\zeta/2}} \right] \gamma d\zeta \right. \\
&\quad \left. + \frac{1}{C_2^3} \int_0^{\tilde{\zeta}} G'''(\eta_2) \left[\frac{-\mu\zeta(1+\zeta/2)^{1/2}(1+\zeta)}{\sqrt{2\zeta}} \right] d\zeta \right] \sin \theta
\end{aligned} \tag{4.29}$$

The same numerical integration procedure that was used earlier in this chapter and derived in Appendix A may be applied. Equations 4.29 may be written using summations for the integrals as follows:

$$\begin{aligned}
\tilde{\sigma}_{rr} &= \left[\sum_{n=0}^{P-1} \sqrt{\Delta\zeta} \left[(F'''(\eta_1))_{P-n} (\tilde{R}_{B_1}^F)_{n,n} A_n + (F'''(\eta_1))_{P-n-1} (\tilde{R}_{B_1}^F)_{n+1,n} B_n \right] \right. \\
&\quad \left. + \sum_{n=0}^{P-1} \sqrt{\Delta\zeta} \left[(G'''(\eta_2))_{P-n} (\tilde{R}_{B_1}^G)_{n,n} A_n + (G'''(\eta_2))_{P-n-1} (\tilde{R}_{B_1}^G)_{n+1,n} B_n \right] \right] \sin \theta \\
\tilde{\sigma}_{r\theta} &= \left[\sum_{n=0}^{P-1} \sqrt{\Delta\zeta} \left[(F'''(\eta_1))_{P-n} (\tilde{R}_{A_1}^F)_{n,n} A_n + (F'''(\eta_1))_{P-n-1} (\tilde{R}_{A_1}^F)_{n+1,n} B_n \right] \right. \\
&\quad \left. + \sum_{n=0}^{P-1} \sqrt{\Delta\zeta} \left[(G'''(\eta_2))_{P-n} (\tilde{R}_{A_1}^G)_{n,n} A_n + (G'''(\eta_2))_{P-n-1} (\tilde{R}_{A_1}^G)_{n+1,n} B_n \right] \right] \cos \theta
\end{aligned} \tag{4.31}$$

$$\begin{aligned} \tilde{z}_{\theta\theta} = & \left[\sum_{m=0}^{p-1} \sqrt{\Delta\zeta} \left[(F''''(\eta_1))_{p-m} (\tilde{R}_{D1}^F)_{m,m}^A + (F''''(\eta_1))_{p-m-1} (\tilde{R}_{D1}^F)_{m+1,m}^B \right] \right. \\ & \left. + \sum_{m=0}^{p-1} \sqrt{\Delta\zeta} \left[(G''''(\eta_2))_{p-m} (\tilde{R}_{D1}^G)_{m,m}^A + (G''''(\eta_2))_{p-m-1} (\tilde{R}_{D1}^G)_{m+1,m}^B \right] \right] \sin \theta \end{aligned}$$

where

$$\tilde{R}_{B1}^F = - \left[\frac{(2\mu(1+\gamma\zeta)^2 + \lambda)(1+\gamma\zeta)}{\sqrt{2\gamma} \sqrt{1+\gamma\zeta/2} \gamma^3 c_2^3} \right] \gamma$$

$$\tilde{R}_{B1}^G = - \left[\frac{4\mu\zeta(1+\zeta/2)^{1/2}(1+\zeta)}{\sqrt{2} c_2^3} \right]$$

$$\tilde{R}_{A1}^F = + \left[\frac{4\mu\gamma\zeta(1+\gamma\zeta/2)^{1/2}(1+\gamma\zeta)}{\sqrt{2\gamma} \gamma^3 c_2^3} \right] \gamma$$

$$\tilde{R}_{A1}^G = + \left[\frac{\mu(1+\zeta)(1+4\zeta+2\zeta^2)}{\sqrt{2} (1+\zeta/2)^{1/2} c_2^3} \right]$$

$$\tilde{R}_{D1}^F = - \left[\frac{(\lambda - 4\mu\gamma\zeta(1+\gamma\zeta/2))(1+\gamma\zeta)}{\sqrt{2\gamma} (1+\gamma\zeta/2)^{1/2} \gamma^3 c_2^3} \right] \gamma$$

$$\tilde{R}_{D1}^G = + \left[\frac{4\mu\zeta(1+\zeta/2)^{1/2}(1+\zeta)}{\sqrt{2} c_2^3} \right]$$

by replacing the integrals in Eqs. 3.42 with the summations of Eqs. 3.43 and factoring out the unknown terms $(F''''(\eta_1))_F$ and $(G''''(\eta_2))_F$, one obtains the following equations for the case $n = 1$,

$$\begin{aligned} (F''''(\eta_1))_F (\tilde{R}_{B1}^F)_{cA_1} + (G''''(\eta_2))_F (\tilde{R}_{B1}^G)_{cA_1} &= - \frac{(\tilde{b}_1(t))_F}{\sqrt{\Delta\zeta}} - (\tilde{S}_{B1})_F \\ (F''''(\eta_1))_F (\tilde{R}_{A1}^F)_{cA_2} + (G''''(\eta_2))_F (\tilde{R}_{A1}^G)_{cA_2} &= - \frac{(\tilde{a}_1(t))_F}{\sqrt{\Delta\zeta}} - (\tilde{S}_{A1})_F \end{aligned} \quad 4.32$$

where $\tilde{b}_1(t)$ and $\tilde{a}_1(t)$ are given by setting $n = 1$ in the first two of Eqs. 3.13 for $+C_2/a \leq 1$ and by Eqs. 3.14 for $+C_2/a \geq 2$.

$$\tilde{v}_1(t) = \frac{\tau}{\pi} \left[\sin \varphi_2 - \frac{1}{3} \sin 3\varphi_2 \right]$$

$$\tilde{u}_1(t) = \frac{\tau}{\pi} \left[\sin \varphi_2 + \frac{1}{3} \sin 3\varphi_2 \right]$$

$$\text{or } \tilde{v}_1(t) = 0, \quad \tilde{u}_1(t) = 0.$$

The summations, $(\tilde{S}_{B1})_F$ and $(\tilde{S}_{A1})_F$, in Eqs. 4.32 may be expressed

$$(\tilde{S}_{B1})_F = \sum_{m=0}^{F-2} \left[(F''''(\eta_1))_{F-m-1} (\tilde{R}_{B1}^F)_{m+1} + (G''''(\eta_2))_{F-m-1} (\tilde{R}_{B1}^G)_{m+1} \right] (B_m + A_{m+1}) \\ + \left[(F''''(\eta_1))_0 (\tilde{R}_{B1}^F)_F + (G''''(\eta_2))_0 (\tilde{R}_{B1}^G)_F \right] B_{F-1}$$

$$(\tilde{S}_{A1})_F = \sum_{m=0}^{F-2} \left[(F''''(\eta_1))_{F-m-1} (\tilde{R}_{A1}^F)_{m+1} + (G''''(\eta_2))_{F-m-1} (\tilde{R}_{A1}^G)_{m+1} \right] (B_m + A_{m+1}) \\ + \left[(F''''(\eta_1))_0 (\tilde{R}_{A1}^F)_F + (G''''(\eta_2))_0 (\tilde{R}_{A1}^G)_F \right] B_{F-1}.$$

Once the values of displacement potentials have been computed, the expression for total hoop stress is obtained by combining the last of Eqs. 3.13 and 3.14 with the last of Eqs. 4.32.

$$\tilde{\sigma}_{\theta\theta} = (\tilde{v}_1(t))_F + \sqrt{\Delta\zeta} \left[(F''''(\eta_1))_F (\tilde{R}_{D1}^F)_F A_c + (G''''(\eta_2))_F (\tilde{R}_{D1}^G)_F A_c \right] \\ + \sqrt{\Delta\zeta} \left[\sum_{m=0}^{F-2} \left[(F''''(\eta_1))_{F-m-1} (\tilde{R}_{D1}^F)_{m+1} + (G''''(\eta_2))_{F-m-1} (\tilde{R}_{D1}^G)_{m+1} \right] (B_m + A_{m+1}) \right] \\ + \sqrt{\Delta\zeta} \left[(F''''(\eta_1))_0 (\tilde{R}_{D1}^F)_F + (G''''(\eta_2))_0 (\tilde{R}_{D1}^G)_F \right] B_{F-1} \quad (4.33)$$

where $\tilde{v}_1(t)$ is given by Eqs. 4.31 for $tC_2/\pi \leq 1$ and by Eqs. 3.14 for $tC_2/\pi \geq 2$.

$$\tilde{v}_1(t) = -\frac{\tau}{\pi} \left[\sin \varphi_1 - \frac{1}{3} \sin 3\varphi_1 \right], \quad \text{or } \tilde{v}_1(t) = 0. \quad (4.34)$$

The results of the solution of the above equations for the hoop stress and the corresponding equations for the case $n = 2$ are shown in Fig. 4.4 for

$\bar{\nu} = 0$ and $\bar{\nu} = 1/3$. The mode, $n = 0$, does not contribute to the hoop stress at the boundary in an incident shear wave.

4.3 Equations for Stress in the Medium

Consider the stress field at some point away from the boundary but behind the incident wave front. The stress at this point consists only of the incident stress if the reflected wave has not reached the point, and the combination of the reflected and incident stresses if the reflected wave has reached the point. In Section 4.1 the equations found in Section 3.1 and 3.3 for an incident wave of dilatation were applied at the boundary in order to find the functions $F^{n+2}(\eta_1)$ and $G^{n+2}(\eta_2)$. Each of these is a function of a single argument given by Eqs. 4.3. These arguments are in turn functions of r and t . In order to find $F^{n+2}(\eta_1)$ and $G^{n+2}(\eta_2)$, a particular value of r , $r = a$, was taken where the stresses were known. Once these functions have been determined, any value of r may be considered in the arguments, and the variation with t can be directly computed.

For convenience the case $n = 1$ will again be considered to illustrate the method of computation. The general expressions for stress due to the diverging wave given by Eqs. 4.6 through 4.8 may be used to compute the stress at any point in the medium with the upper limit given by Eq. 4.5. This upper limit is inconvenient, however, because it leads to values of η_1 and η_2 less than $-a/C_1$ and $-a/C_2$, respectively, in the range of integration. These values represent time for which the reflected waves have not reached the radius in question. It is more convenient to use the upper limit which corresponds to the first value of $F'''(\eta_1)$ and $G'''(\eta_2)$ which is not zero. These limits may be obtained from the arguments η_1 and η_2 . Consider first the integrals involving $F'''(\eta_1)$ when a new variable \bar{t}_1 is introduced

$$\bar{t}_1 = t - \frac{(r-a)}{C_1} \quad 4.30$$

Then \bar{t}_1 is the time elapsed after the reflected wave reached the radius r , and t is the total time elapsed. Solving for t

$$t = \bar{t}_1 + \frac{r}{c_1} - \frac{a}{c_1}.$$

Substitute this into the first of Eqs. 4.3,

$$\eta_1 = \bar{t}_1 - \frac{a}{c_1} - \frac{r}{c_1} \xi. \quad 4.36$$

The upper limit on ξ , ξ_1 , must be chosen so that η_1 becomes $-a/c_1$. Then

$$\bar{t}_1 = \frac{r}{c_1} \xi_1, \quad \xi_1 = \frac{\bar{t}_1 c_1}{r}. \quad 4.37$$

The variable of integration ξ , then, has the upper and lower limits

$$0 \leq \xi \leq \xi_1 = \frac{\bar{t}_1 c_1}{r}.$$

In the same way, the limits on the integrals involving $G'''(\eta_2)$ may be found from η_2 . The time variable \bar{t}_2 may be defined as

$$\bar{t}_2 = t - \frac{r-a}{c_2} \quad 4.38$$

$$\text{or} \quad t = \bar{t}_2 + \frac{r}{c_2} - \frac{a}{c_2}.$$

Substituting this into the second of Eqs. 4.3 and recalling that ξ becomes $\alpha\xi$ in these integrals, one obtains

$$\eta_2 = \bar{t}_2 - \frac{a}{c_2} - \frac{r}{c_2} \alpha\xi. \quad 4.39$$

The upper limit on ξ becomes

$$\begin{aligned} \bar{t}_2 &= \frac{r}{c_2} \alpha\xi_2 \\ \xi_2 &= \frac{\bar{t}_2 c_2}{\alpha r} = \frac{\bar{t}_2 c_1}{r} \end{aligned} \quad 4.40$$

and ξ varies in the interval

$$0 \leq \xi \leq \xi_2 = \frac{\bar{t}_2 C_1}{r}.$$

In the machine computations, where discrete time steps are used, the total time is given as before by $t = p\Delta t$. Also the radius may be written

$$r = a + n\Delta t C_1.$$

From Eqs. 4.37 and 4.38

$$\begin{aligned}\bar{t}_1 &= (p-n)\Delta t \\ \bar{t}_2 &= (p-n/\alpha)\Delta t.\end{aligned}$$

In general the variable ξ may be written

$$\xi = \frac{\tau C_1}{r} \quad 4.41$$

where τ varies from zero to \bar{t}_1 or \bar{t}_2 and may be expressed in general as $\tau = m\Delta t$.

Using the above substitutions, Eqs. 4.36 and 4.39 become

$$\begin{aligned}\eta_1 &= (p-n)\Delta t - a/C_1 - m\Delta t \\ \eta_2 &= (p-n/\alpha)\Delta t - a/C_2 - m\Delta t\end{aligned}$$

where

$$0 \leq m \leq (p-n)$$

in the equation for η_1 and

$$0 \leq m \leq (p-n/\alpha)$$

in the equation for η_2 .

From Eqs. 4.37 and 4.40 the upper limits on the $F'''(\eta_1)$ and $G'''(\eta_2)$ integrals may be written

$$\xi_1 = \frac{(p-n)\Delta t C_1}{a+n\Delta t C_1}, \quad \xi_2 = \frac{(p-n/\alpha)\Delta t C_1}{a+n\Delta t C_1}. \quad 4.42$$

Since ξ varies with radius, the quantities R_{A1}^F , R_{A1}^G , R_{B1}^F , R_{B1}^G , R_{D1}^F , and R_{D1}^G must be recomputed at each radius using Eqs. 4.10 and 4.12. Once the new

values of R have been computed for a particular radius, the equations for stress in the summation form given by Eqs. 4.13 through 4.15 may be used with the appropriate limits.

If the above computational procedure is adopted and if the same steps in time, Δt , that were used at the boundary are chosen, the set of values of the argument of $F'''(\eta_1)$ used in the computations is the same set as were used when the original computations were carried out at the boundary. Therefore, the limits of integration fall on known values of $F'''(\eta_1)$. This is not the case with $G'''(\eta_2)$, however, since the upper limit on m , as shown above, is $p\pi/\alpha$. Then if m is allowed to vary as $m = 0, 1, 2, \dots$ none of the values of η_2 will be the same as at the boundary (see expression for η_2 above). It is simpler to perform the integrations to known values of η_2 (the same values that were used to find the function at the boundary) realizing that these integrals involving $G'''(\eta_2)$, $H_2(r, t)$, do not correspond to the same times as the integrals involving $F'''(\eta_1)$, $H_1(r, t)$. After the integrations are performed and the integrals are to be combined in order to obtain the stress, $H_2(r, t)$ must be shifted in time so that values of $H_1(r, t)$ and $H_2(r, t)$ corresponding to the same total time are combined. This shift will in general involve interpolation in $H_2(r, t)$. A parabolic interpolation was used for this purpose.

The general expressions for stress due to the incident wave given by Eqs. 4.23 and 4.24 are valid at any radius except that θ_1 must be redefined ($\bar{\theta}_1$). From Fig. 4.3

$$C_1 t = a - r \cos \bar{\theta}_1$$

$$\bar{\theta}_1 = \cos^{-1} \left(\frac{a - tC_1}{r} \right)$$

or for machine use

$$\bar{\theta}_1 = \cos^{-1} \left(\frac{a - p\Delta t C_1}{a + n\Delta t C_1} \right) . \quad 4.43$$

Considering the changes in $\bar{\theta}_1$ and in the integration limits, one has the same basic equations for stress in the medium as were used at the boundary. The total stress is the sum of the stress in the diverging wave given by Eqs. 4.13, 4.14, and 4.15 plus the corresponding stress in the incident wave given by Eqs. 4.23 or 4.24.

$$\begin{aligned}
 \sigma_{rr} = & \left\{ (a_1(t))_{p-n} + \sum_{m=0}^{p-n-1} \sqrt{\Delta \xi} \left[(F''''(\eta_1))_{p-m} (R_{A1}^F)_{m,m} A_m + (F''''(\eta_1))_{p-m-1} (R_{A1}^F)_{m+1,m} B_m \right] \right. \\
 & \left. + \sum_{m=0}^{p-n/\alpha-1} \sqrt{\Delta \xi} \left[(G''''(\eta_2))_{p-m} (R_{A1}^G)_{m,m} A_m + (G''''(\eta_2))_{p-m-1} (R_{A1}^G)_{m+1,m} B_m \right] \right\} \cos \theta \\
 \sigma_{r\theta} = & \left\{ (b_1(t))_{p-n} + \sum_{m=0}^{p-n-1} \sqrt{\Delta \xi} \left[(F''''(\eta_1))_{p-m} (R_{B1}^F)_{m,m} A_m + (F''''(\eta_1))_{p-m-1} (R_{B1}^F)_{m+1,m} B_m \right] \right. \\
 & \left. + \sum_{m=0}^{p-n/\alpha-1} \sqrt{\Delta \xi} \left[(G''''(\eta_2))_{p-m} (R_{B1}^G)_{m,m} A_m + (G''''(\eta_2))_{p-m-1} (R_{B1}^G)_{m+1,m} B_m \right] \right\} \sin \theta \\
 \sigma_{\theta\theta} = & \left\{ (c_1(t))_{p-n} + \sum_{m=0}^{p-n-1} \sqrt{\Delta \xi} \left[(F''''(\eta_1))_{p-m} (R_{D1}^F)_{m,m} A_m + (F''''(\eta_1))_{p-m-1} (R_{D1}^F)_{m+1,m} B_m \right] \right. \\
 & \left. + \sum_{m=0}^{p-n/\alpha-1} \sqrt{\Delta \xi} \left[(G''''(\eta_2))_{p-m} (R_{D1}^G)_{m,m} A_m + (G''''(\eta_2))_{p-m-1} (R_{D1}^G)_{m+1,m} B_m \right] \right\} \cos \theta .
 \end{aligned}$$

4.44

V. DERIVATION OF THE SHORT TIME SOLUTION

5.1 Short-Time Solution for Hoop Stress at the Boundary

The short-time solution to be described is useful for several reasons: (1) it serves as a check on the machine solution of the problem for a short time after the plane wave reaches the opening; (2) it provides the initial values of the function $F^{n+2}(\eta_1)$ and $G^{n+2}(\eta_2)$; and (3) it determines the analytic character of the solution at short times, and gave insights useful in developing the integration process. The functions $F^{n+2}(\eta_1)$ and $G^{n+2}(\eta_2)$ which were obtained in Chapter IV by numerical integration are now found by a different technique, using the same basic integral equations. Therefore the method does not check the derivation of these equations; it checks only the solution of the equations for short time.

The same boundary equations given by Eqs. 3.41 for the case of an incident wave of dilatation are again used. The functions $F^{n+2}(\eta_1)$ and $G^{n+2}(\eta_2)$ are expanded in Taylor series (with unknown coefficients) about the initial values of η_1 and η_2 . Then the integrand of each integral as well as the incident stresses are expanded in Taylor series and the integrations performed. By satisfying the boundary equations for each power of t it is possible to evaluate the unknown coefficients in the series for $F^{n+2}(\eta_1)$ and $G^{n+2}(\eta_2)$ successively. Once the series for $F^{n+2}(\eta_1)$ and $G^{n+2}(\eta_2)$ are known, these functions may be used to find the hoop stress at the boundary or the stresses in the medium.

Consider Eqs. 4.6, 4.7 and 4.8 in which the stresses in the diverging wave are written in terms of ξ in a form suitable for combination with an incident wave of dilatation for the case $n = 1$.

If the value of stress is required at some time, t , then the limits of integration of the $F'''(\eta_1)$ and $G'''(\eta_2)$ terms extend from

$$0 \leq \xi \leq \bar{\xi} \quad \text{where} \quad \bar{\xi} = tC_1/a. \quad 5.1$$

However, ξ may be made to vary from zero to its upper limit by letting

$$\xi = \beta \bar{\xi}, \quad 0 \leq \beta \leq 1. \quad 5.2$$

Then $\bar{\xi}$ is a constant and the variable of integration becomes β with the limits zero to one. In order to expand the function $F'''(\eta_1)$ in a Taylor series, consider the argument η_1 (Eq. 4.3),

$$\eta_1 = t - \frac{a}{C_1} (1 + \xi) = t - \frac{a}{C_1} - \frac{a}{C_1} \xi.$$

The variable ξ goes from zero to the value which causes η_1 to become $-a/C_1$. Then the limit of ξ is

$$\frac{a}{C_1} \bar{\xi} = t \quad \text{or} \quad \bar{\xi} = \frac{tC_1}{a}.$$

Using Eq. 5.2

$$\eta_1 = \frac{a}{C_1} \bar{\xi}(1-\beta) - \frac{a}{C_1}.$$

Then $F'''(\eta_1)$ may be expanded about $-a/C_1$ in powers of $\frac{a}{C_1} \bar{\xi}(1-\beta)$. In a similar manner the argument η_2 is

$$\eta_2 = t - \frac{a}{C_2} (1 + \xi) = t - \frac{a}{C_2} - \frac{a}{C_2} \xi$$

and $t = (a/C_2) x \bar{\xi}$. Then the argument η_2 may be written

$$\eta_2 = \frac{a}{C_2} \bar{\xi}(1-\beta) - a/C_2,$$

and $G'''(\eta_2)$ may also be expanded in powers of $\frac{a}{C_2} \bar{\xi}(1-\beta)$, but now about $-a/C_2$.

$$F''(\xi_1) = \frac{1}{\xi_1^2} \left[\frac{1}{\xi_1} - \frac{1}{\xi_1^2} \bar{F}(1-\beta) + \frac{1}{\xi_1^3} \left[\frac{\mu}{\xi_1} \bar{F}(1-\beta) \right]^2 + \dots \right] \quad 5.3$$

$$G''(\xi_1) = \frac{1}{\xi_1^2} \left[\frac{1}{\xi_1} - \frac{1}{\xi_1^2} \bar{F}(1-\beta) + \frac{1}{\xi_1^3} \left[\frac{\mu}{\xi_1} \bar{F}(1-\beta) \right]^2 + \dots \right] \quad 5.4$$

In other words the integrands of Eqs. 4.6 through 4.8 may be expressed in series for $\xi_1 \rightarrow 0$, using the binomial expansion for the square root terms and the series for \bar{F} and \bar{G} in Eq. (4.5). For the case $\bar{v} = 1/3$ ($\mu = 1/4$, $\nu = \alpha$) these terms may be written as follows:

$$\begin{aligned} \frac{(1+\alpha\mu)+(1+\alpha\mu)\xi_1+\mu\xi_1^2+\alpha\mu\xi_1^3}{\sqrt{1\xi_1}\sqrt{1-\xi_1}} &= \frac{\mu}{\xi_1^2\sqrt{1\xi_1}} \left[3 + \frac{2\alpha}{3}\xi_1 + \frac{4\alpha^2}{3^2}\xi_1^2 + \frac{13\alpha^3}{128}\xi_1^3 + \dots \right] \\ \frac{4\alpha\xi_1(1+\alpha\xi_1)(1+\alpha\xi_1/c)^{-1/2}}{\sqrt{2\alpha\xi_1}\sqrt{1-\xi_1^2}} &= \frac{\mu}{\alpha^2\xi_1^2\sqrt{2\alpha\xi_1}} \left[\alpha\xi_1^2 + \alpha^2\xi_1^3 + \frac{7}{8}\alpha^3\xi_1^3 + \dots \right] \\ \frac{1-\xi_1(1-\xi_1)(1-\xi_1/c)^{-1/2}}{\sqrt{1\xi_1}\sqrt{1-\xi_1^2}} &= \frac{1}{\xi_1^2\sqrt{1\xi_1}} \left[1 + \frac{1}{2}\xi_1 + \frac{1}{8}\xi_1^2 + \dots \right] \\ \frac{1(1+\alpha\xi_1+\alpha\xi_1^2+\alpha^2\xi_1^3)}{\sqrt{2\alpha\xi_1}\sqrt{1+\xi_1^2}} &= \frac{\mu}{\alpha^2\xi_1^2\sqrt{2\alpha\xi_1}} \left[1 + \frac{2\alpha}{3}\xi_1 + \frac{1\alpha^2}{3^2}\xi_1^2 + \frac{11\alpha^3}{128}\xi_1^3 + \dots \right] \\ \frac{1(1-\xi_1)+\alpha\mu\xi_1(1+\xi_1/c)^{-1/2}}{\sqrt{1\xi_1}\sqrt{1-\xi_1^2}} &= \frac{\mu}{\xi_1^2\sqrt{1\xi_1}} \left[1 + \frac{1}{2}\xi_1 + \frac{1\alpha}{3^2}\xi_1^2 + \frac{13\alpha^3}{128}\xi_1^3 + \dots \right] \\ \frac{1-\alpha\xi_1(1+\alpha\xi_1)(1+\alpha\xi_1/c)^{-1/2}}{\sqrt{1\xi_1}\sqrt{1-\xi_1^2}} &= \frac{1}{\xi_1^2\sqrt{1\xi_1}} \left[1 - \alpha\xi_1^2 + \alpha^2\xi_1^3 - \alpha^3\xi_1^3 + \dots \right] \end{aligned} \quad 5.5$$

Substituting Eqs. 5.3 through 5.5 into

4.7 and 4.8 and making the substitution $\xi_1 = \beta\bar{\xi}_1$, one obtains the following expressions for stress due to the diverging wave:

$$\begin{aligned}
\sigma_{rr} = & -\frac{\mu\sqrt{\xi}}{c_1^3} \int_0^1 \frac{1}{\sqrt{2\beta}} \left[F'''' \left(-\frac{a}{c_1} \right) \left(3 + \frac{25}{4} \beta \bar{\xi} + \frac{145}{32} \beta^2 \bar{\xi}^2 + \frac{133}{128} \beta^3 \bar{\xi}^3 + \dots \right) \right. \\
& + A_1 \frac{a}{c_1} \left(3 \bar{\xi} (1-\beta) + \frac{25}{4} \beta \bar{\xi}^2 (1-\beta) + \frac{145}{32} \beta^2 \bar{\xi}^3 (1-\beta) + \dots \right) \\
& + A_2 \left(\frac{a}{c_1} \right)^2 \left(3 \bar{\xi}^2 (1-\beta)^2 + \frac{25}{4} \beta \bar{\xi}^3 (1-\beta)^2 + \dots \right) + A_3 \left(\frac{a}{c_1} \right)^3 \left(3 \bar{\xi}^3 (1-\beta)^3 + \dots \right) \left. \right] d\beta \\
& + \frac{\mu\sqrt{\xi}}{\alpha^2 c_1^3 \sqrt{\alpha}} \int_0^1 \frac{1}{\sqrt{2\beta}} \left[G'''' \left(-\frac{a}{c_2} \right) \left(4 \bar{\xi} \beta + 5 \alpha \beta^2 \bar{\xi}^2 + \frac{7}{8} \alpha^2 \beta^3 \bar{\xi}^3 + \dots \right) \right. \\
& + B_1 \frac{a}{c_1} \left(4 \beta \bar{\xi}^2 (1-\beta) + 5 \alpha \beta^2 \bar{\xi}^3 (1-\beta) + \dots \right) + B_2 \left(\frac{a}{c_1} \right)^2 \left(\bar{\xi}^2 (1-\beta)^2 \right. \\
& \left. \left. + \frac{19}{4} \alpha \bar{\xi}^3 \beta (1-\beta)^2 + \dots \right) + B_3 \left(\frac{a}{c_1} \right)^3 \left(\bar{\xi}^3 (1-\beta)^3 + \dots \right) \right] d\beta
\end{aligned} \tag{5.6}$$

$$\begin{aligned}
\sigma_{r\theta} = & -\frac{\sqrt{\xi}}{c_1^3} \int_0^1 \frac{1}{\sqrt{2\beta}} \left[F'''' \left(-\frac{a}{c_1} \right) \left(4 \beta \bar{\xi} + 5 \beta^2 \bar{\xi}^2 + \frac{7}{8} \beta^3 \bar{\xi}^3 + \dots \right) \right. \\
& + A_1 \frac{a}{c_1} \left(4 \beta \bar{\xi}^2 (1-\beta) + 5 \beta^2 \bar{\xi}^3 (1-\beta) + \dots \right) + A_2 \left(\frac{a}{c_1} \right)^2 \left(4 \beta \bar{\xi}^3 (1-\beta)^2 + \dots \right) \left. \right] d\beta \\
& + \frac{\mu\sqrt{\xi}}{\alpha^2 \sqrt{\alpha} c_1^3} \int_0^1 \frac{1}{\sqrt{2\beta}} \left[G'''' \left(-\frac{a}{c_2} \right) \left(1 + \frac{19}{4} \alpha \beta \bar{\xi} + \frac{155}{32} \alpha^2 \beta^2 \bar{\xi}^2 + \frac{114}{128} \alpha^3 \beta^3 \bar{\xi}^3 + \dots \right) \right. \\
& + B_1 \frac{a}{c_1} \left(\bar{\xi} (1-\beta) + \frac{19}{4} \alpha \beta \bar{\xi}^2 (1-\beta) + \frac{155}{32} \alpha^2 \beta^2 \bar{\xi}^3 (1-\beta) + \dots \right) \\
& + B_2 \left(\frac{a}{c_1} \right)^2 \left(\bar{\xi}^2 (1-\beta)^2 + \frac{19}{4} \alpha \beta \bar{\xi}^3 (1-\beta)^2 + \dots \right) + B_3 \left(\frac{a}{c_1} \right)^3 \left(\bar{\xi}^3 (1-\beta)^3 + \dots \right) \left. \right] d\beta
\end{aligned} \tag{5.7}$$

$$\begin{aligned}
\sigma_{\theta\theta} = & -\frac{\mu\sqrt{\xi}}{c_1^3} \int_0^1 \frac{1}{\sqrt{2\beta}} \left[F'''' \left(-\frac{a}{c_1} \right) \left(3 + \frac{25}{4} \beta \bar{\xi} + \frac{145}{32} \beta^2 \bar{\xi}^2 + \frac{105}{128} \beta^3 \bar{\xi}^3 + \dots \right) \right. \\
& + A_1 \frac{a}{c_1} \left(3 \bar{\xi} (1-\beta) + \frac{25}{4} \beta \bar{\xi}^2 (1-\beta) + \frac{145}{32} \beta^2 \bar{\xi}^3 (1-\beta) + \dots \right) \\
& + A_2 \left(\frac{a}{c_1} \right)^2 \left(3 \bar{\xi}^2 (1-\beta)^2 + \frac{25}{4} \beta \bar{\xi}^3 (1-\beta)^2 + \dots \right) + A_3 \left(\frac{a}{c_1} \right)^3 \left(3 \bar{\xi}^3 (1-\beta)^3 + \dots \right) \left. \right] d\beta \\
& - \frac{\mu\sqrt{\xi}}{\alpha^2 \sqrt{\alpha} c_1^3} \int_0^1 \frac{1}{\sqrt{2\beta}} \left[G'''' \left(-\frac{a}{c_2} \right) \left(4 \alpha \beta \bar{\xi} + 5 \alpha^2 \beta^2 \bar{\xi}^2 + \frac{7}{8} \alpha^3 \beta^3 \bar{\xi}^3 + \dots \right) \right. \\
& + B_1 \frac{a}{c_1} \left(4 \alpha \beta \bar{\xi}^2 (1-\beta) + 5 \alpha^2 \beta^2 \bar{\xi}^3 (1-\beta) + \dots \right) + B_2 \left(\frac{a}{c_1} \right)^2 \left(4 \alpha \beta \bar{\xi}^3 (1-\beta)^2 + \dots \right) \left. \right] d\beta
\end{aligned} \tag{5.8}$$

the series for σ_{rr} and $\sigma_{\theta\theta}$ are obtained by a suitable grouping of terms results in:

$$\begin{aligned} \sigma_{rr} = & \frac{A\sqrt{\bar{\xi}}}{\sqrt{1-\bar{\xi}}^2} \left[G^{(1)} \left(-\frac{4}{C_2} \right) \left(-\frac{1}{C_1} \bar{\xi} + \frac{1}{C_1} \bar{\xi} + \frac{1}{C_1} \bar{\xi}^2 + \frac{1}{C_1} \bar{\xi}^3 + \dots \right) \right. \\ & + A_1 \left(\frac{2}{C_1} \right) \left(\bar{\xi} + \frac{1}{C_1} \bar{\xi} + \frac{1}{C_1} \bar{\xi}^2 + \dots \right) + A_2 \left(\frac{2}{C_1} \right)^2 \left(\frac{16}{15} \bar{\xi}^2 + \frac{20}{21} \bar{\xi}^3 + \dots \right) \\ & + A_3 \left(\frac{2}{C_1} \right)^3 \left(\frac{1}{2} \bar{\xi}^2 + \dots \right) \left. \right] + \frac{A\sqrt{\bar{\xi}}}{\sqrt{1-\bar{\xi}}^2} \left[G^{(1)} \left(-\frac{4}{C_2} \right) \left(\frac{2}{C_2} \bar{\xi} + 2\alpha\bar{\xi}^2 + \frac{1}{4}\alpha^2\bar{\xi}^3 + \dots \right) \right. \\ & \left. + B_1 \left(\frac{2}{C_1} \right) \left(\frac{16}{15} \bar{\xi}^2 + \frac{2}{3}\alpha\bar{\xi}^3 + \dots \right) + B_2 \left(\frac{2}{C_1} \right)^2 \left(\frac{64}{105} \bar{\xi}^3 + \dots \right) \right] \quad 5.9 \end{aligned}$$

$$\begin{aligned} \sigma_{\theta\theta} = & \frac{A\sqrt{\bar{\xi}}}{\sqrt{1-\bar{\xi}}^2} \left[G^{(1)} \left(-\frac{4}{C_2} \right) \left(-\bar{\xi} + \frac{1}{C_1} \bar{\xi} + \frac{1}{C_1} \bar{\xi} + \frac{1}{C_1} \bar{\xi}^2 + \dots \right) + A_1 \left(\frac{2}{C_1} \right) \left(\frac{16}{15} \bar{\xi}^2 + \frac{4}{7} \bar{\xi}^3 + \dots \right) \right. \\ & \left. + A_2 \left(\frac{2}{C_1} \right)^2 \left(\frac{16}{15} \bar{\xi}^3 + \dots \right) \right] + \frac{A\sqrt{\bar{\xi}}}{\sqrt{1-\bar{\xi}}^2} \left[G^{(1)} \left(-\frac{4}{C_2} \right) \left(2 + \frac{19}{6} \alpha\bar{\xi} + \frac{31}{16} \alpha^2\bar{\xi}^2 \right. \right. \\ & \left. \left. + \frac{1}{12} \alpha^3\bar{\xi}^3 + \dots \right) + B_1 \left(\frac{2}{C_1} \right) \left(\frac{2}{3} \bar{\xi} + \frac{1}{C_1} \alpha\bar{\xi} + \frac{1}{C_1} \alpha^2\bar{\xi}^2 + \dots \right) \right. \\ & \left. + B_2 \left(\frac{2}{C_1} \right)^2 \left(\frac{16}{15} \bar{\xi}^2 + \frac{2}{3} \alpha\bar{\xi}^3 + \dots \right) + B_3 \left(\frac{2}{C_1} \right)^3 \left(\frac{64}{105} \bar{\xi}^3 + \dots \right) \right] \quad 5.10 \end{aligned}$$

$$\begin{aligned} \sigma_{\phi\phi} = & \frac{A\sqrt{\bar{\xi}}}{\sqrt{1-\bar{\xi}}^2} \left[G^{(1)} \left(-\frac{4}{C_2} \right) \left(-\frac{1}{C_1} \bar{\xi} + \frac{1}{C_1} \bar{\xi} + \frac{1}{C_1} \bar{\xi} + \frac{1}{C_1} \bar{\xi}^2 + \dots \right) \right. \\ & + A_1 \left(\frac{2}{C_1} \right) \left(-\frac{1}{C_1} \bar{\xi} + \frac{1}{C_1} \bar{\xi} + \frac{1}{C_1} \bar{\xi}^2 + \dots \right) + A_2 \left(\frac{2}{C_1} \right)^2 \left(-\frac{16}{15} \bar{\xi}^2 + \frac{62}{105} \bar{\xi}^3 + \dots \right) \\ & + A_3 \left(\frac{2}{C_1} \right)^3 \left(\frac{1}{2} \bar{\xi}^2 + \dots \right) \left. \right] + \frac{A\sqrt{\bar{\xi}}}{\sqrt{1-\bar{\xi}}^2} \left[G^{(1)} \left(-\frac{4}{C_2} \right) \left(\frac{2}{C_2} \alpha\bar{\xi} + \alpha^2\bar{\xi}^2 \right. \right. \\ & \left. \left. + \frac{1}{4} \alpha^3\bar{\xi}^3 + \dots \right) + B_1 \left(\frac{2}{C_1} \right) \left(\frac{1}{C_1} \alpha\bar{\xi} + \frac{1}{C_1} \alpha^2\bar{\xi}^2 + \frac{1}{C_1} \alpha^3\bar{\xi}^3 + \dots \right) \right. \\ & \left. + B_2 \left(\frac{2}{C_1} \right)^2 \left(\frac{16}{105} \alpha\bar{\xi}^3 + \dots \right) \right] \quad 5.11 \end{aligned}$$

The stresses on the cylindrical boundary due to the incident wave may also be written in terms of powers of $\bar{\xi}$ by using the series form of the

trigonometric functions. For $n = 1$ the incident stresses are given by Eq. 4.23.

In series form these become

$$a_1(t) = -\frac{\sigma \sqrt{2\xi}}{3\pi} \left[6 - \frac{25}{6} \xi + \frac{29}{16} \xi^2 - \frac{19}{64} \xi^3 + \dots \right] \quad 5.12$$

$$b_1(t) = +\frac{\sigma \sqrt{2\xi}}{3\pi} \left[\frac{8}{3} \xi - 2\xi^2 + \frac{1}{4} \xi^3 + \dots \right] \quad 5.13$$

$$d_1(t) = -\frac{\sigma \sqrt{2\xi}}{3\pi} \left[2 + \frac{13}{6} \xi - \frac{33}{16} \xi^2 + \frac{15}{64} \xi^3 + \dots \right] \quad 5.14$$

In order to satisfy the conditions of a traction free boundary, the sum of corresponding boundary tractions for the incident and diverging waves must equal zero. The radial and shear stresses due to the $n = 1$ terms of the diverging wave are given by Eqs. 5.9 and 5.10, respectively. These stresses are given by Eqs. 5.12 and 5.13 for the incident wave. A series for the total radial stress at the boundary results from the sum of Eqs. 5.9 and 5.12. A similar series for shear stress at the boundary results from the sum of Eqs. 5.10 and 5.13. If these boundary stresses are to equal zero, each term of the series must equal zero. In this way the unknown constants in Eqs. 5.9 and 5.10 may be evaluated successively, resulting in the following:

$$\begin{aligned} F'''(-\frac{a}{C_1}) &= \frac{-2}{3\pi} \frac{C_1^3}{\mu} \sigma & G'''(-\frac{a}{C_2}) &= 0 \\ A_1 &= +0.4421 \frac{C_1^4}{\mu a} \sigma & B_1 &= -0.2150 \frac{C_1^4}{\mu a} \sigma \\ A_2 &= -0.3936 \frac{C_1^5}{\mu a^2} \sigma & B_2 &= +0.2594 \frac{C_1^5}{\mu a^2} \sigma \\ A_3 &= +0.1716 \frac{C_1^6}{\mu a^3} \sigma & B_3 &= -0.3989 \frac{C_1^6}{\mu a^3} \sigma \end{aligned}$$

By substituting these quantities into Eqs. 5.3 and 5.4, one obtains expressions for $F'''(\eta_1)$ and $G'''(\eta_2)$.

$$\begin{aligned}
 F''(r_1) &= \frac{c^3}{\mu} \sigma \left[-0.2122 + 0.4421\bar{\xi} - 0.3936\bar{\xi}^2 + 0.1716\bar{\xi}^3 + \dots \right] \\
 G''(r_2) &= \frac{c^3}{\mu} \sigma \left[-0.2150\bar{\xi} + 0.2994\bar{\xi}^2 - 0.3989\bar{\xi}^3 + \dots \right]
 \end{aligned}
 \tag{5.15}$$

Finally, a power series for the hoop stress in the diverging wave is found by substituting the above constants into Eq. 5.11. The total stress at any point is the sum of the incident and diverging stresses, that is the sum of Eqs. 5.11 and 5.14.

$$\sigma_{\theta\theta} = \sigma \sqrt{\bar{\xi}} \left[-1.0670\bar{\xi} + 0.9374\bar{\xi}^2 - 0.2754\bar{\xi}^3 + \dots \right]
 \tag{5.16}$$

The procedure outlined above for $n = 1$ may be applied for other values of n in the same manner except for certain simplifications when $n = 0$. The expressions for the modewise hoop stresses for other values of n are

for $n = 0$

$$\sigma_{\theta\theta} = \sigma \sqrt{\bar{\xi}} \left[-0.5335\bar{\xi} + 0.1160\bar{\xi}^2 + 0.001641\bar{\xi}^3 + \dots \right]
 \tag{5.17}$$

for $n = 2$

$$\sigma_{\theta\theta} = \sigma \sqrt{\bar{\xi}} \left[-1.0670\bar{\xi} + 3.0962\bar{\xi}^2 - 2.1392\bar{\xi}^3 + \dots \right]
 \tag{5.18}$$

for $n = 3$

$$\sigma_{\theta\theta} = \sigma \sqrt{\bar{\xi}} \left[-1.0670\bar{\xi} + 6.9574\bar{\xi}^2 - 9.6148\bar{\xi}^3 + \dots \right]
 \tag{5.19}$$

for $n = 4$

$$\sigma_{\theta\theta} = \sigma \sqrt{\bar{\xi}} \left[-1.0670\bar{\xi} + 15.2681\bar{\xi}^2 - 34.7894\bar{\xi}^3 + \dots \right]
 \tag{5.20}$$

In Fig. 5.1 the results of the short time solution given by each of Eqs. 5.16 through 5.20 for the first five modes are plotted along with the first three modes as obtained in the computer solution. In the short time solution all

terms in $\bar{\xi}$ out to $\bar{\xi}^{7/2}$ were carried in the computations. From these curves it may be seen that a larger number of terms of the series must be used for higher than for lower values of n to obtain comparable accuracy.

From the shape of $F'''(\eta_1)$ as shown in Fig. 4.1 agreement would not be expected beyond one time of transit in view of the singularity at $\bar{\xi} = 2$. On Fig. 5.1 the sum of the first three modes for $\sigma_{\theta\theta}$ as computed in the machine is compared with the sum of the first three and the first five terms as computed by the short time method. Also shown on Fig. 5.1 is the first three modes of the outgoing wave combined with the exact representation for the incident stresses. These stresses correspond to an angle around the opening of $\theta = 0^\circ$, $\cos n\theta = 1.0$.

The procedure just described is quite similar in the case of an incident shear wave. The mode $n = 0$ does not produce a hoop stress. This may be shown by observing that the first of Eqs. 3.13 for $\tilde{b}_n(t)$ is always zero for $n = 0$. By placing this result into the first of the boundary equations (Eq. 3.42), one observes that $F''(\eta_1)$ is always zero for this case. Then the hoop stress in the outgoing wave given by the last of Eqs. 3.39 is always zero since $F''(\eta_1) = 0$ in the first integral and $\sinh nu = 0$ in the second. The dimensionless time, $\bar{\xi}$, used in the incident shear computations is equal to tC_2/a rather than tC_1/a as used in the case of an incident wave of dilatation. The series form of the hoop stress in the diverging wave only, has been computed for $n = 1$ and 2. These stresses are,

For $n = 1$

$$\sigma_{\theta\theta} = \sigma \frac{\sqrt{\bar{\xi}}}{\sqrt{2}} \left[-2.8294\bar{\xi} + 4.5799\bar{\xi}^2 - 1.0197\bar{\xi}^3 + \dots \right] \quad 5.21$$

For $n = 2$

$$\sigma_{\theta\theta} = \sigma \frac{\sqrt{\bar{\xi}}}{\sqrt{2}} \left[-5.6588\bar{\xi} + 13.6325\bar{\xi}^2 - 18.4427\bar{\xi}^3 + \dots \right] \quad 5.22$$

The results of Eqs. 5.21 and 5.22 are shown in Fig. 5.2 with the corresponding results of the computer solution.

5.3 Short Time Solution for Stresses in the Medium

In Section 4.3 the method of computation used in the computer solution for stresses away from the boundary was discussed for the case $n = 1$. The short time solution derived in Section 5.1 will now be extended to obtain the stresses in the medium. As an example of the computation procedure, the hoop stress away from the boundary in the diverging wave will be considered. The equation for this stress is given in general form by Eq. 3.35. By setting $n = 1$, substituting $1 + \zeta$ for $\cosh u$ as given by Eq. 4.2, and using the limits defined by Eqs. 4.1, one obtains the general expression for hoop stress

$$\begin{aligned} \sigma_{\theta\theta} = & \left[+ \frac{1}{c_1^3} \int_0^{\bar{\zeta}_1} F'''(\eta_1) \left[\frac{-\lambda - (\lambda - 4\mu)\zeta + 6\mu\zeta^2 + 2\mu\zeta^3}{\sqrt{2\zeta} \sqrt{1+\zeta/2}} \right] d\zeta \right. \\ & \left. - \frac{1}{c_2^3} \int_0^{\bar{\zeta}_2} G'''(\eta_2) \left[\frac{4\mu\zeta(1+\zeta)(1+\zeta/2)}{\sqrt{2\zeta} \sqrt{1+\zeta/2}} \right] d\zeta \right] \cos \theta \end{aligned} \quad 5.23$$

It is convenient in this case not to use the dimensionless time variable $\bar{\zeta}$ until the last step of the derivation.

It is apparent that Eqs. 4.3 may be written in the equivalent form

$$\eta_1 = t - \frac{r}{c_1} \left(1 + \frac{\tau c_1}{r} \right) \quad \text{and} \quad \eta_2 = t - \frac{r}{c_2} \left(1 + \frac{\tau c_2}{r} \right) \quad 5.24$$

where the dummy τ ranges from zero to t . First consider the argument η_1 . This argument may be written in the equivalent form

$$\eta_1 = \bar{t}_1 - \frac{a}{c_1} - \tau$$

where
$$\bar{t}_1 = t - \frac{r-a}{c_1} .$$

The time \bar{t}_1 represents the time after the reflected wave has reached the radius r , and τ varies from zero to \bar{t}_1 . This variation in τ may be accomplished by setting

$$\tau = \beta \bar{t}_1, \quad 0 \leq \beta \leq 1. \quad 5.25$$

By using this substitution, η_1 may be written

$$\eta_1 = \bar{t}_1(1-\beta) - a/C_1.$$

From this form of η_1 it is seen that $F'''(\eta_1)$ may be expanded about $-a/C_1$ in powers of $\bar{t}_1(1-\beta)$. Therefore, by using the coefficients given in the first of Eqs. 5.15, $F'''(\eta_1)$ may be written

$$F'''(\eta_1) = \frac{C_1^3}{\mu} \sigma \left[-0.2122 + 0.4421 \frac{C_1}{a} \bar{t}_1(1-\beta) - 0.3936 \frac{C_1^2}{a^2} \bar{t}_1^2 (1-\beta)^2 + 0.1716 \frac{C_1^3}{a^3} \bar{t}_1^3 (1-\beta)^3 + \dots \right] \quad 5.26$$

In the remaining factors of the integrals involving $F'''(\eta_1)$ the variable ζ may be written as follows using the substitution of Eq. 5.25

$$\zeta = \frac{\tau C_1}{r} = \frac{\beta \bar{t}_1 C_1}{r}.$$

In view of this substitution for ζ in the fifth series of Eqs. 5.5 and of Eq. 5.26, the first integral of Eq. 5.23, $\sigma_{\theta\theta}^F$, may be written in series form:

$$\begin{aligned} \sigma_{\theta\theta}^F = \sigma \int_0^1 \frac{C_1^3}{\mu} \left[-0.2122 + 0.4421 \frac{C_1}{a} \bar{t}_1(1-\beta) - 0.3936 \frac{C_1^2}{a^2} \bar{t}_1^2 (1-\beta)^2 + 0.1716 \frac{C_1^3}{a^3} \bar{t}_1^3 (1-\beta)^3 + \dots \right] \\ \left\{ \frac{\mu}{C_1^3} \sqrt{\frac{r}{2\beta \bar{t}_1 C_1}} \left[-1 + \frac{13}{4} \left(\frac{\beta \bar{t}_1 C_1}{r} \right) + \frac{165}{32} \left(\frac{\beta \bar{t}_1 C_1}{r} \right)^2 + \frac{105}{128} \left(\frac{\beta \bar{t}_1 C_1}{r} \right)^3 + \dots \right] \right\} \left(\frac{\bar{t}_1 C_1}{r} \right) d\beta. \end{aligned} \quad 5.27$$

This solution is restricted to the case $\bar{\nu} = 1/3$ since this value was used in the series expansions of Eqs. 5.5 and the computation of the coefficients used in Eq. 5.26.

In a similar manner the series expansion for $G'''(\eta_2)$ may be determined. From Eq. 5.24 the argument η_2 may be written

$$\eta_2 = \bar{t}_2 - \frac{a}{C_2} - \tau$$

where

$$\bar{t}_2 = t - \frac{r-a}{C_2}.$$

The time \bar{t}_2 represents the time after the reflected wave has reached the radius r , and τ varies from zero to \bar{t}_2 . This variation may be accomplished by setting

$$\tau = \beta \bar{t}_2, \quad 0 \leq \beta \leq 1. \quad 5.29$$

The argument η_2 becomes

$$\eta_2 = \bar{t}_2(1-\beta) - a/C_2$$

and the function $G'''(\eta_2)$ may be expanded about $-a/C_2$ in powers of $\bar{t}_2(1-\beta)$ by using the coefficients given by the second of Eqs. 5.15.

$$G'''(\eta_2) = \frac{\sigma C_1^3}{\mu} \left[-0.2150 \frac{C_1}{a} \bar{t}_2(1-\beta) + 0.2594 \frac{C_1^2}{a^2} \bar{t}_2^2 (1-\beta)^2 - 0.3989 \frac{C_1^3}{a^3} \bar{t}_2^3 (1-\beta)^3 + \dots \right]. \quad 5.30$$

The variable ζ in the integrals involving $G'''(\eta_2)$ of Eq. 5.23 may be written in the following form,

$$\zeta = \frac{\tau C_2}{r}.$$

By using Eq. 5.29 to vary τ from zero to \bar{t}_2 and, by letting $C_2 = \alpha C_1$, one may rewrite this expression

$$\zeta = \frac{\beta \bar{t}_2 \alpha c_1}{r} .$$

It follows from Eq. 5.30 and the above substitution for ζ in the sixth series of Eqs. 5.5 that the second integral, $\sigma_{\theta\theta}^G$, of Eq. 5.23 may be written in series form.

$$\begin{aligned} \sigma_{\theta\theta}^G = \sigma \int_0^1 \frac{c_1^3}{\mu} \left[-0.2150 \frac{c_1}{a} \bar{t}_2 (1-\beta) + 0.2594 \frac{c_1^2}{2} \bar{t}_2^2 (1-\beta)^2 \right. \\ \left. - 0.3989 \frac{c_1^3}{a} \bar{t}_2^3 (1-\beta)^3 + \dots \right] \left\{ \frac{\mu}{c_1^3} \alpha \sqrt{\frac{r}{2\alpha\beta\bar{t}_2 c_1}} \left[4 \left(\frac{\alpha\beta\bar{t}_2 c_1}{r} \right) \right. \right. \\ \left. \left. + 5 \left(\frac{\alpha\beta\bar{t}_2 c_1}{r} \right)^2 + \frac{7}{8} \left(\frac{\alpha\beta\bar{t}_2 c_1}{r} \right)^3 + \dots \right] \right\} \left(\frac{\bar{t}_2 \alpha c_1}{r} \right) d\beta \end{aligned} \quad 5.31$$

The following equations result from performing the integrations on the right sides of Eq. 5.27 and 5.31, for the case $\lambda = \mu$, $\nu = 1/4$, yielding $\alpha = \frac{1}{\sqrt{3}}$.

$$\begin{aligned} \sigma_{\theta\theta}^F = \sigma \sqrt{\frac{\bar{t}_1 c_1}{2r}} \left[+0.4244 - 0.5894 \bar{t}_1 \frac{c_1}{a} + 0.4199 \bar{t}_1^2 \frac{c_1^2}{a^2} \right. \\ - 0.1569 \bar{t}_1^3 \frac{c_1^3}{a^3} - 0.4598 \bar{t}_1 \frac{c_1}{r} + 0.3832 \bar{t}_1^2 \frac{c_1^2}{ar} \\ - 0.1949 \bar{t}_1^3 \frac{c_1^3}{a^2 r} - 0.4377 \bar{t}_1^2 \frac{c_1^2}{r^2} + 0.2605 \bar{t}_1^3 \frac{c_1^3}{ar^2} \\ \left. - 0.04974 \bar{t}_1^3 \frac{c_1^3}{r^3} + \dots \right] \end{aligned} \quad 5.32$$

$$\begin{aligned} \sigma_{\theta\theta}^G = \sigma \sqrt{\frac{\bar{t}_2 c_1}{r}} \left[-0.5227 \bar{t}_2^2 \frac{c_1^2}{ar} + 0.3604 \bar{t}_2^3 \frac{c_1^3}{a^2 r} \right. \\ \left. - 0.1617 \bar{t}_2^3 \frac{c_1^3}{ar^2} + \dots \right] . \end{aligned} \quad 5.33$$

The results obtained in Eqs. 5.32 and 5.33 may not be added directly. Equal

values of \bar{t}_1 and \bar{t}_2 correspond to different times t , \bar{t}_1 being the interval after the reflected dilatation wave has reached r and \bar{t}_2 being the interval after the shear wave has reached the radius r . For this reason the two parts of the hoop stress will be evaluated and compared with the machine solution separately. Equations 5.32 and 5.33 may be written in terms of the dimensionless times

$$\zeta_1 = \frac{\bar{t}_1 c_1}{a} \quad \text{and} \quad \zeta_2 = \frac{\bar{t}_2 c_1}{a}$$

as follows

$$\begin{aligned} \sigma_{\theta\theta}^F = \sigma \sqrt{\frac{\zeta_1 a}{2r}} \left[+ 0.4244 - 0.5894\zeta_1 + 0.4199\zeta_1^2 \right. \\ - 0.1569\zeta_1^3 - 0.4598\zeta_1 \frac{a}{r} + 0.3832\zeta_1^2 \frac{a}{r} - 0.1949\zeta_1^3 \frac{a}{r} \\ \left. - 0.4377\zeta_1^2 \frac{a^2}{r^2} + 0.2605\zeta_1^3 \frac{a^2}{r^2} - 0.04974\zeta_1^3 \frac{a^3}{r^3} + \dots \right] \end{aligned} \quad 5.34$$

$$\sigma_{\theta\theta}^G = \sigma \sqrt{\frac{\zeta_2 a}{2r}} \left[-0.5227\zeta_2^2 \frac{a}{r} + 0.3604\zeta_2^3 \frac{a}{r} - 0.1617\zeta_2^3 \frac{a^2}{r^2} + \dots \right]. \quad 5.35$$

In Fig. 5.3 the stresses given by Eqs. 5.34 and 5.35 are shown along with the corresponding results from the computer solution for a value of $\frac{r}{a} = 1.25$. It may be seen from these curves that the difference in the two solutions is quite small out to ζ_1 and $\zeta_2 = 0.6$.

VI. RESULTS AND INTERPRETATION

6.1 Incident Wave of Dilatation

The results of the computer solution for hoop stress at the boundary due to three terms of the Fourier series representation of an incident wave of dilatation are shown in Figs. 6.1 and 6.2. The most important information which follows from an examination of these curves is summarized in the following table.

\bar{v}	θ	Maximum Stress $\sigma_{\theta\theta}/\sigma$	Time of Max. Stress Transit Times	Static Value $\sigma_{\theta\theta}/\sigma$
0	0°	+1.29	4.8	+1.00
	90°	-3.33	3.3	-3.00
1/3	0°	+0.11	4.0	0
	90°	-2.93	3.7	-2.67

In Sections 5.1 and 5.2 a method was discussed which provides a check on the machine solution of the basic equations at short time. After several transit times have passed the stresses should approach the static values as given above. This provides not only another check on the solution of the basic equations but to some extent, on the formulation of the solution to the problem. The static stresses in the case of plane stress are given by the well known Kirsch formulas, which are shown as follows in Ref. (11):

$$\begin{aligned}
 \sigma_{rr} &= \frac{\sigma}{2} \left(1 - \frac{a^2}{r^2}\right) + \frac{\sigma}{2} \left(1 + \frac{3a^4}{r^4} - \frac{4a^2}{r^2}\right) \cos 2\theta \\
 \sigma_{\theta\theta} &= \frac{\sigma}{2} \left(1 + \frac{a^2}{r^2}\right) - \frac{\sigma}{2} \left(1 + \frac{3a^4}{r^4}\right) \cos 2\theta \\
 \sigma_{r\theta} &= -\frac{\sigma}{2} \left(1 - \frac{3a^4}{r^4} + \frac{2a^2}{r^2}\right) \sin 2\theta .
 \end{aligned}
 \tag{6.1}$$

These equations may be used to solve the plane strain problem by superimposing on the stress field σ the stresses due to another stress field acting in the perpendicular direction and of magnitude $\bar{\nu} \sigma$. By this means the static solution for $\sigma_{\theta\theta}$ around the opening as well as stresses in the medium can be found for all the problems considered, and in all cases the stresses approach the static values quite closely after 5 to 7 transit times.

The results shown in Figs. 6.1 and 6.2 are compared in Figs. 6.3 and 6.4 with the corresponding results from Refs. (3) and (4). The hoop stress on the boundary at $\theta = 0^\circ$ from Ref. (3) is shown in Fig. 6.3 to be quite different from that given by Ref. (4) and the present work. Also the hoop stress at $\theta = 90^\circ$ from Ref. (3) is shown in Fig. 6.4 to be less than that given by Ref. (4), but the difference is not as large as for $\theta = 0^\circ$. It is interesting to note that all three computations give quite close results for the maximum values of tensile and compressive stresses. In Ref. (4) the reason for the difference in stresses given by Ref. (3) is explained. In using the Duhamel integral for computation of the boundary tractions from the diverging step wave, singularities of the same type as in the present work occur at values of $tC_1/a = 0$ and 2.0 . For this reason great care must be taken in the numerical integrations in this region. In Ref. (3) a constant time interval was used throughout this integration; however, as shown in Ref. (4) it is necessary to reduce the length of time interval in the region of the singularities. It is suggested that the integration technique discussed in Appendix A would have been useful for the computations of Refs. (3) and (4) since the singularities have the general form of $t^{-1/2}$. The method discussed in Appendix A is a more accurate means of accounting for the singularities than is provided by reducing the length of the integration interval.

The hoop stresses at $\theta = 0^\circ$ and 90° from Ref. (4) agree with the present work as closely as the curves in Ref. (4) can be read, except during

the first transit time. With regard to this difference it should be recalled that the incident stress was represented by three terms of Fourier series and that diverging wave stresses were computed to correspond to these three terms. Once the diverging wave stresses are found, they must be combined with the incident stresses in order to find the total stresses. However, it must be decided whether the three modes of diverging wave stresses should be combined with the same three modes of the incident wave stresses or with the total incident stresses which may be represented exactly. In Figs. 6.3 and 6.4 the results of both methods of representing the incident stresses are shown. Both Refs. (3) and (4) apparently used the exact representation of the incident hoop stress; however, the hoop stresses shown in Figs. 6.1 and 6.2 as well as the stresses in the medium and the stresses caused by decaying waves found in the present investigation were computed using the first three modes of the series representation for the incident stresses. It was not possible to determine the cause of the disagreement between the results for hoop stress from Ref. (4) and the present work during the first transit time when the same incident stress was used. In view of the excellent agreement with the independently computed short-time stresses, the present computer solution acquires considerable credibility at least for early times. Moreover, if one considers the present method of solution, it hardly seems possible that the hoop stress could be considerably in error during the first quarter transit time without causing a large difference at one transit time.

The use of the total incoming wave causes the total hoop stress at $\theta = 0^0$ to have an improper initial value. This may be shown in the following way. For $\bar{v} = 1/3$, $\theta = 0^0$ and the incident stress $\sigma = -1.0$, the incident hoop stress is $\bar{v}\sigma = -1/3$; however, at the same point the diverging radial stress must equal $\sigma_{rr} = \sigma = +1$ at $t = 0$ and therefore the diverging hoop stress $\sigma_{\theta\theta} - \bar{v}\sigma_{rr} = +\frac{1}{3}$

since it may be argued that there is no strain in the θ direction for $\theta = 0$ at this time. Therefore the diverging wave should have an initial value of hoop stress equal to $+1/3$ if all the modes were considered, and the initial value of total incident and diverging stress at $\theta = 0^\circ$ combined should be zero.

In Figs. 6.3 and 6.4 the hoop stresses at $\theta = 0^\circ$ and 90° are shown using the first 5 modes as given in Ref. (4). By comparison of these curves with those given for 3 modes, the magnitude of error may be estimated. The error appears to be quite large at $\theta = 0^\circ$ for the first two transit times as would be expected. At 90° the addition of two more modes makes very little difference. Also the use of 5 modes gives the initial value of $\sigma_{\theta\theta}$ at $\theta = 0^\circ$ much closer to the required value of zero.

By comparing Figs. 6.1 and 6.2 it may be seen that a reduction in Poisson's ratio increases both the maximum tensile and maximum compressive stresses.

In Figs. 6.5 through 6.8 is shown the variation of stress with time at several radii for $\bar{v} = 0$ and for $\bar{v} = 1/3$ due to an incident wave of dilatation. These curves show the free field stress until the reflected wave reaches the point, at which time there is a sharp change. At some time after the reflected wave passes the point, however, the stress approaches the long time or static value consistent with the particular point. From these stress-time plots at various radii it may be seen that the dynamic effect on the peak stress is not as great away from the boundary as at the edge of the opening. The static variation of stress with radius as found from Eqs. 6.1 are shown in Fig. 6.9. Also shown in Fig. 6.9 is the variation of radial and hoop stresses with radius at several times.

In Fig. 6.7, which shows the radial stress vs. time curve for $\theta = 0^\circ$ and $\bar{v} = 1/3$, an indication of the mechanism which might cause spalling is

observed. The stresses should be considered only qualitatively during the transit of the wave across the opening since only three modes are used. At $r/a = 1.25$ for example the stress drops very sharply from -1.00 to -0.05 when the reflected tension reaches the point. If the incident stress wave had a decay behind the front, this drop in stress could easily produce a total tensile stress σ_{rr} . A sufficiently large tension would cause failure of the medium. Since the slab bounded by the region of tensile failure and the free surface of the opening has a particle velocity equal to the sum of that in the incident compression wave plus that in the reflected tension wave (both in the inward direction) it would tend to fly inward. This slab remains continuous with the adjacent material in a circumferential direction, however, and the energy trapped in it must be sufficient to break it away to form a spall.

From the results of an incident step wave it is possible to find the stresses caused by an incident wave of any other form using the Duhamel integral.

$$\sigma_{mn} = \sigma_{mn}^{(S)}(t) - \int_0^t \frac{dP(\tau)}{d\tau} \left[\sigma_{mn}^{(S)}(t - \tau) \right] d\tau \quad 6.2$$

where $\sigma_{mn}^{(S)}$ is any stress due to a unit step wave, and σ_{mn} is the corresponding stress due to an arbitrary stress wave $P(t)$. To illustrate the use of the Duhamel integral and study the effect of a decaying stress wave the hoop stress was computed at $\theta = 0^\circ$ and 90° for $\bar{v} = 1/3$ and $a = 17.5$ ft. The variation of stress behind the wave front was assumed to be of the following form

$$P(t) = P_0 \left(1 - \frac{t}{t_0}\right) e^{-Kt/t_0}$$

where K is a constant and t_0 is the total positive duration of the wave. Hoop stresses are shown in Fig. 6.10 and 6.11 for $P_0 = 4000$ psi, $t_0 = 1.8$ sec.,

$C_1 = 17,300$ ft./sec. and $K = 100, 250$ and 400 . Also shown is the stress due to a step wave with a stress of 4000 psi. By increasing K , the rate of decay behind the shock front is increased. The values of K used represent a rather sharp decay which would be consistent with high stresses produced by a large-yield nuclear weapon. The peak compressive stress at $\theta = 90^\circ$ is reached within 3 transit times, or, in terms of the wave velocity, only the first 6 ms of the wave. In the case of the tensile stress the peak occurs within 5 transit times or within 10 ms. after the wave reaches the opening. Therefore only the very early portion of the wave history is pertinent in determining the maximum stress. In 5 ms. the pressure has decreased to 3020 psi for $K = 100$ and to 1316 psi for $K = 400$.

In general only the maximum tensile and compressive stresses have been shown since these stresses are critical in determining the failure of the medium. The computer code which was written to compute these stresses can also compute stresses at any number of evenly spaced angles around the opening and at any radius cut from the boundary so long as the radius is an integral number of distances $\Delta r C_1$. This code is considerably less complex than that used by the authors of Refs. (3) and (4). To solve a problem in which the stresses are computed at 13 equiangular increments around half the opening and for sufficient time to reach the static solution requires approximately 20 minutes of machine time for 3 modes. For a problem in which the stresses are computed at $1/4$ radius spacing for 4 radii cut from the boundary and with the same angular increments requires approximately 50 minutes.

It is of particular interest to notice the effect of changing the length of time steps in the computations. The following table shows the hoop stress at the boundary for $\theta = 90^\circ$ and $\bar{v} = 1/3$ at several times as the length of time steps are varied.

Time steps per transit time	Peak stress σ_{yy}/σ	σ_{yy}/σ at $tc_1/a=1.0$	$\sigma_{\theta\theta}/\sigma$ at $tc_1/a=2.0$
20	-2.9307	-0.7958	-1.8327
40	-2.9306	-0.7905	-1.8334
60	-2.9305	-0.7832	-1.8336
100	-2.9305	-0.7839	-1.8336

The effect of changing the length of time step on the peak stress is negligible. At earlier times the effect is larger, but still unimportant from a practical standpoint. The value of 40 steps per transit time was used for the computation of stresses due to an incident wave of dilatation. The incident shear problem was found to be somewhat more sensitive to changes in the length of time step, so 80 steps per transit time was used in those computations.

6.2 Incident Shear Wave

In Figs. 6.12 and 6.13 are shown the results of the computer solution for hoop stress on the boundary due to three modes of an incident shear wave with magnitude of stress $\bar{\tau}$. The most important information shown by these curves is summarized in the following table.

$\bar{\tau}$	θ	Maximum Stress $\sigma_{\theta\theta}/\bar{\tau}$	Time of Max. Stress, Transit Times	Static value $\sigma_{\theta\theta}/\bar{\tau}$
0	0	4.000	2.0	+4.00
	90	-4.00	2.0	-4.00
1/2	0	4.00	3.0	+4.00
	90	-4.00	3.0	-4.00

The stresses around the opening due to a shear wave should approach the static values after a long time. These static values may be obtained using Eqs. 6.1 by superimposing equal compressive and tensile stress fields acting 90° apart. In this way a field of pure shear is created around the opening. The maximum

static stresses obtained in this way are found to occur on the boundary at 45° and 135° measured from the direction of wave travel. These static values of maximum hoop stress are shown in the above table.

Also shown in Fig. 6.13 is the hoop stress at $\theta = 45^\circ$ due to an incident shear wave as shown in Ref. (12) for $\bar{v} = 1/3$. In Ref. (12) the authors of Ref. (3) use the same method that they used to solve the incident dilatational wave problem to solve the incident shear problem. Therefore, a constant time step in the Duhamel integral near the singularities at $tC_2/a = 0$ and 2 was probably used as before. This would explain why the curve of Ref. (3) does not agree with that from the present computation. The case of an incident shear wave was not solved in Ref. (4).

Also Ref. (12) shows a hoop stress at $\theta = 0^\circ$ which is not found by the present theory and which, in fact, can be shown to be nonexistent by a simple symmetry argument. For, by inspection

$$\gamma_{xy} = \frac{\partial u}{\partial y} + \frac{\partial v}{\partial x} \text{ and } u, v \text{ are even in } y.$$

Therefore

$$\frac{\partial v}{\partial x} \text{ and } \frac{\partial u}{\partial y} \text{ are even in } y.$$

This requires that

$$u, \frac{\partial u}{\partial x} = \epsilon_x, \quad \frac{\partial v}{\partial y} = \epsilon_y \text{ be odd in } y.$$

Since ϵ_x and ϵ_y are both odd in y , they are zero at $y = 0$, and as a consequence the stresses σ_{rr} and $\sigma_{\theta\theta}$ are zero at $y = 0$.

The passage of a shear wave across an opening results in a higher concentration factor for both tension and compression than the passage of a wave of dilatation and therefore may cause the more critical situation. However, the intensity of stress in a shear wave is much less than the stress

in a wave of dilatation for an air induced ground shock, and may be absent altogether for the direct ground shock. The effect on the stress concentration factors of varying Poisson's ratio is small as shown by comparing the curves of Fig. 6.12 and 6.13.

The computer code written to solve the incident shear wave problem for hoop stress at the boundary is quite similar to that discussed for an incident dilatational wave, and therefore requires approximately the same amount of time for solution on the machine. This code was found to be somewhat more sensitive to changes in the time interval than was that for an incident dilatational wave. The reason for this is probably the sharper slope of the Fourier coefficients, $\tilde{a}_n(t)$ and $\tilde{b}_n(t)$, in the series for incident shear stress when the wave front is near the front and rear of the opening.

6.3 Use in Protective Construction

The results of this investigation may be used as a guide in the study of effects of stress waves on openings in rock. Among the first things to be decided in such a study is the type of failure to be expected. For example the maximum compressive stress, which occurs at the ends of the diameter parallel to the wave front for incident waves of dilatation, may cause crushing of the rock in these regions. The maximum tensile stress, which occurs at the ends of the diameter perpendicular to the wave front, may cause tensile failure in these regions, creating loose rock which would fall into the opening. Since the tensile strength of materials such as rock is much less than the compressive strength, tension failure may occur at a free field stress which is not sufficient to cause compression failure. Thus the ratio of maximum tensile stress to maximum compressive stress becomes important in deciding which of these types of failure will occur. Another type of damage

and possible failure may occur from spalling which was described earlier. If the free field stress is high enough, the material in the entire region of the opening may fail and close the opening. This could occur if the opening were sufficiently close to the center of burst of a nuclear weapon. Construction of a lining within the cavity would afford some protection against spalling or loose rock.

Though the maximum stresses in the region of a cylindrical opening have been determined for a homogeneous medium and ideal wave forms, there is still considerable uncertainty in the practical case. The results obtained may only be used as a guide. For example rock contains faults and/or joints and therefore is often weaker than the conventional strength tests would indicate. Furthermore rock may be so cracked or so damaged by the mining operation that it has no tensile strength near the opening. Also the wave form is surely altered in traveling through a nonhomogeneous medium and probably does not have a sharp front. The effect of a rise time would be to reduce the dynamic stress concentration factor and to reduce the possibility of spalling failure. From this discussion it may be seen that considerable judgment is required in making allowances for these uncertainties.

In Ref. (13) many of the practical problems encountered in the application of theoretical results of the type obtained in the present work are discussed. Also the various wave types are discussed and a method for combining the effects of waves of dilatation and shear waves when both are created by an air blast wave moving on the surface is presented.

V. 1. CONCLUSIONS

Stresses in the vicinity of a cylindrical cavity due to two types of stress waves have been studied. Also the effect of changing the shape of the stress wave behind the front and of varying the properties of the material have been considered. From these studies certain conclusions may be made concerning the method of solution used to solve the problem under consideration.

(1) The method of solution described in the present work can be used successfully and efficiently to solve the problem under consideration. Once the solution for a unit step pulse is known, it is possible to find the stresses for a stress wave of any shape using the Duhamel integral.

(2) The short time solution may be used to check the initial portion of the machine solution. By using a larger number of terms in the Taylor expansions, this solution could be extended to apply to longer times.

(3) The location of maximum stress in the solution appears to give maximum stresses in the vicinity of the cavity with sufficient accuracy for practical purposes. In order to study the spalling phenomenon, however, it is necessary to know the stresses in the vicinity of the cavity at short times are required.

The problem could be studied in further detail, either by extending the present solution or applying the method to other problems. A few of the problems that might be considered are the following:

(1) A computer program could be written as described in Appendix C could be written for a general case and sufficient data used to obtain any accuracy desired.

(2) By using a large number of modes either with the computer solution or the short time solution the stresses at early time could be obtained with sufficient accuracy to make a complete study of the spalling problem.

(3) A complete study of various wave forms such as effect of rise time and decay rate would be possible. If wave forms with rapid changes in stress were to be considered, it would be necessary first to obtain the solution with more modes included.

(4) The problem of a cylindrical opening with a lining could be solved by the method presented. Either the case of a thin lining or that of a thick lining could be considered.

BIBLIOGRAPHY

1. Gilbert, J. F., "Planar Wave Interaction with Cylindrical Cavity," Report to ADIR, Air Force Ballistic Missile Division (Contract AFO4(647)-343), E. H. Everett & Associates, Inc., 1 December 1959.
2. Pao, Yih-Hsing, "Dynamical Stress Concentration in an Elastic Plate," Journal of Applied Mechanics, Vol. 19, June 1962, p. 299.
3. Baron, M. L. and Matthews, A. L., "Diffraction of a Pressure Wave by a Cylindrical Cavity in an Elastic Medium," Journal of Applied Mechanics, Vol. 28, September 1961, p. 747.
4. Logcher, R. D., "A Method for the Study of Failure Mechanisms in Cylindrical Rock Cavities Due to the Diffraction of a Pressure Wave," School of Engineering, Massachusetts Institute of Technology, Technical Report 162-5, July 1962.
5. Soldate, A. M. and Hook, J. E., "A Theoretical Study of Structure-Medium Interaction," AFOSR-TH-61-8, Air Force Special Weapons Center, Kirtland Air Force Base, New Mexico, December 1961.
6. Riley, W. E. and Carpenter, R. J., "Application of Moire Methods to the Determination of Tensile Stress and Strain Distribution," Journal of Applied Mechanics, Vol. 19, March 1962, p. 27.
7. Hirschert, L. L., "Model Experiment Pertaining to the Design of Underground Openings Subjected to Blast Ground Shock," Technical Report of the Colorado School of Mines Research Foundation, January 1960.
8. Larr, E., Hydrodynamics, Cambridge, MA, Cambridge University Press, 1961.
9. von Karman, H. and Biot, J. N., "The Motion of Slender Bodies Moving with Superimposed Rotation and Translation Relative to Projectile," Transactions ASEE Applied Mechanics, Vol. 1, 1951, p. 177.
10. Courant, R. and Hilbert, E., Methods of Mathematical Physics, Vol. 1, Interscience Publishers, New York, 1953.
11. Timoshenko, S. and Woinowsky-Krieger, I., Theory of Plates, Second Edition, New York, McGraw-Hill, 1959.
12. Baron, M. L. and Matthews, A. L., "Diffraction of a Linear Wave by a Cylindrical Cavity in an Elastic Medium," Journal of Applied Mechanics, Vol. 19, March 1962, p. 27.
13. Baron, M. L. and Matthews, A. L., "Theoretical Studies on Blast-Induced Failure of Structures," More Corporation, SR-19, 1961, 20 pp.

APPENDIX A

DERIVATION OF THE NUMERICAL INTEGRATION FORMULA

From the form of the stress equations for diverging waves written in terms of ξ , Eqs. 4.6 - 4.8 for example, it may be seen that one term of each expression has an integrable singularity at $\xi = 0$ due to the term $\xi^{1/2}$ in the denominator. It is apparent that a trapezoidal or parabolic approximation would not give a finite result in the first step of the numerical integration even though the integral converges. An integration procedure was derived to avoid this difficulty, and is described in this appendix. After this procedure had been in use for some time, it was found that a very similar procedure was described by Jeffreys and Jeffreys in Ref. (9).

Consider the second integral involved in the computation of $\sigma_{r\theta}$ in mode 1 given by Eq. 4.7.

$$\int_0^{\xi} g^{(1)}(\xi_0) \left[\frac{a(1 + \alpha\xi_0 + \alpha^2\xi_0^2 + \alpha^3\xi_0^3)}{\sqrt{2a\xi_0} \sqrt{1 + \alpha\xi_0} - \alpha^2\xi_0^3} \right] d\xi_0$$

Let all the integrand except $\xi^{1/2}$ be approximated by a linear relation in the interval $\Delta\xi$. Then

$$g^{(1)}(\xi_0) \left[\frac{a(1 + \alpha\xi_0 + \alpha^2\xi_0^2 + \alpha^3\xi_0^3)}{\sqrt{2a\xi_0} \sqrt{1 + \alpha\xi_0} - \alpha^2\xi_0^3} \right] \approx g_r + \frac{(g_{r+1} - g_r)}{\Delta\xi} (\xi - \xi_r) \quad A.1$$

in the interval $\xi = r\Delta\xi$ to $\xi = (r+1)\Delta\xi$. With this substitution, the integral in this interval becomes,

$$\begin{aligned}
& \int_{m\Delta\xi}^{(m+1)\Delta\xi} \frac{1}{\sqrt{\xi}} \left[g_m + \frac{(g_{m+1} - g_m)}{\Delta\xi} (\xi - m\Delta\xi) \right] d\xi \\
& = \left[2g_m \xi^{1/2} + \frac{(g_{m+1} - g_m)}{\Delta\xi} \left(\frac{2}{3} \xi^{3/2} \right) - \frac{(g_{m+1} - g_m)}{\Delta\xi} m\Delta\xi (2\xi^{1/2}) \right]_{m\Delta\xi}^{(m+1)\Delta\xi} \quad A.2
\end{aligned}$$

Straightforward evaluation of this expression leads to the following value for the left side of Eq. A.2.

$$\begin{aligned}
& \sqrt{\Delta\xi} \left[g_m \left\{ 2(1+m) [(m+1)^{1/2} - m^{1/2}] - \frac{2}{3} [(m+1)^{3/2} - m^{3/2}] \right\} \right. \\
& \quad \left. + g_{m+1} \left\{ \frac{2}{3} [(m+1)^{3/2} - m^{3/2}] - 2m [(m+1)^{1/2} - m^{1/2}] \right\} \right] \quad A.3
\end{aligned}$$

This expression gives the value of the integral between $m\Delta\xi$ and $(m+1)\Delta\xi$ as long as the values of g_m and g_{m+1} are defined according to Eq. A.1. The functions of m by which each ordinate is multiplied differs for each step, since m changes, but will be the same for integration of $F'''(\eta_1)$ and $G'''(\eta_2)$ terms. Also, this expression is not limited to $n = 1$; it is a general integration formula for which g is any function. From Eq. A.3 let

$$\begin{aligned}
A_m &= 2(1+m) [(m+1)^{1/2} - m^{1/2}] - \frac{2}{3} [(m+1)^{3/2} - m^{3/2}] \\
B_m &= \frac{2}{3} [(m+1)^{3/2} - m^{3/2}] - 2m [(m+1)^{1/2} - m^{1/2}] \quad A.4
\end{aligned}$$

With these substitutions the integral to be evaluated may be written

$$\begin{aligned}
& \frac{1}{\alpha^2} \int_{\alpha\xi}^{(n+1)\Delta\xi} G'''(\eta_2) \left[\frac{\mu(1+\alpha\xi+6\alpha^2\xi^2+2\alpha^3\xi^3)}{\sqrt{2\alpha\xi} \sqrt{1+\alpha\xi/2}} \right] \alpha d\xi \\
& = \sqrt{\Delta\xi} \left[(G'''(\eta_2))_{p=n} R_n^G A_m + (G'''(\eta_2))_{p=n-1} R_{n+1}^G B_m \right] \quad A.5
\end{aligned}$$

where R_n^G is the factor

$$\frac{\mu(1+5\alpha\zeta+6\alpha^2\zeta^2+2\alpha^3\zeta^3)\alpha}{\sqrt{2\alpha}\sqrt{1+\alpha\zeta/2}\alpha^3c_1^3}$$

evaluated at $\zeta = m\Delta\zeta$ and R_{m+1}^G is the same factor evaluated at $\zeta = (m+1)\Delta\zeta$.

In computing the factors A_m and B_m , the small difference between large numbers are involved when m gets fairly large if the computation is made in a straightforward manner. Therefore these weighting factors were also written as asymptotic series which were used after m reached a certain value. These series are as follows

$$A_m = \frac{1}{2\sqrt{m}} \left[1 - \frac{1}{6m} + \frac{1}{16m^2} - \frac{1}{32m^3} + \dots \right]$$

A.6

$$B_m = \frac{1}{2\sqrt{m}} \left[1 - \frac{1}{3m} + \frac{1}{16m^2} - \frac{1}{8m^3} + \dots \right] .$$

APPENDIX B
SOME PROPERTIES OF THE DISPLACEMENT POTENTIALS

B.1 General Solution of the Wave Equation in Cylindrical Coordinates.

In Section 3.3 it is shown that two hyperbolic partial differential equations in two independent variables result from substituting Fourier series for ϕ and ψ into the wave equations. These differential equations are Eqs. 3.21. The relevant parts of the general solutions of these equations were stated as Eqs. 3.22. It will now be shown that these solutions satisfy the differential equations. Since both differential equations and both solutions are of the same form, it is only necessary to show the validity of one of the solutions.

Then it is to be shown that for $n = 0, 1, 2, \dots$

$$f_n = \left(\frac{1}{r} \frac{\partial}{\partial r}\right)^n f_0 \quad \text{B.1}$$

satisfies the equation

$$c_1^2 \left(\frac{\partial^2 f_n}{\partial r^2} + \frac{2n+1}{r} \frac{\partial f_n}{\partial r} \right) = \ddot{f}_n \quad \text{B.2}$$

It is first assumed that f_n is a solution to Eq. B.2. Then it will be shown that f_{n+1} given by Eq. B.1 is also a solution, and therefore the general solution for any value of n is given by Eq. B.1 provided f_0 is a solution with $n=0$. The expression for f_{n+1} is given by Eq. B.1 as

$$f_{n+1} = \left(\frac{1}{r} \frac{\partial}{\partial r}\right) f_n \quad \text{B.3}$$

and the differential equation becomes (by replacing n by $n+1$ in Eq. B.2)

$$c_1^2 \left(\frac{\partial^2 f_{n+1}}{\partial r^2} + \frac{2n+3}{r} \frac{\partial f_{n+1}}{\partial r} \right) = \ddot{f}_{n+1} \quad \text{B.4}$$

Substitute Eq. B.3 into Eq. B.4.

$$c_1^2 \left[\frac{\partial^2}{\partial r^2} \left(\frac{1}{r} \frac{\partial f_n}{\partial r} \right) + \frac{2n+3}{r} \frac{\partial}{\partial r} \left(\frac{1}{r} \frac{\partial f_n}{\partial r} \right) \right] = \frac{\partial^2}{\partial t^2} \left(\frac{1}{r} \frac{\partial f_n}{\partial r} \right)$$

$$\begin{aligned}
c_1^2 \left[\left(\frac{1}{r} \frac{\partial^3 f_n}{\partial r^3} - \frac{2}{r^2} \frac{\partial^2 f_n}{\partial r^2} + \frac{2}{r^3} \frac{\partial f_n}{\partial r} \right) + \frac{2n+3}{r} \left(\frac{1}{r} \frac{\partial^2 f_n}{\partial r^2} - \frac{1}{r^2} \frac{\partial f_n}{\partial r} \right) \right] \\
= \frac{1}{r} \frac{\partial^3 f_n}{\partial t^2 \partial r} \\
c_1^2 \left[\frac{1}{r} \frac{\partial^3 f_n}{\partial r^3} + \frac{2n+1}{r} \left(\frac{1}{r} \frac{\partial^2 f_n}{\partial r^2} - \frac{1}{r^2} \frac{\partial f_n}{\partial r} \right) \right] = \frac{1}{r} \frac{\partial^3 f_n}{\partial t^2 \partial r} .
\end{aligned} \tag{B.5}$$

However

$$\frac{1}{r} \frac{\partial^2 f_n}{\partial r^2} - \frac{1}{r^2} \frac{\partial f_n}{\partial r} = \frac{\partial}{\partial r} \left(\frac{1}{r} \frac{\partial f_n}{\partial r} \right) .$$

Therefore Eq. B.5 may be written

$$c_1^2 \left[\frac{1}{r} \frac{\partial}{\partial r} \left(\frac{\partial^2 f_n}{\partial r^2} \right) + \frac{1}{r} \frac{\partial}{\partial r} \left(\frac{2n+1}{r} \frac{\partial f_n}{\partial r} \right) \right] = \frac{1}{r} \frac{\partial}{\partial r} \frac{\partial^2 f_n}{\partial t^2} .$$

It is apparent that this is an identity since the same expression may be obtained by taking the partial derivative of both sides of Eq. B.2 with respect to r and dividing through by r . Therefore Eq. B.3 satisfies the differential equation and as a consequence Eq. B.1 is a general solution for any value of n provided f_0 is a solution.

It was shown in Chapter III by a physical argument that f_0 has the form given by Eq. 3.26. It is of interest to show directly that f_0 in this form satisfies the differential equation given by Eq. B.2 with $n = 0$. This is

$$f_0 = \int_0^{+\infty} F(t - \frac{r}{c_1} \cosh u) du \tag{B.6}$$

is a solution of

$$c_1^2 \left(\frac{\partial^2 f_0}{\partial r^2} + \frac{1}{r} \frac{\partial f_0}{\partial r} \right) = \frac{\partial^2 f_0}{\partial t^2} , \tag{B.7}$$

provided that all derivatives which appear are continuous in u and r .^{*} Take the derivatives of Eq. B.6

$$\frac{\partial f_0}{\partial r} = \frac{-1}{c_1} \int_0^\infty F'(t - \frac{r}{c_1} \cosh u) \cosh u \, du$$

$$\frac{\partial^2 f_0}{\partial r^2} = \frac{+1}{c_1^2} \int_0^\infty F''(t - \frac{r}{c_1} \cosh u) \cosh^2 u \, du$$

$$\frac{\partial^2 f_0}{\partial t^2} = + \int_0^\infty F''(t - \frac{r}{c_1} \cosh u) \, du .$$

Substitute these derivatives into Eq. B.7.

$$c_1^2 \left[\frac{1}{c_1^2} \int_0^\infty F''(t - \frac{r}{c_1} \cosh u) \cosh^2 u \, du - \frac{1}{rc_1} \int_0^\infty F'(t - \frac{r}{c_1} \cosh u) \cosh u \, du \right] = \int_0^\infty F''(t - \frac{r}{c_1} \cosh u) \, du$$

The second term on the left may be integrated by parts as follows.

$$- \frac{1}{rc_1} \int_0^\infty F'(t - \frac{r}{c_1} \cosh u) \cosh u \, du = + \frac{1}{rc_1} F'(t - \frac{r}{c_1} \cosh u) \sinh u \Big|_0^\infty + \frac{1}{c_1^2} \int_0^\infty F''(t - \frac{r}{c_1} \cosh u) \sinh^2 u \, du$$

The first term on the right equals zero since $\sinh u = 0$ at $u = 0$ and

$F'(t - \frac{r}{c_1} \cosh u) = 0$ as u tends to infinity, for a disturbance which starts

* In the computations of Chapters IV and V, the function $F''(\eta_1)$ is not continuous through $\eta_1 = -a/c_1$. In this case it is not difficult to alter the proof so that the result will hold

at a finite time. Then

$$\begin{aligned} & -\frac{1}{rC_1} \int_0^\infty F'(t - \frac{r}{C_1} \cosh u) \cosh u \, du \\ & = -\frac{1}{C_1^2} \int_0^\infty F''(t - \frac{r}{C_1} \cosh u) \sinh^2 u \, du \end{aligned}$$

By making this substitution into Eq. B.8 and observing that $(\cosh^2 u - \sinh^2 u) = 1$, one obtains an equality.

$$\begin{aligned} & C_1^2 \left[\frac{1}{C_1^2} \int_0^\infty F''(t - \frac{r}{C_1} \cosh u) (\cosh^2 u - \sinh^2 u) \, du \right] \\ & = \int_0^\infty F''(t - \frac{r}{C_1} \cosh u) \, du \end{aligned}$$

B.2 General Form of ϕ and ψ for Arbitrary n .

The general expression for the displacement potentials ϕ and ψ , as given by Eq. 3.29, may be written in the much more convenient form of Eq. 3.30. The derivation is shown for the function ϕ . For ψ the proof is the same.

From the first of Eqs. 3.29, the n th term of the series for ϕ , say ϕ_n , may be written

$$\phi_n = \Omega_n(r, t) \cos n\theta$$

where

$$\Omega_n = r^n \left(\frac{1}{r} \frac{\partial}{\partial r} \right)^n \int_0^\infty F(t - \frac{r}{C_1} \cosh u) \, du. \quad \text{E.9}$$

The term $n + 1$ takes the form

$$\Omega_{n+1} = r^{n+1} \left(\frac{1}{r} \frac{\partial}{\partial r} \right)^{n+1} \int_0^\infty F(t - \frac{r}{C_1} \cosh u) \, du$$

or

$$\Omega_{n+1} = r^n \frac{\partial}{\partial r} \left(\frac{1}{r} \frac{\partial}{\partial r} \right)^n \int_0^\infty F\left(t - \frac{r}{c_1} \cosh u\right) du.$$

This expression may be written in the equivalent form

$$\Omega_{n+1} = \left\{ \frac{\partial}{\partial r} \left[r^n \left(\frac{1}{r} \frac{\partial}{\partial r} \right)^n \right] - \frac{n}{r} r^n \left(\frac{1}{r} \frac{\partial}{\partial r} \right)^n \right\} \int_0^\infty F\left(t - \frac{r}{c_1} \cosh u\right) du.$$

By comparing this expression with Eq. B.9 it may be seen that

$$\Omega_{n+1} = \frac{\partial}{\partial r} \Omega_n - \frac{n}{r} \Omega_n. \quad \text{B.10}$$

The derivation of Eqs. 3.30 from Eqs. 3.29 may now proceed by mathematical induction. Let it be assumed that the first of Eqs. 3.30 is correct for Ω_n . Then it will be shown that Eqs. 3.30 hold for Ω_{n+1} with $n = 0, 1, 2, \dots$. Once this is shown it only remains to notice that the expression is correct for $n = 0$. From the first of Eqs. 3.30, φ_n may be written

$$\varphi_n = \Omega_n(r, t) \cos n\theta,$$

$$\Omega_n = \frac{(-1)^n}{c_1^n} \int_0^\infty F^n\left(t - \frac{r}{c_1} \cosh u\right) \cosh nu \, du. \quad \text{B.11}$$

By performing the operation indicated by Eq. B.10, one obtains

$$\begin{aligned} \Omega_{n+1} &= \frac{-(-1)^n}{c_1^{n+1}} \int_0^\infty F^{n+1}\left(t - \frac{r}{c_1} \cosh u\right) \cosh nu \cosh u \, du \\ &\quad - \frac{n}{r} \frac{(-1)^n}{c_1^n} \int_0^\infty F^n\left(t - \frac{r}{c_1} \cosh u\right) \cosh nu \, du. \end{aligned} \quad \text{B.12}$$

The second integral on the right may be written as follows by integrating by parts

$$\begin{aligned}
& \frac{n}{r} \frac{(-1)^n}{C_1^n} \int_0^\infty F^n\left(t - \frac{r}{C_1} \cosh u\right) \cosh nu \, du = \\
& \left[\frac{n}{r} \frac{(-1)^n}{C_1^n} F^n\left(t - \frac{r}{C_1} \cosh u\right) \left(\frac{1}{n} \sinh nu\right) \right]_0^\infty \\
& + \frac{n}{r} \frac{(-1)^n r}{C_1^{n+1}} \int_0^\infty F^{n+1}\left(t - \frac{r}{C_1} \cosh u\right) \left(\frac{1}{n} \sinh nu \sinh u\right) du .
\end{aligned} \tag{B.13}$$

The first term on the right is zero, however, since $\sinh nu = 0$ at $u = 0$ and $F^n\left(t - \frac{r}{C_1} \cosh u\right) = 0$ as u tends to infinity. By using Eq. B.13, one may write Eq. B.12 in the following form

$$\begin{aligned}
\Omega_{n+1} &= \frac{(-1)^{n+1}}{C_1^{n+1}} \int_0^\infty F^{n+1}\left(t - \frac{r}{C_1} \cosh u\right) \cosh nu \cosh u \, du \\
&+ \frac{(-1)^{n+1}}{C_1^{n+1}} \int_0^\infty F^{n+1}\left(t - \frac{r}{C_1} \cosh u\right) \sinh nu \sinh u \, du ,
\end{aligned}$$

or by combining terms

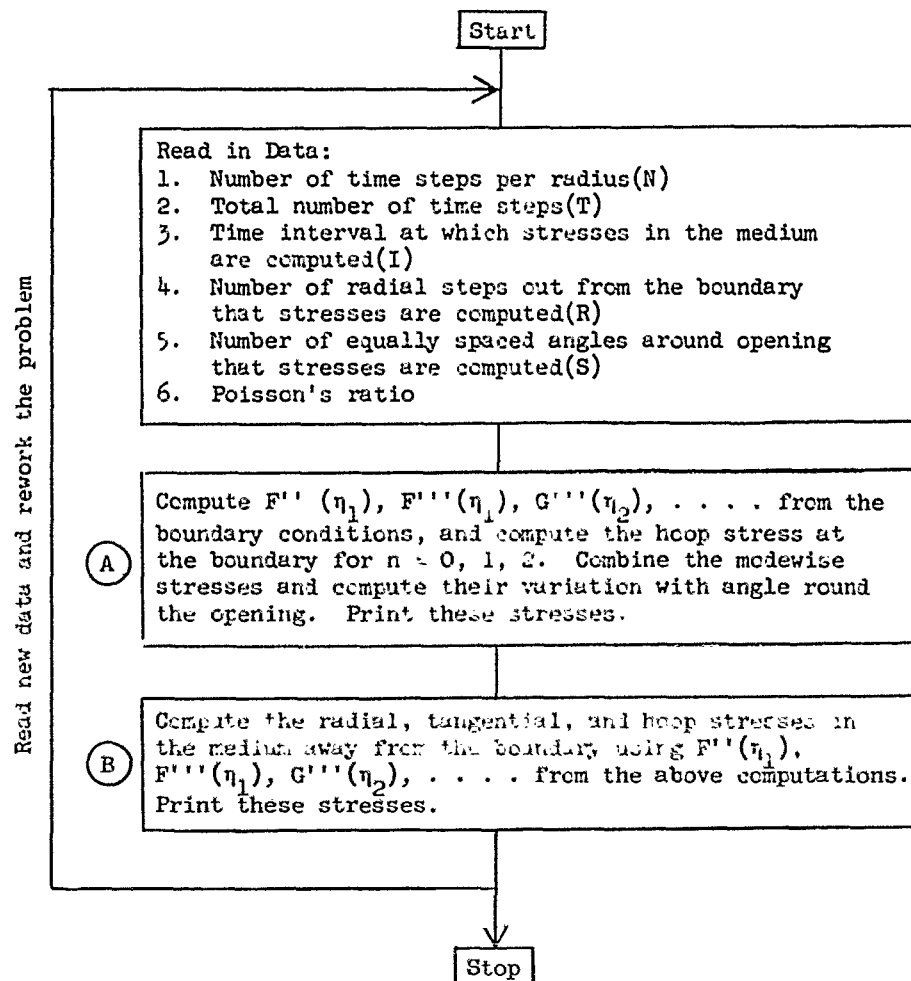
$$\begin{aligned}
\Omega_{n+1} &= \frac{(-1)^{n+1}}{C_1^{n+1}} \int_0^\infty F^{n+1}\left(t - \frac{r}{C_1} \cosh u\right) \left[\cosh nu \cosh u \right. \\
&\quad \left. + \sinh nu \sinh u \right] du .
\end{aligned}$$

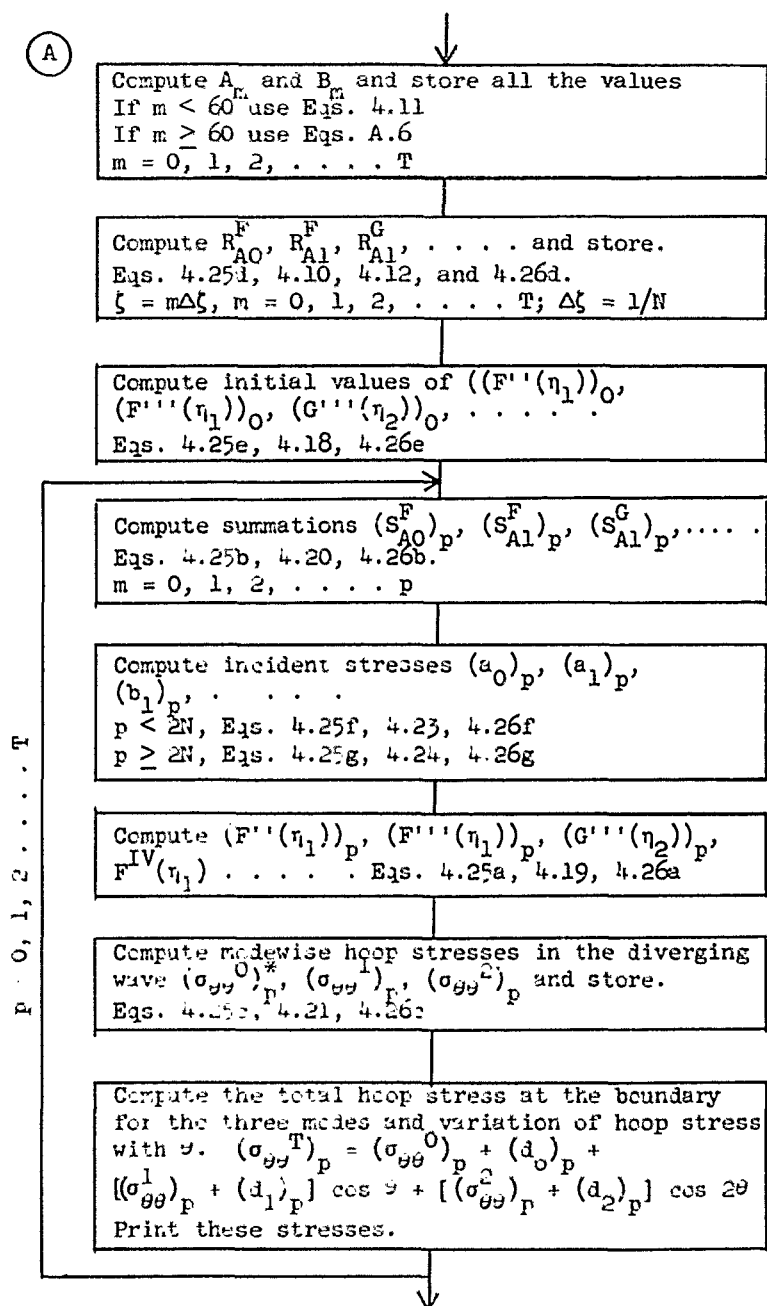
The quantity in brackets is, however, equal to $\cosh (n+1)u$. With this substitution, the expression for Ω_{n+1} is identical to Eq. 3.30 with $n+1$ replacing n . The conclusion holds even for $n = 0$ since only the first term on the right-hand side of Eq. B.12 appears in that case. It has thus been shown that the first of Eqs. 3.30 holds for $n+1$ if it is assumed to be correct for n , $n = 0, 1, 2, \dots$.

To complete the demonstration, it is only necessary to note that the first of Eqs. 3.30 is correct for $n = 0$, since it is identical to the first of Eqs. 3.29.

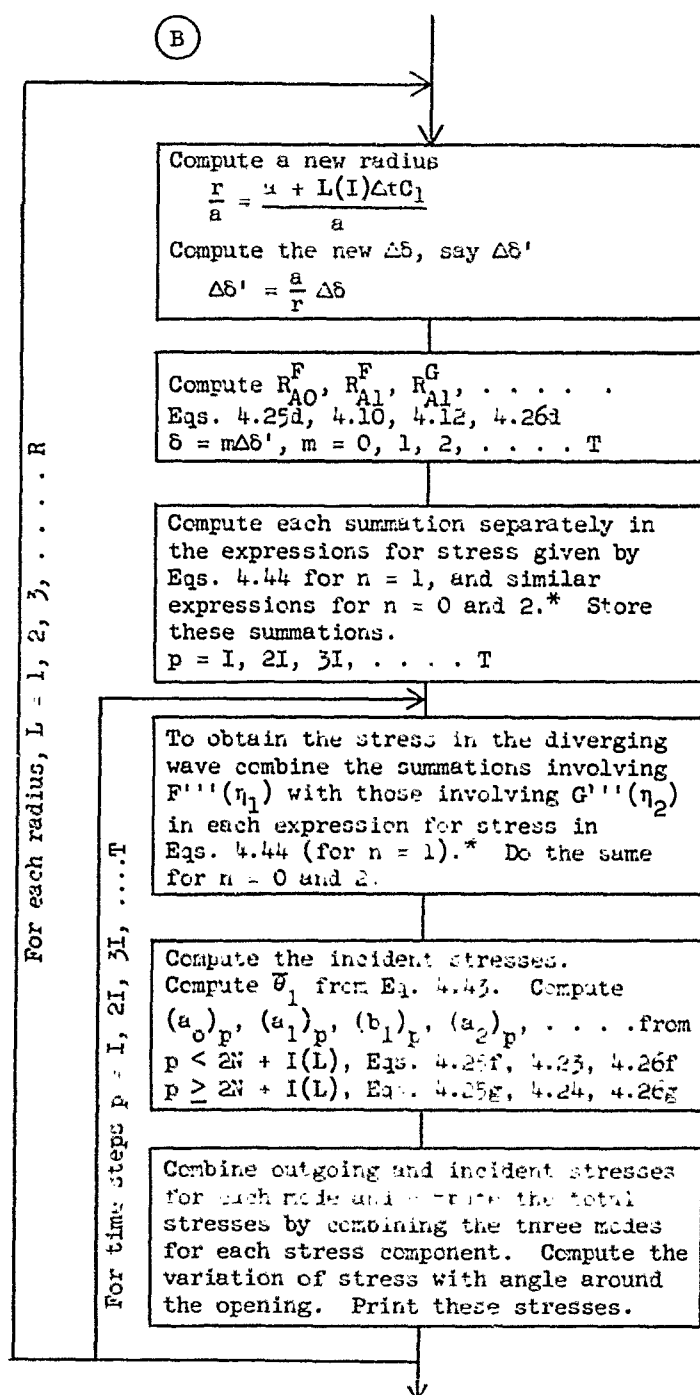
APPENDIX C DESCRIPTION OF THE COMPUTER PROGRAM

A program was written in FORTRAN language to solve the problem on an electronic digital computer. The computer used was a CDC 1604. The sequence of operations performed by the computer in the solution of the problem is shown in the following diagrams. The computations are indicated together with the appropriate equations to be solved.





* The superscript indicates the mode ($n = 0, 1, 2$). The radial and shear stresses in the diverging wave were also computed at this time so they could later be combined with the corresponding incident stresses to verify that the sums were zero at the boundary.



* As discussed in the text, the upper limit on the summations involving $G'''(\eta_2)$ actually used in the machine was not $p - n/\alpha$, but $p - n$. Therefore a shift in time must be made when these summations are combined with those involving $F'''(\eta_1)$ in Eqs. 4.44 and similar equations to obtain the stresses.

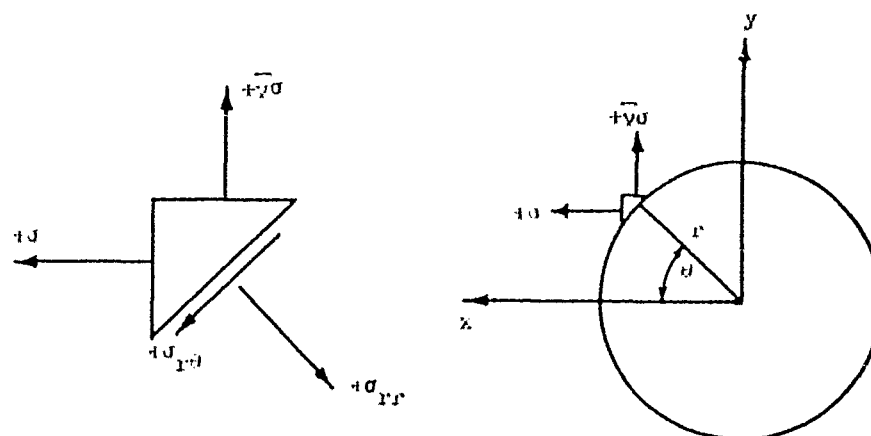


Fig. 3.1 Sign convention for stress at a point.

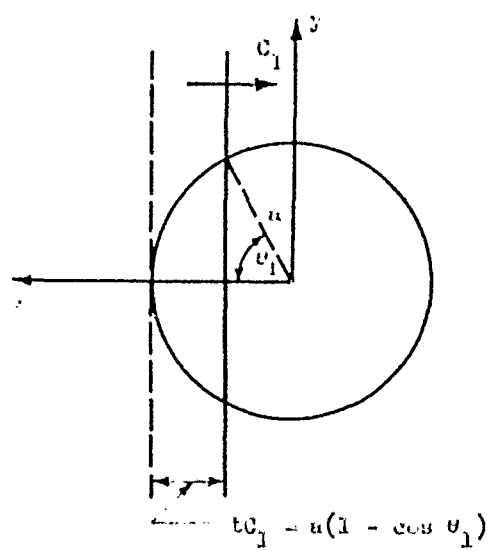


Fig. 3.2 Geometry of envelopment of a cylindrical boundary by a plane wave of dilatation.

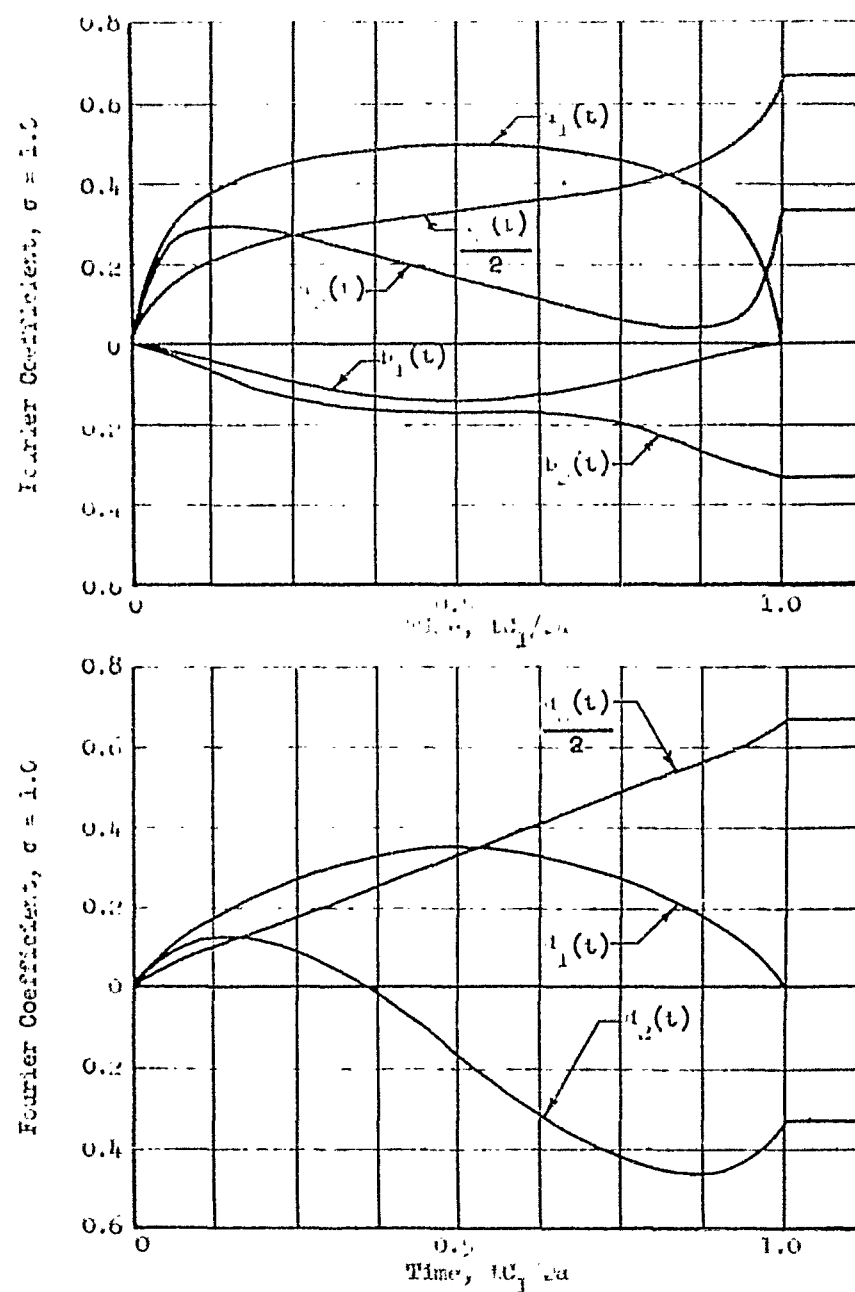


Fig. 3.3 Variation with time of the Fourier coefficients for stress on a cylindrical boundary during envelopment by an incident wave of dilatation, $\bar{\nu} = 1/3$.

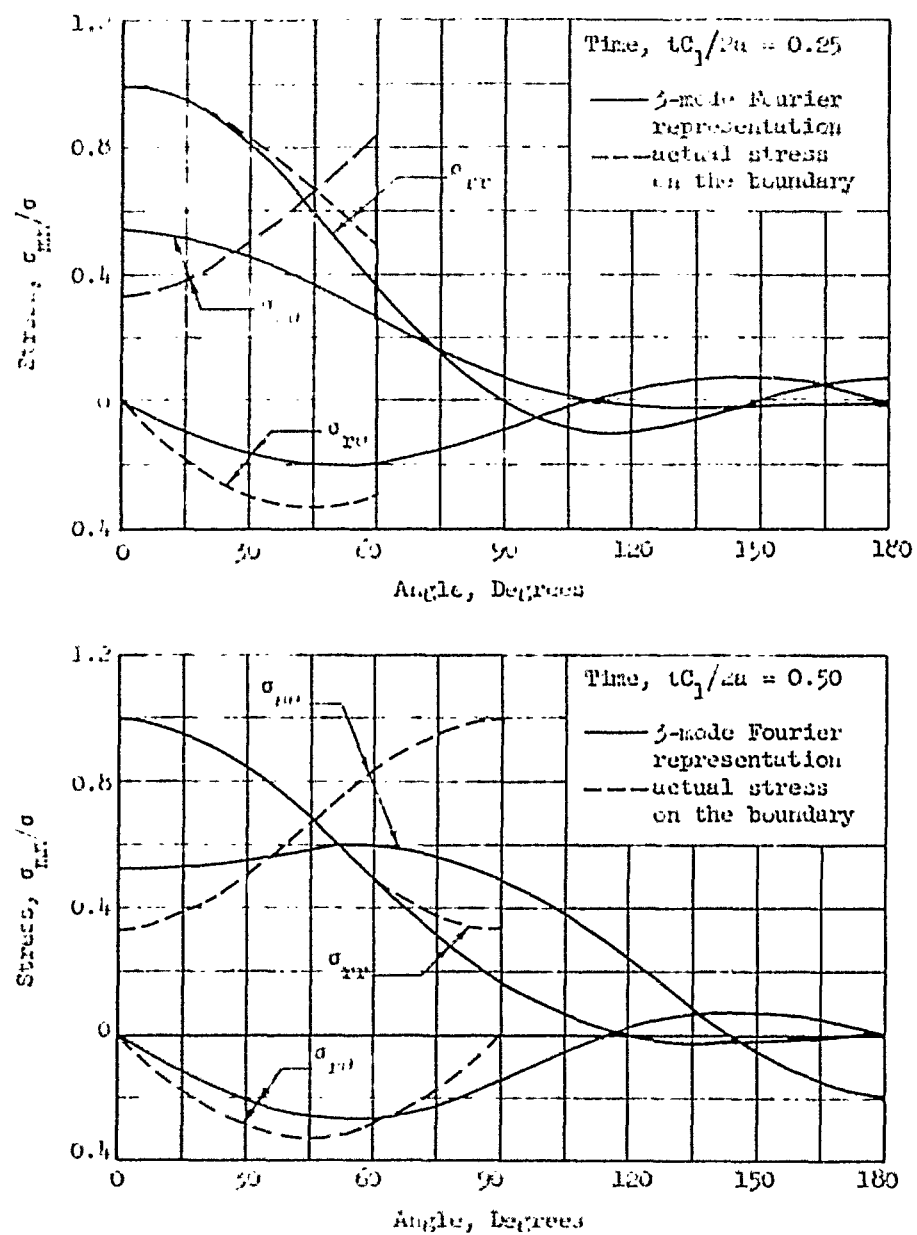


Fig. 3.4 Comparison of actual stress on the boundary during envelopment by the incident plane wave of dilatation with the Fourier representation, $\nu = 1/3$.

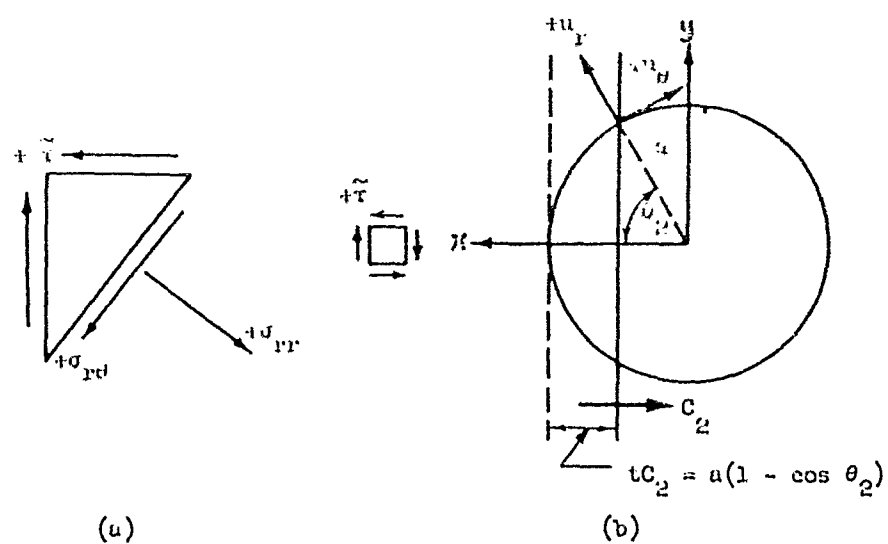


Fig. 3.5 Geometry of envelopment of a cylindrical boundary by an incident shear wave.

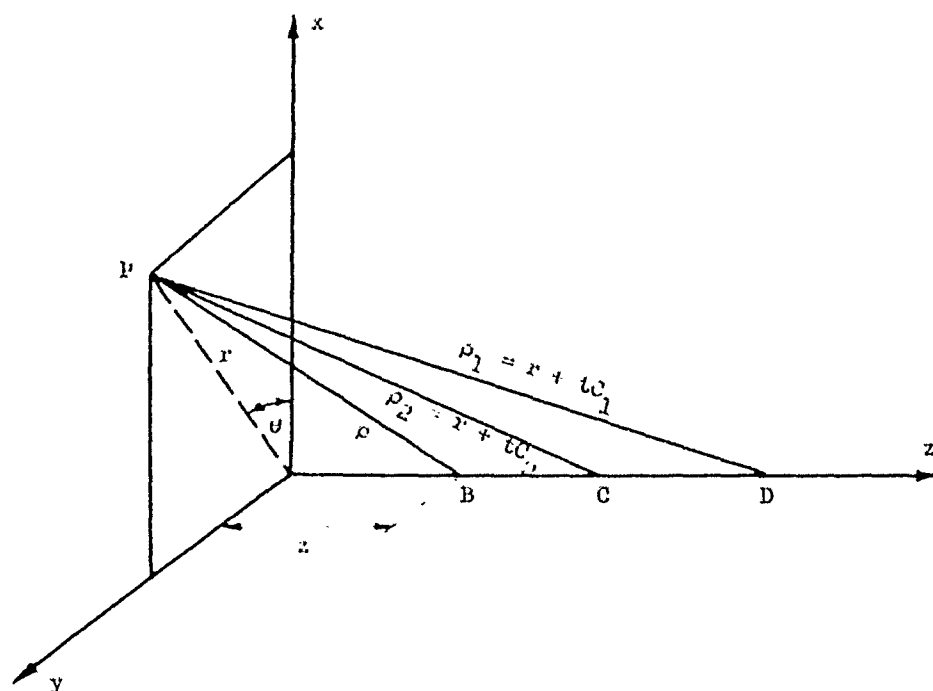


Fig. 3.6 Coordinate system and point-source waves reaching point p at time t.

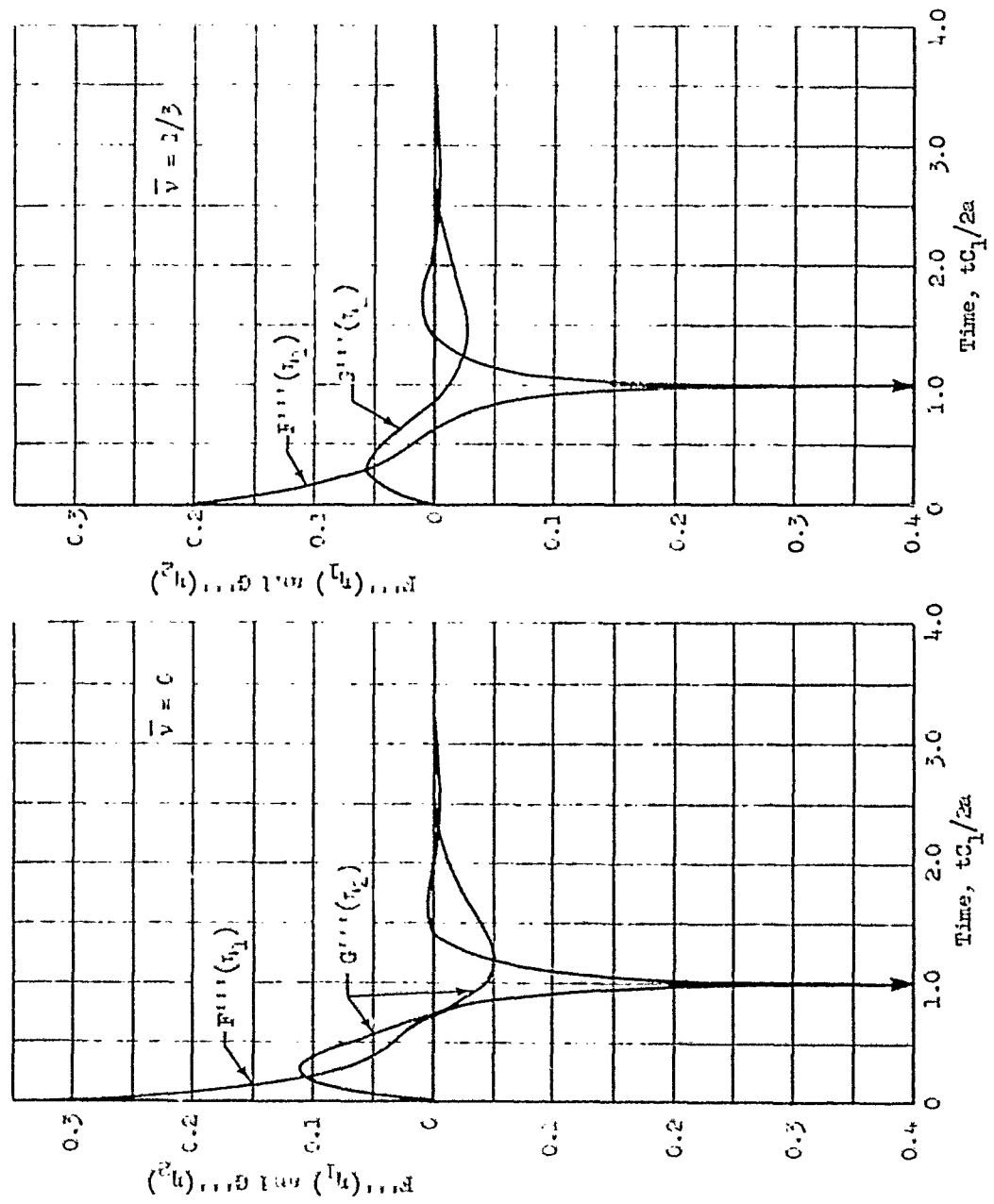


Fig. 4.1 Results of the numerical solution for $F'''(\eta_1)$ and $G'''(\eta_2)$ in the case $n = 1$ ($\bar{v} = 0$ and $\bar{v} = 1/3$).

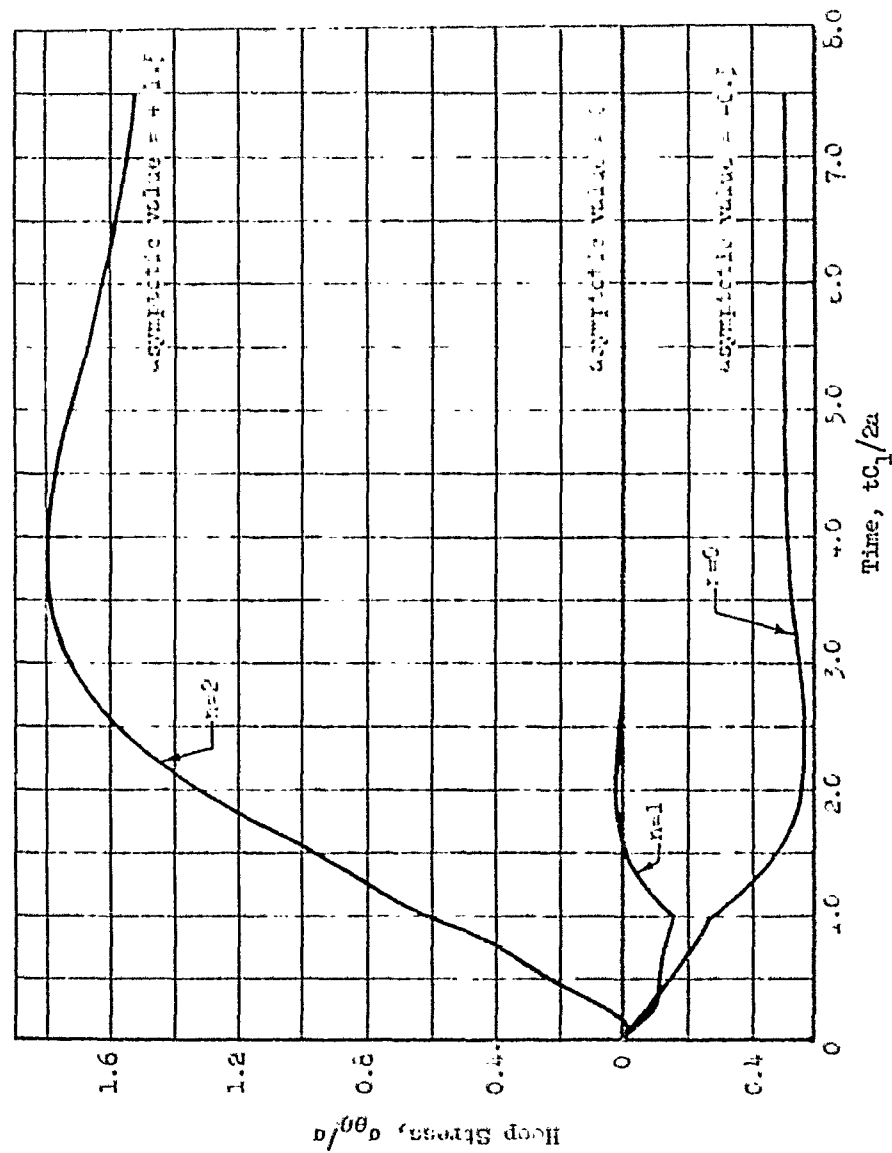


Fig. 4.2 Results of the computer solution for hoop stress in modes 0, 1 and 2 due to an incident wave of dilatation ($\bar{v} = 0$).

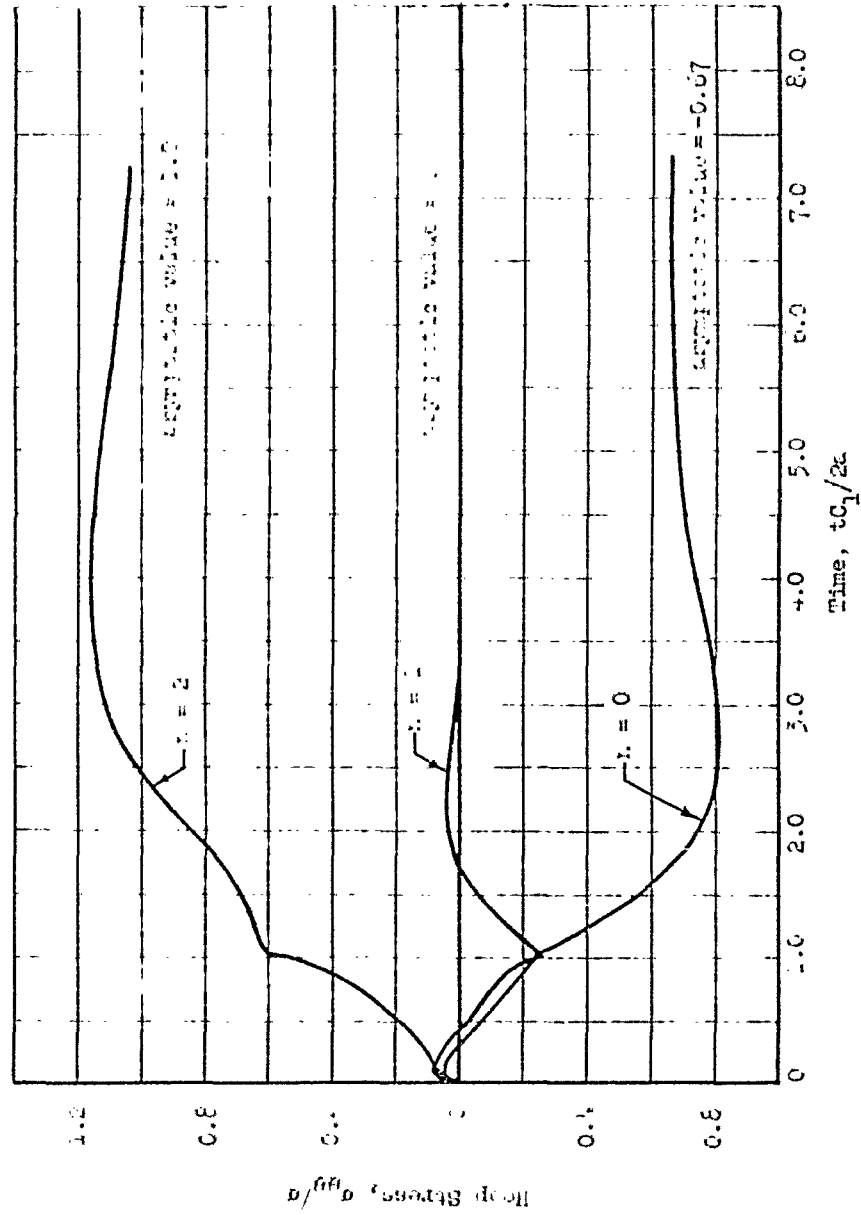


Fig. 4.3 Results of the computer solution for hoop stress in modes 0, 1 and 2 due to an incident wave of dilatation ($\bar{v} = 1/3$).

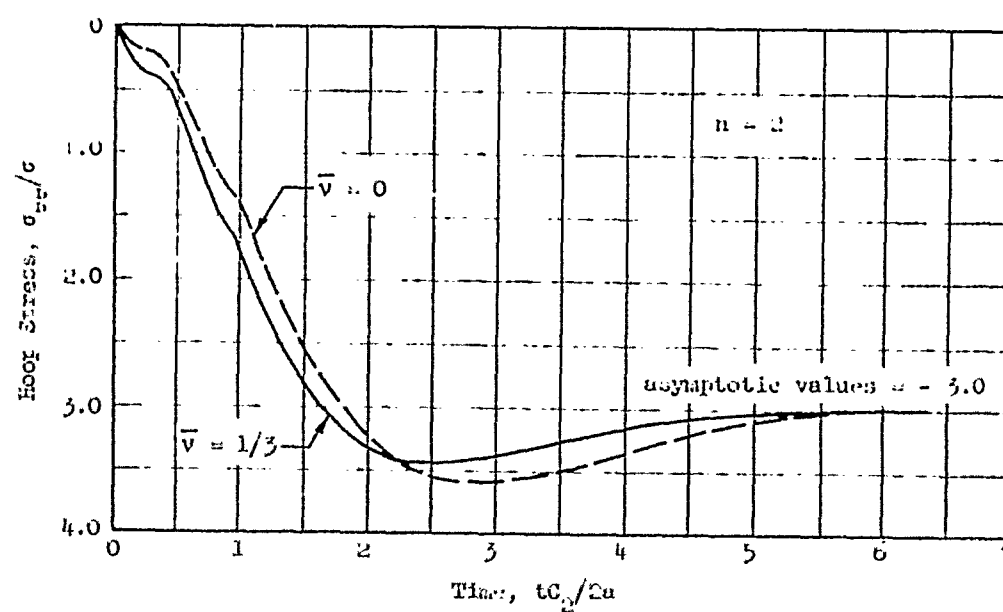
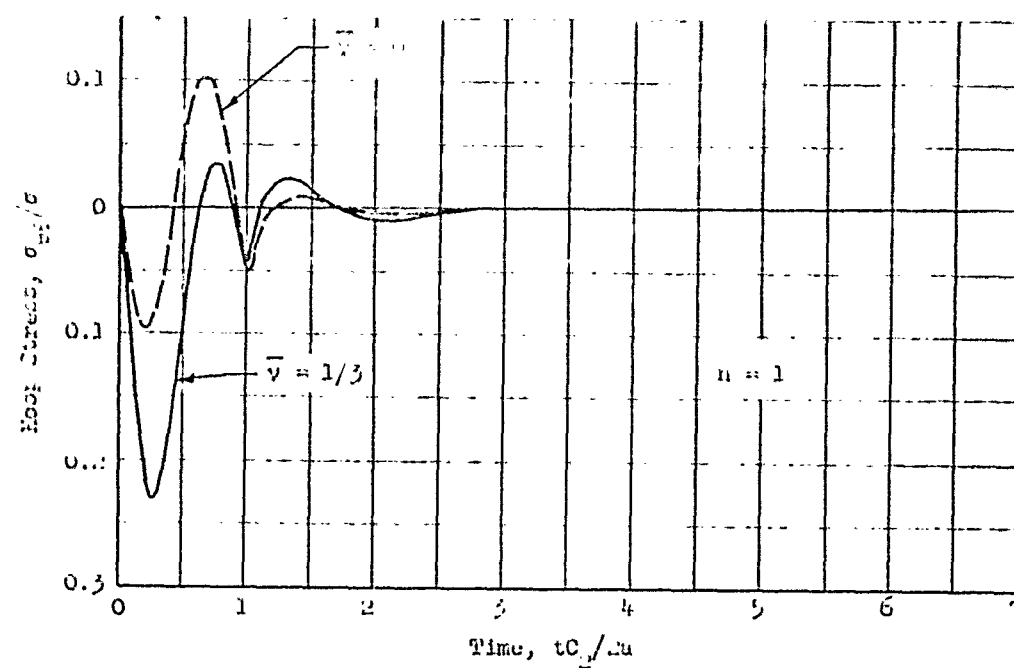


Fig. 4.4 Results of the computer solution for hoop stress in modes 0, 1 and 2 due to an incident shear wave ($\bar{\nu} = 0$ and $1/3$).

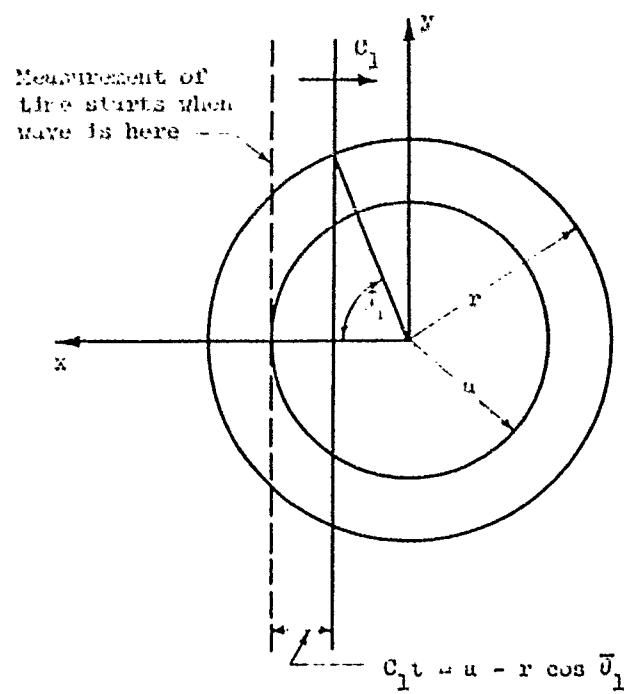


Fig. 4.5 Geometry associated with computation of stress in the medium.

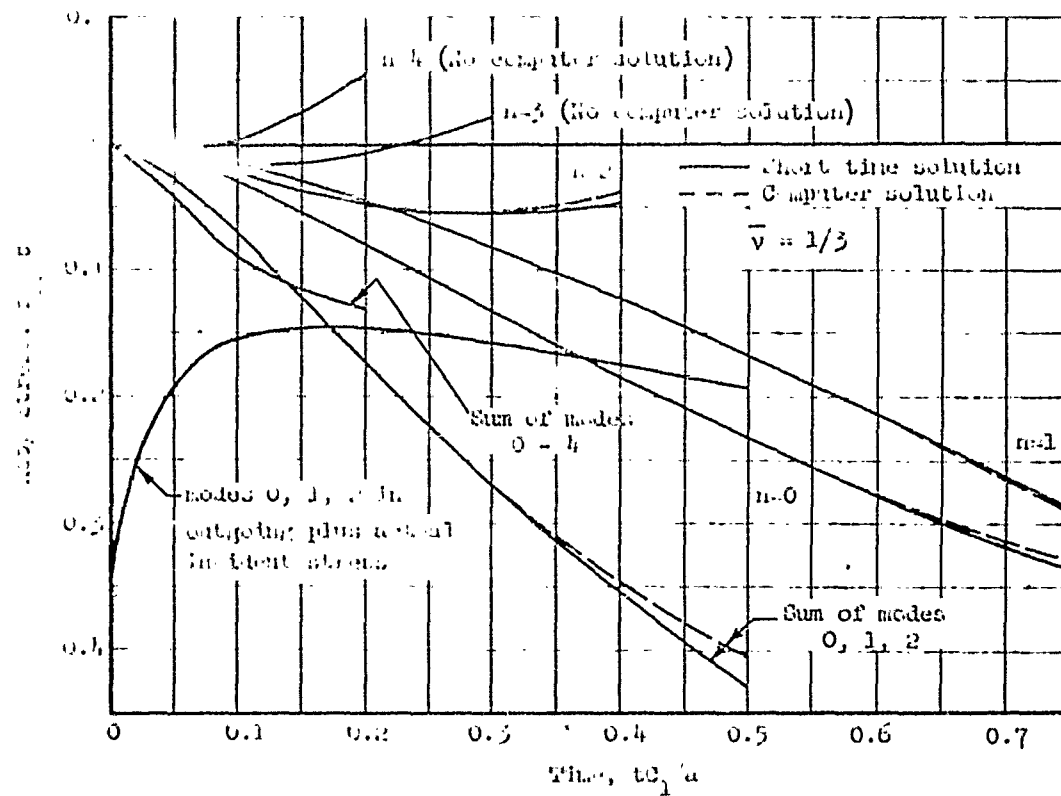


Fig. 5.1 Comparison of the short-time and the computer solutions for total nodewise hoop stress at the boundary in an incident wave of dilatation. The short time solution is also shown for modes $n=3$ and 4.

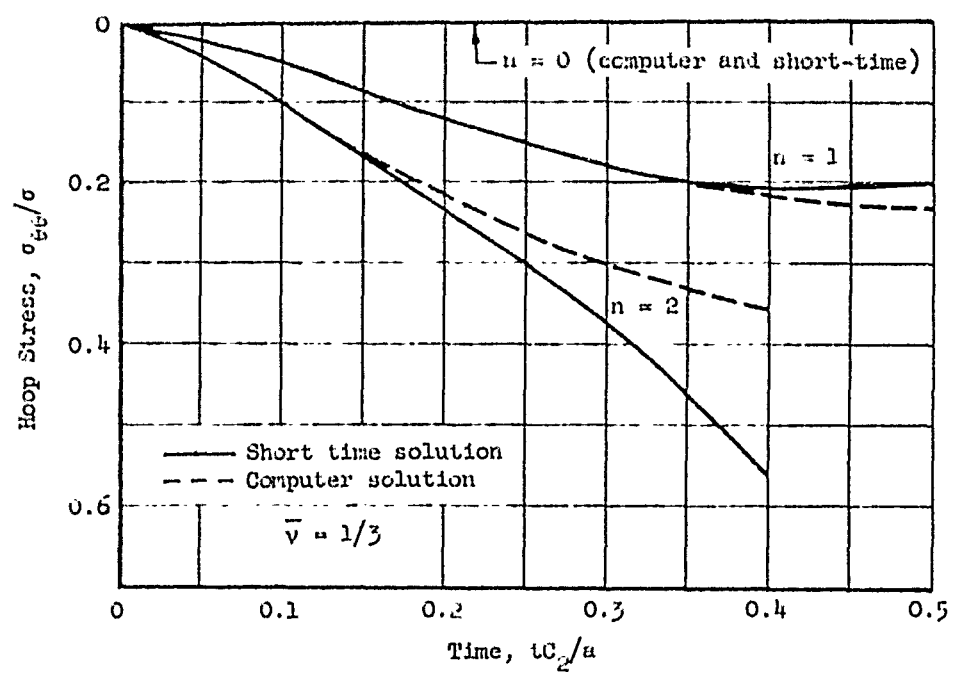


Fig. 5.2 Comparison of the short-time and the computer solutions for hoop stress at the boundary in the diverging wave due to an incident shear wave.

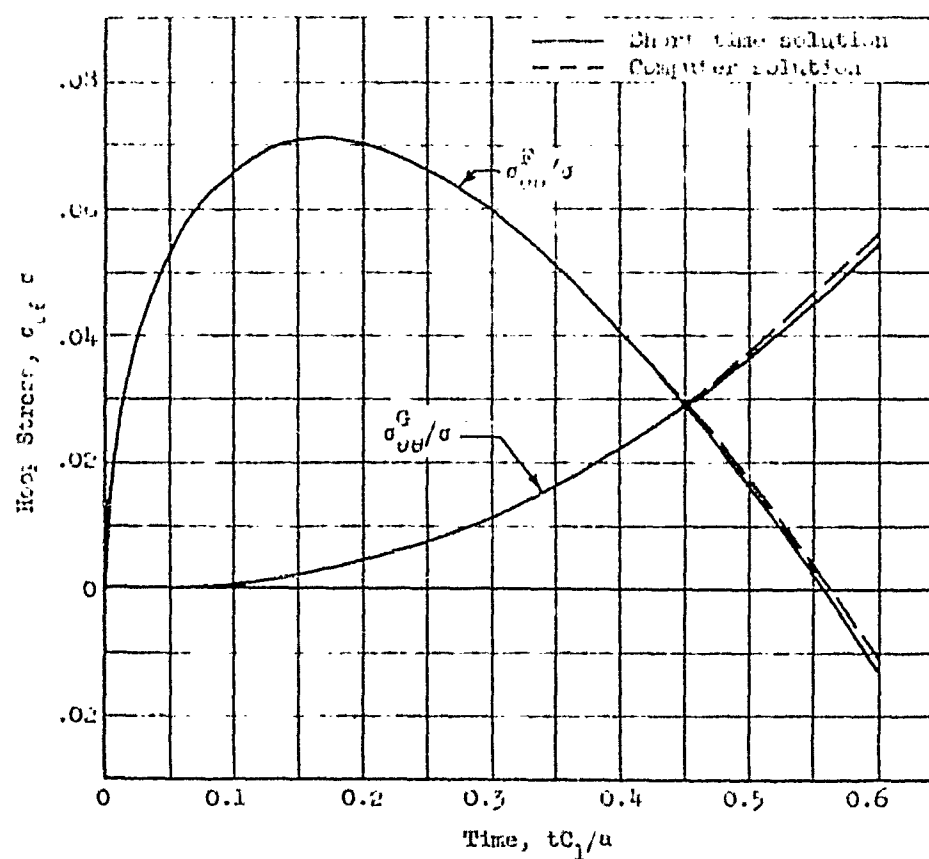


Fig. 5.3 Comparison of the short-time and the computer solutions for hoop stress at $r/a = 1.25$ due to an incident wave of dilatation ($n = 1$, $\bar{\nu} = 1/3$, $\theta = 0^\circ$).

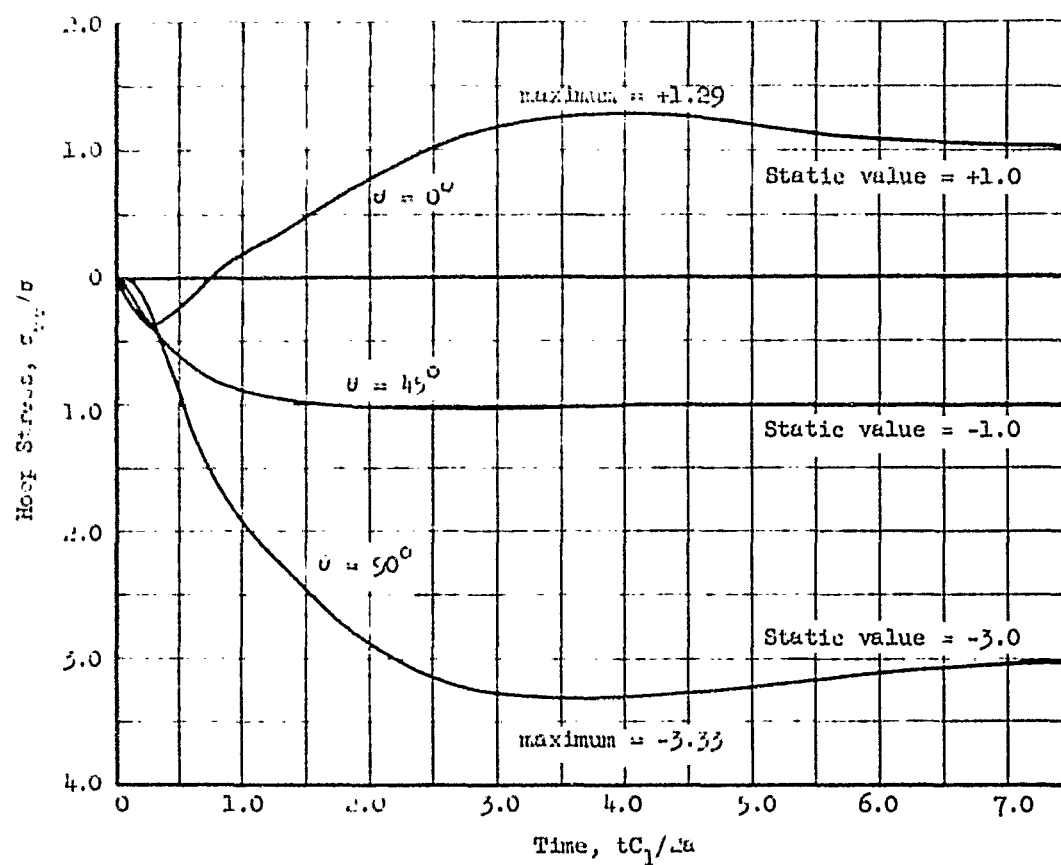


Fig. 6.1 Hoop stress at the boundary due to an incident wave of dilatation using $n = 0, 1, 2$ ($\bar{\nu} = 0$).

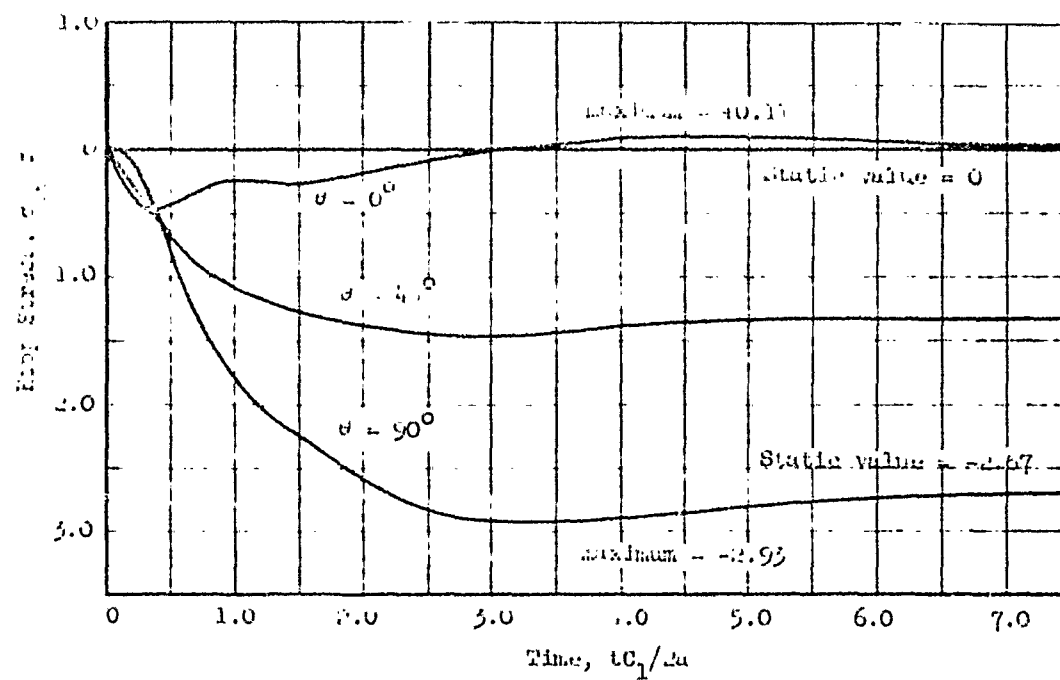


Fig. 6.2 Hoop stress at the boundary due to an incident wave of dilatation using $n = 0, 1, 2$ ($\bar{\nu} = 1/3$).

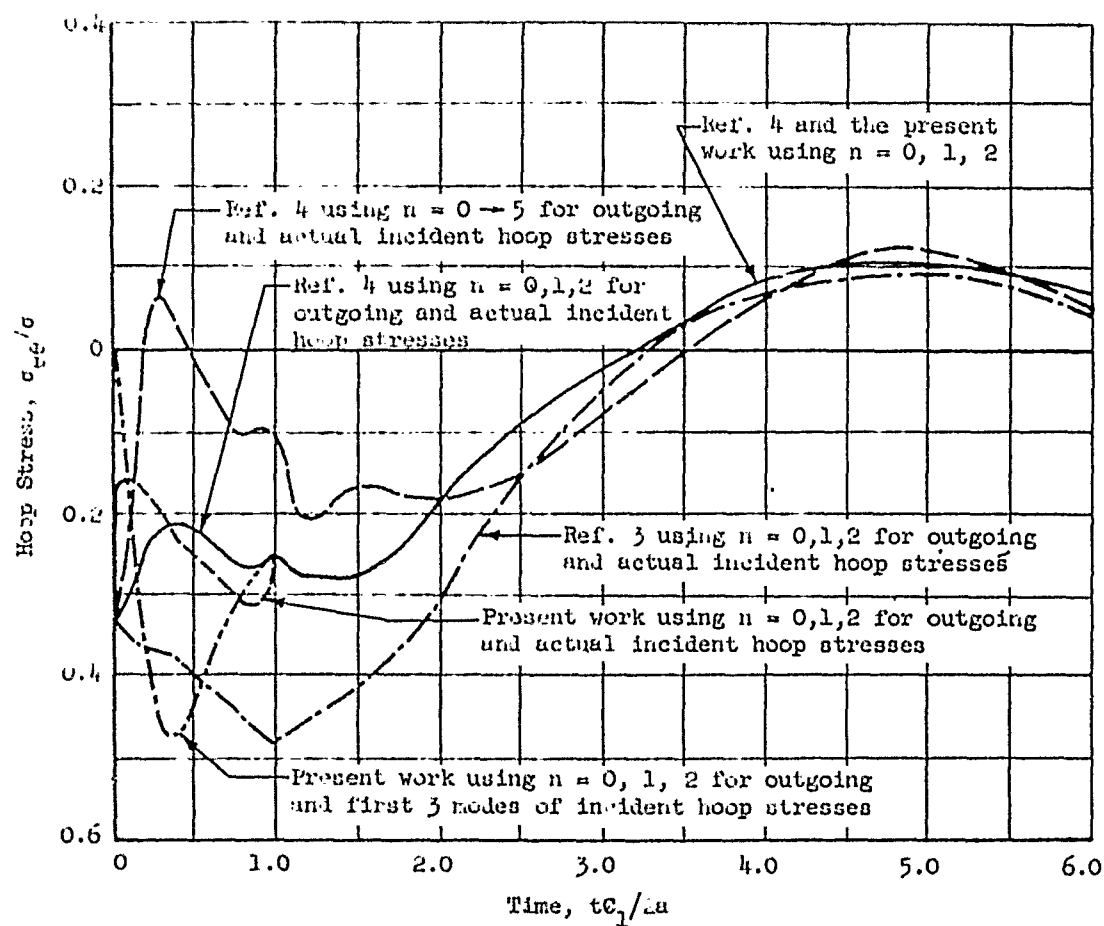


Fig. 6.5 Comparison of the present computations with those of Refs. (3) and (4) for hoop stress at $\theta = 0^\circ$ due to an incident wave of dilatation ($\bar{\nu} = 1/3$).

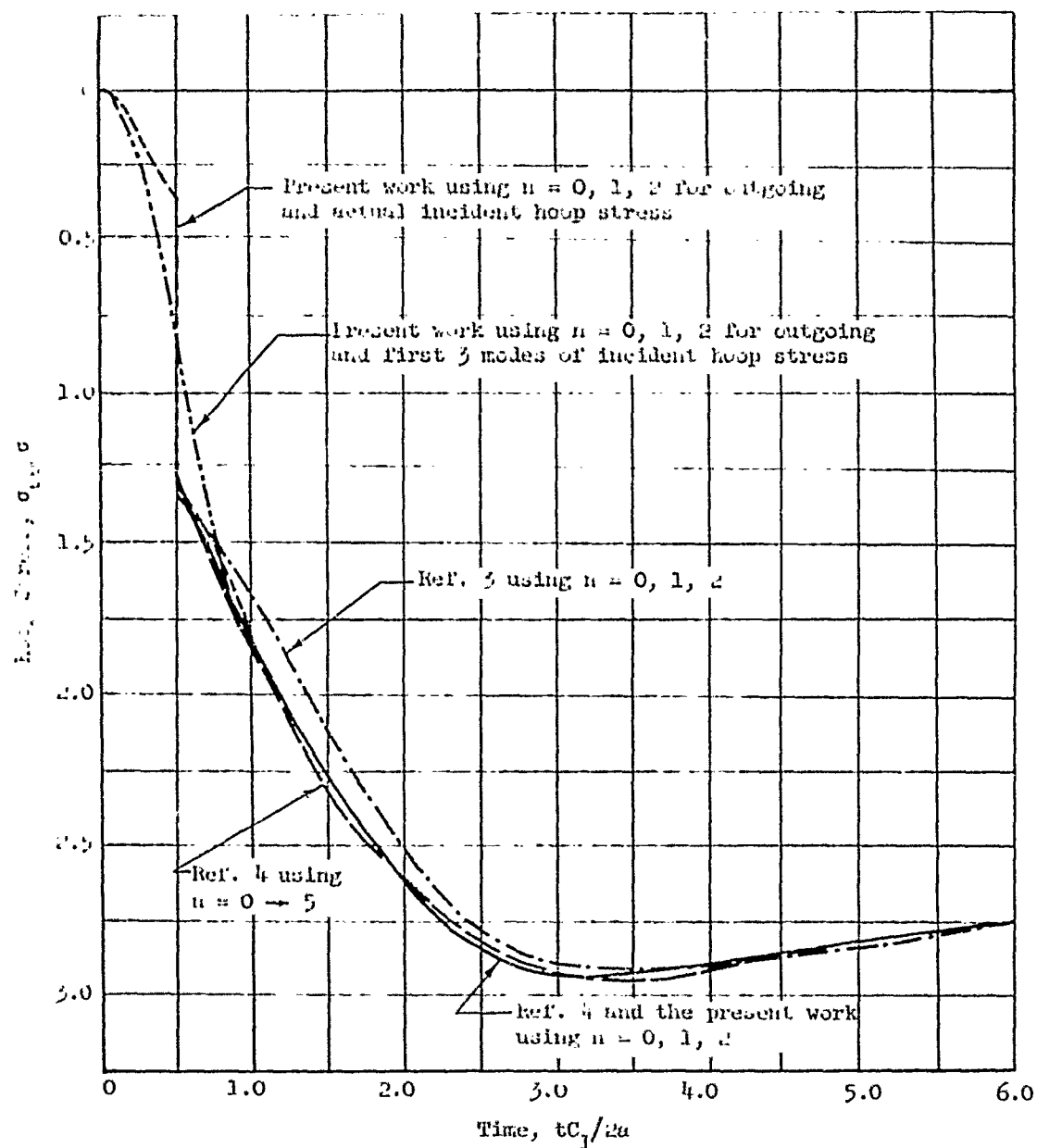


Fig. 6.4 Comparison of the present computations with those of Refs. (3) and (4) for hoop stress at $\theta = 90^\circ$ due to an incident wave of dilatation ($\bar{\nu} = 1/3$).

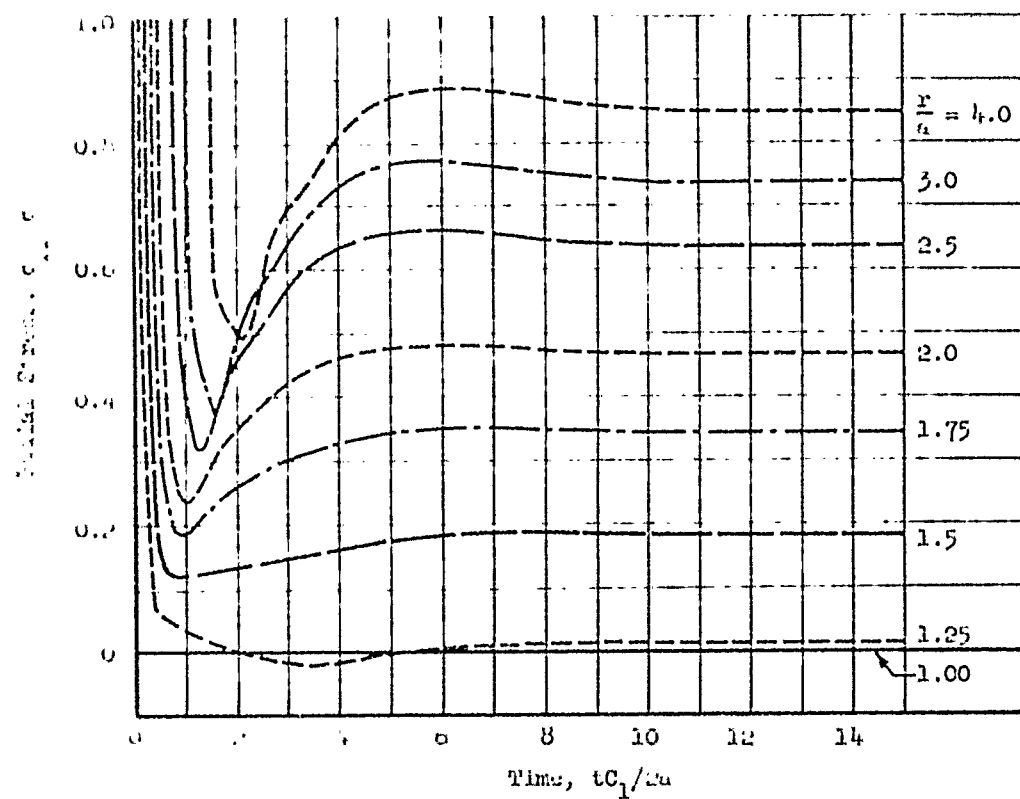


Fig. 6.5 Radial stress vs. time at various radii due to an incident wave of dilatation ($\bar{v} = 0$, $\nu = 0$).

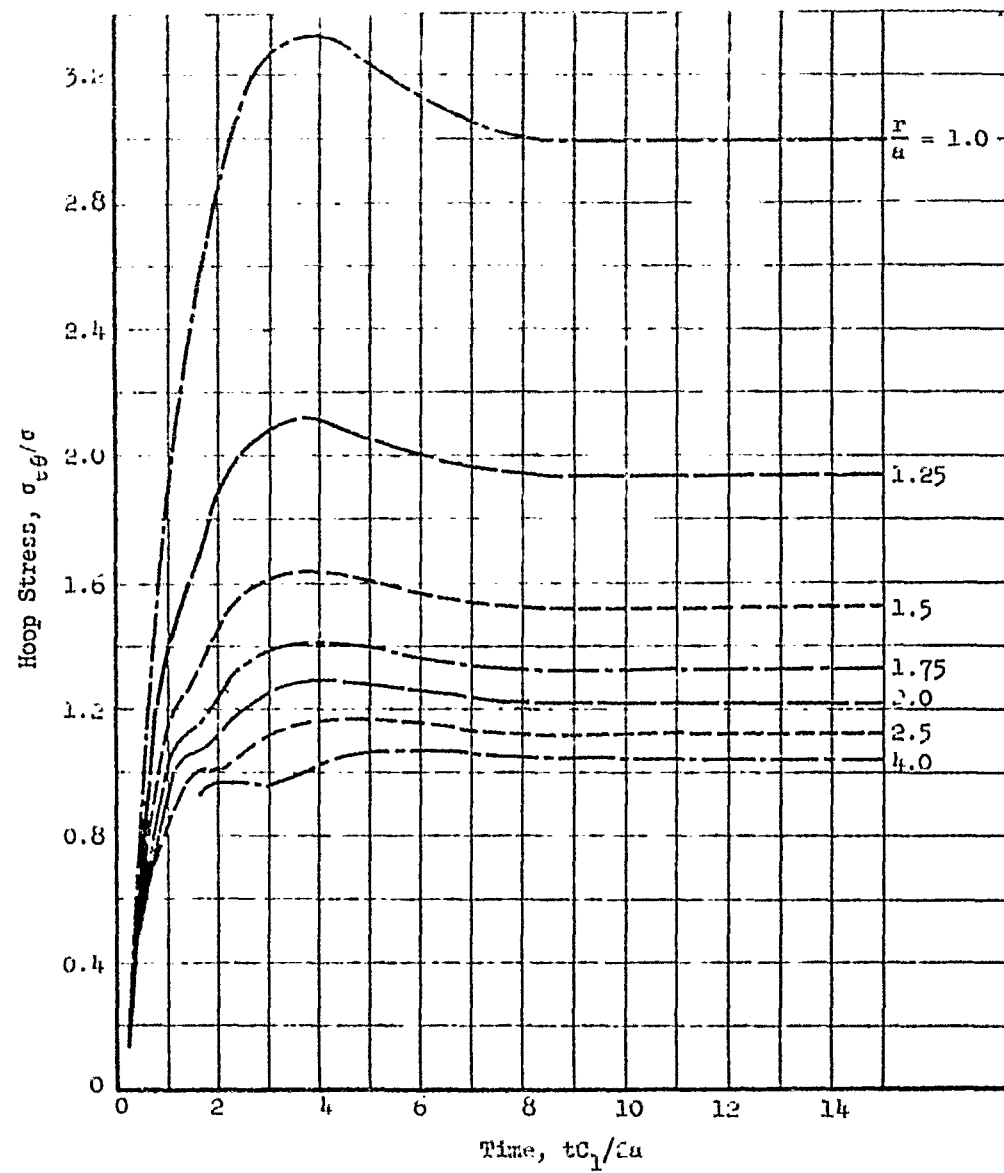


Fig. 6.6 Hoop stress vs. time at various radii due to an incident wave of dilatation ($\bar{v} = 0$, $\theta = 90^\circ$).

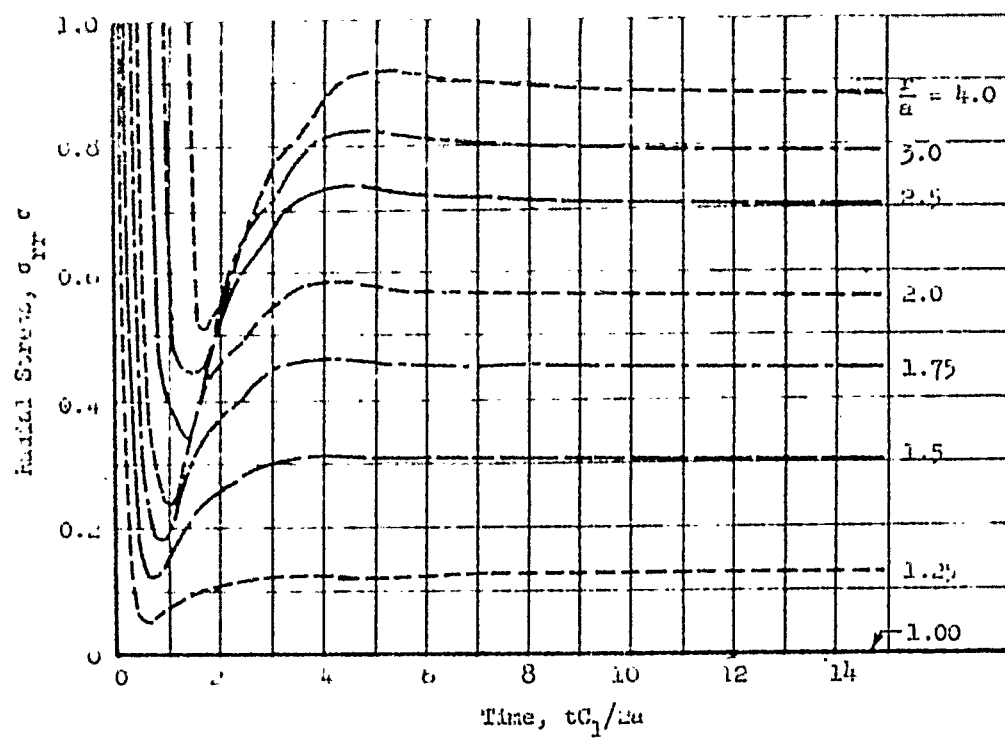


Fig. 6.7 Radial stress vs. time at various radii due to an incident wave of dilatation ($\bar{v} = 1/3$, $\nu = 0$).

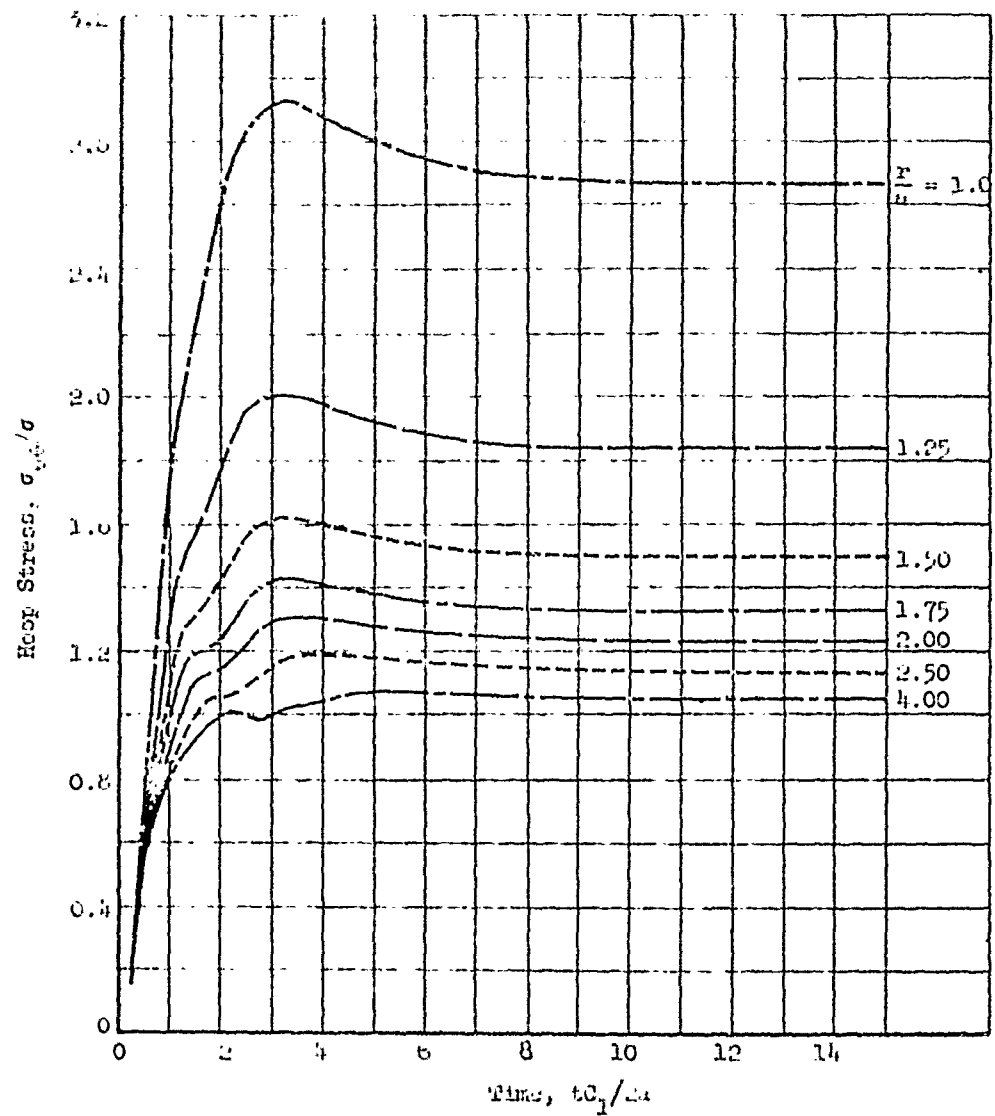


Fig. 6.8 Hoop stress vs. time at various radii due to an incident wave of dilatation ($\bar{v} = 1/3$, $\theta = 90^\circ$).

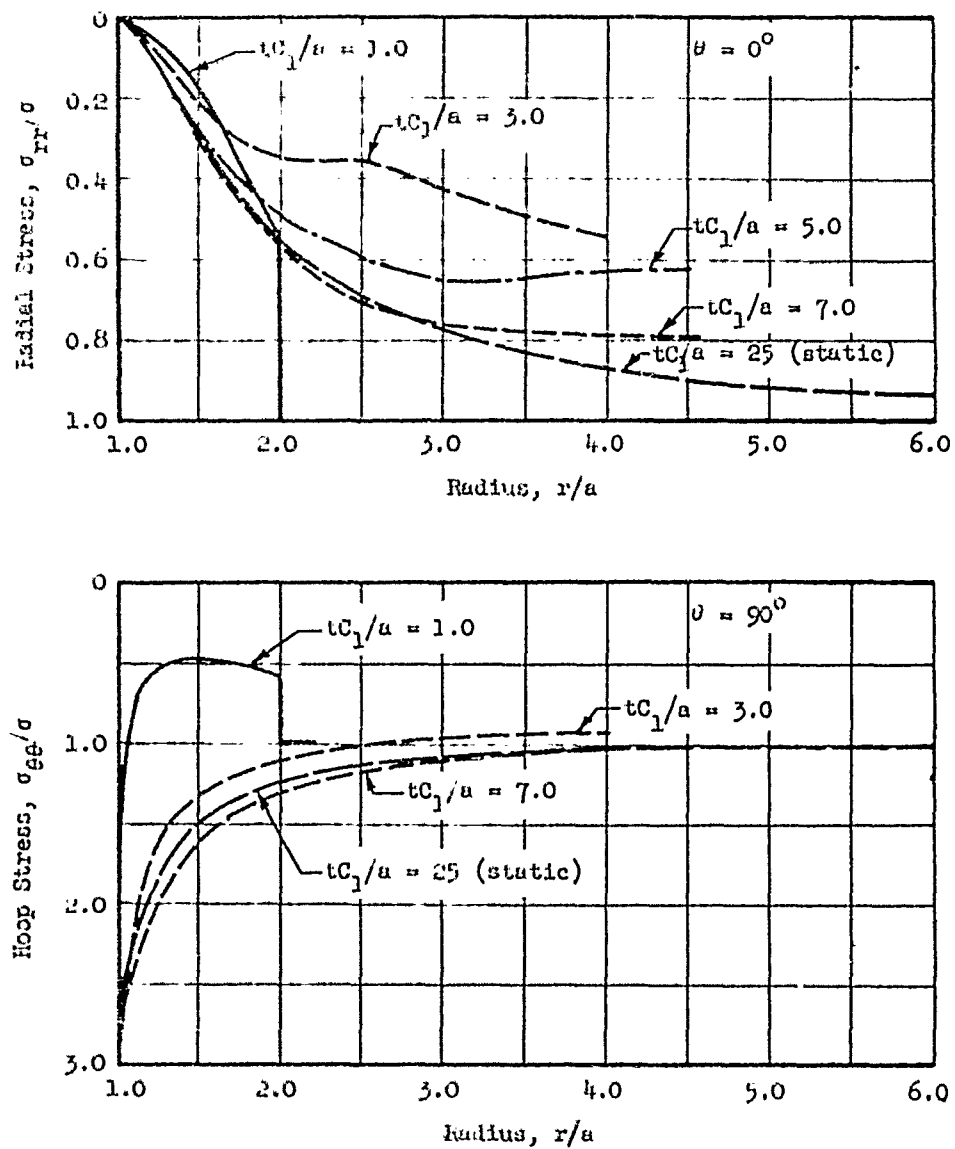


Fig. 6.9 Stress vs. radius at several times due to an incident wave of dilatation ($\bar{\nu} = 1/3$).

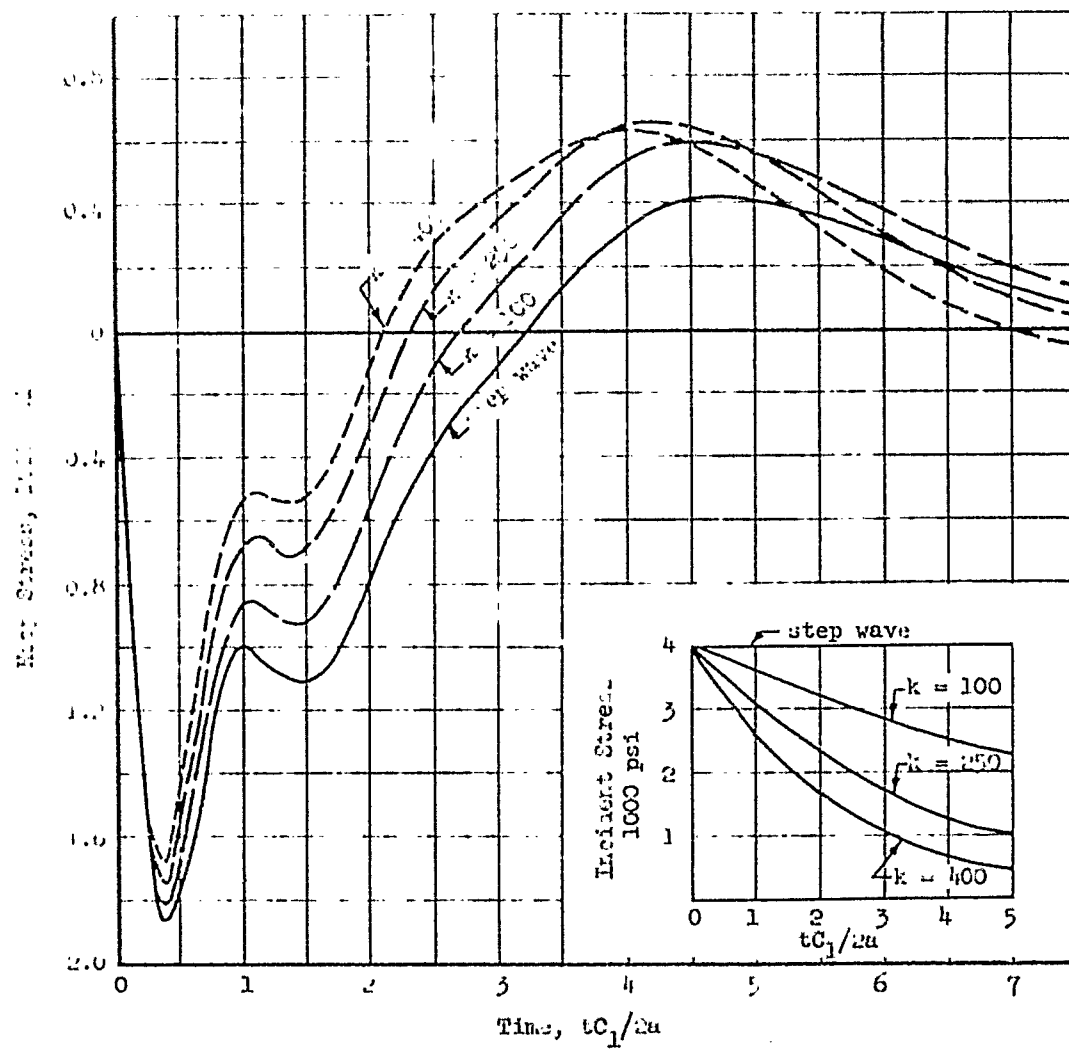


Fig. 6.10 Hoop stress at the boundary vs. time due to an incident wave of dilatation with 4000 psi at the front and various rates of decay behind the front ($\bar{\nu} = 1/3$, $\nu = 0^0$).

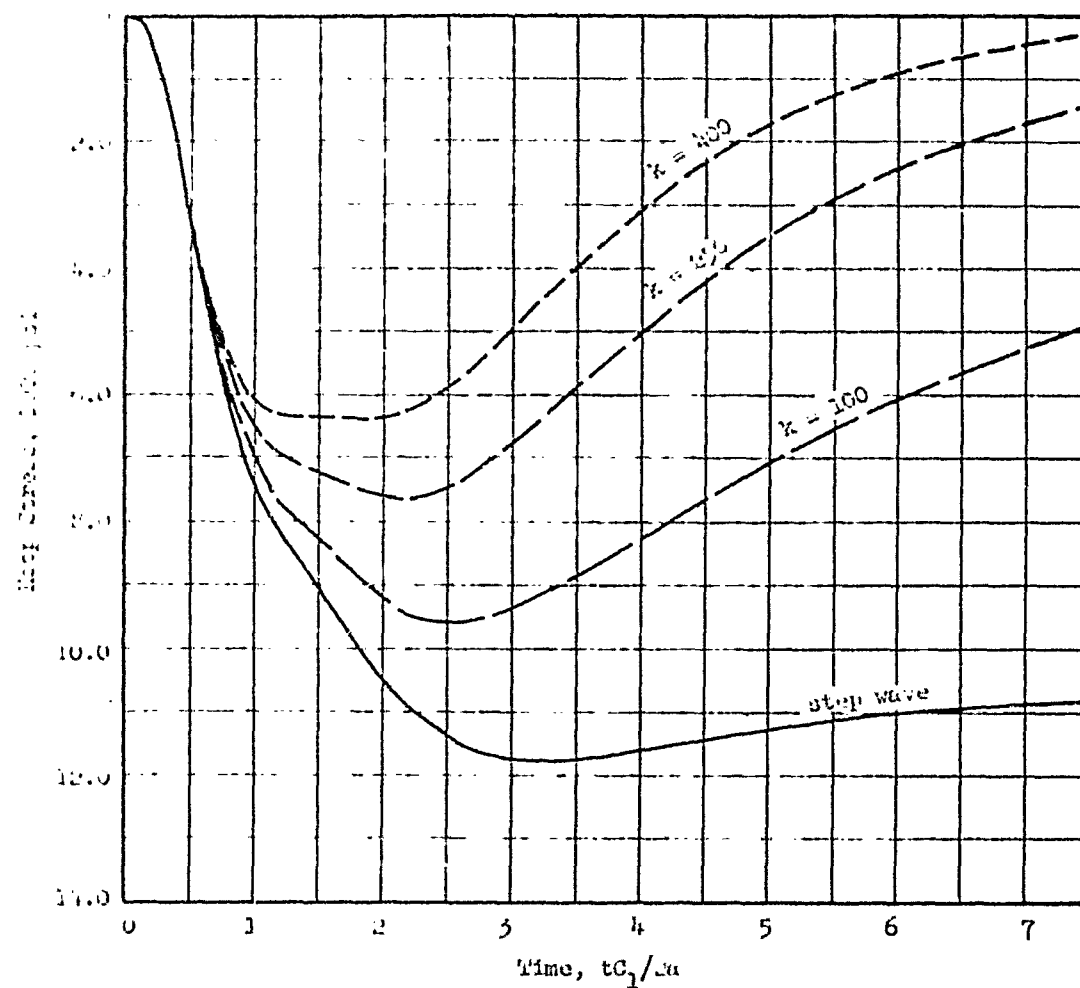


Fig. 6.11 Hoop stress at the boundary vs. time due to an incident wave of elevation with 1000 psi at the front and various rates of decay behind the front ($\bar{v} = 1/3$, $\theta = 90^\circ$).

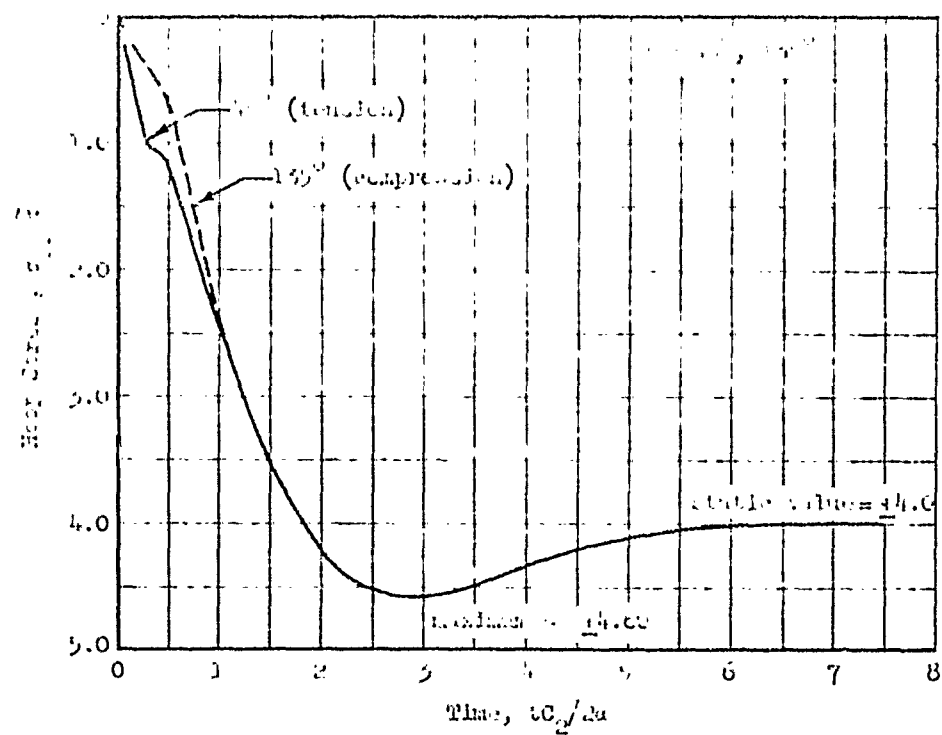


Fig. 6.12 Hoop stress at the boundary due to an incident shear wave using: $\nu = 0, 1, 2$ ($\bar{\nu} = 0$).

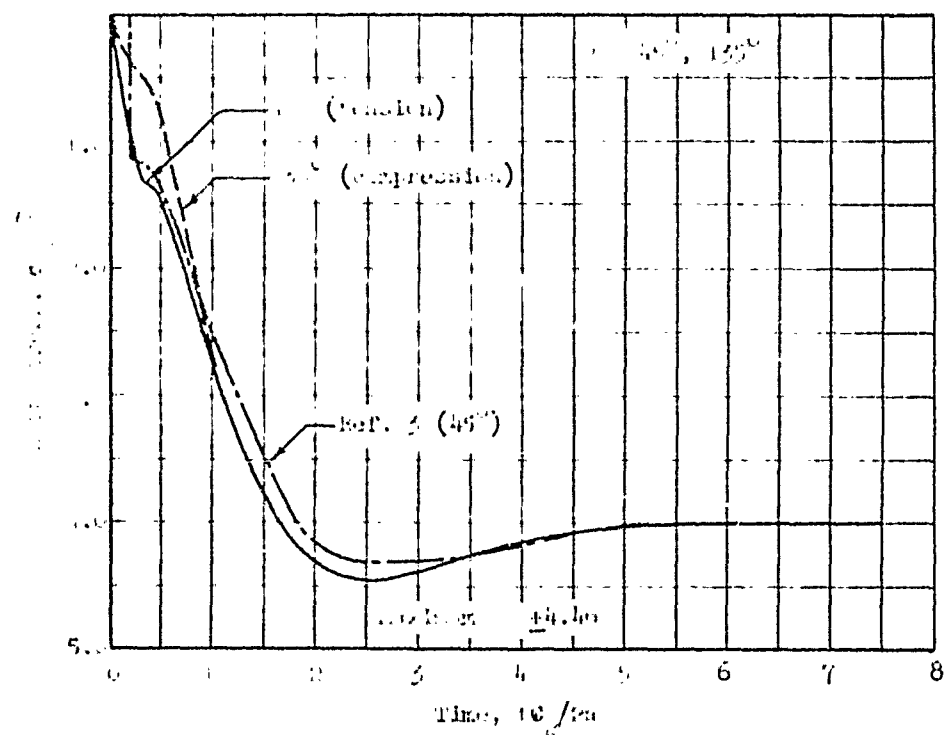


FIG. 6.11.3 Response at the boundary due to an incident wave with $\bar{\gamma} = 0, 1, 2$ ($\bar{\gamma} = 1/3$), (also the response from Ref. (5) is shown for the same conditions.)

DISTRIBUTION

No. cys

HEADQUARTERS USAF

1	Hq USAF (AFOCE), Wash 25, DC
1	Hq USAF (AFRST), Wash 25, DC
1	Hq USAF (AFTAC), Wash 25, DC
1	USAF Dep, The Inspector General (AFIDI), Norton AFB, Calif
1	USAF Directorate of Nuclear Safety (AFINS), Kirtland AFB, NM
1	AFOSR, Bldg T-D, Wash 25, DC

MAJOR AIR COMMANDS

1	AFSC (SCT), Andrews AFB, Wash 25, DC
2	AUL, Maxwell AFB, Ala
2	USAFIT (USAF Institute of Technology), Wright-Patterson AFB, Ohio
2	USAF A, United States Air Force Academy, Colo

AFSC ORGANIZATIONS

1	AF Msl Dev Cen (RRRT), Holloman AFB, NM
---	---

KIRTLAND AFB ORGANIZATIONS

1	AFSWC (SWEH), Kirtland AFB, NM
	AFWL, Kirtland AFB, NM
5	(WLRS)
20	(WLL)

OTHER AIR FORCE AGENCIES

1	Director, USAF Project RAND, via: Air Force Liaison Office, The RAND Corporation, ATTN: RAND Library, 1700 Main Street, Santa Monica, Calif
---	---

ARMY ACTIVITIES

1	Chief of Research and Development, Department of the Army (Special Weapons and Air Defense Division), Wash 25, DC
1	Research Analysis Corp (Document Control Office), 6935 Arlington Road, Bethesda, Md., Wash 14, DC

DISTRIBUTION (cont'd)

No. cys

NAVY ACTIVITIES

- 1 Chief of Naval Research, Department of the Navy, Wash 25, DC
- 1 Commander, Naval Ordnance Laboratory, White Oak, Silver Spring, Md
- 1 Naval Weapons Evaluation Facility (NWEF) (Code 404), Kirtland AFB, NM

OTHER DOD ACTIVITIES

- 1 Chief, Defense Atomic Support Agency (Document Library), Wash 25, DC
- 1 Director, Advanced Research Projects Agency, Department of Defense, The Pentagon, Wash 25, DC
- 1 Director, Defense Research & Engineering, The Pentagon, Wash 25, DC
- 20 Hq Defense Documentation Center for Scientific and Technical Information (DDCI), Comeron Stn, Alexandria, Va. 22314

OTHER

- 1 Institute for Defense Analysis, Room 2B257, The Pentagon, Wash 25, DC
THRU: ARPA
- 25 University of Illinois, Talbot Laboratory, ATTN: Mr. Stan Paul, Urbana, Ill
- 1 Illinois Institute of Technology Research Institute, ATTN: Dr. James Dally, 344 South Dearborn St., Chicago 16, Ill
- 1 Louisiana State University, ATTN: Dr. Dale Carver, Dept. of Engineering Mechanics, Baton Rouge, La
- 1 Grumman Research Dept., Grumman Aircraft Engineering Corp., Bethpage, NY
- 1 General American Transportation Corp., MRD Div., ATTN: Mr. Tom Morrison, 7501 N. Natchez Ave., Niles 48, Ill
- 1 Iowa State University, Dept. of Nuclear Engineering, ATTN: Dr. D. F. Young, Ames, Iowa
- 1 Northrup-Ventura, ATTN: Dr. R. P. Banaugh, 1515 Rancho Conejo Blvd., Newburg Park, Calif
- 1 National Engineering Science Co., ATTN: Dr. Soldate, 711 South Fair Oaks Ave., Pasadena, Calif
- 1 United Research Services, ATTN: Mr. Harold C. Mason, 1811 Trousdale Drive, Burlingame, Calif

DISTRIBUTION (cont'd)

No. cys

- | | |
|---|---|
| 1 | University of New Mexico, AF Shock Tube Facility, Box 188
University Station, Albuquerque, NM |
| 1 | Stanford Research Institute, ATTN: Dr. G. E. Duvall and
Dr. Fred Sauer, Menlo Park, Calif |
| 1 | Purdue University, School of Civil Engineering, ATTN: Prof.
G. A. Leonards, Lafayette, Ind |
| 1 | Physics International Co., ATTN: C. Godfrey, 4229 Fourth
Street, Berkeley 10, Calif |
| 1 | Paul Weidlinger and Associates, 770 Lexington Ave., New
York 21, NY |
| 1 | Professor A. P. Boresi, Department of Theoretical and
Applied Mechanics, 212 Talbot Laboratory, University of
Illinois, Urbana, Ill |
| 1 | Dr. Ralph Fadum School of Engineering, North Carolina State
College, Raleigh, North Carolina |
| 1 | Dr. Eivind Hognestad, Manager, Structural Development
Section, Portland Cement Association, 5420 Old Orchard Road,
Skokie, Ill |
| 1 | Dr. Lydik S. Jacobsen, Agbabian-Jacobsen & Associates, 8939
South Sepulveda Blvd., Los Angeles 45, Calif |
| 1 | Professor Frank Kerekes, Dean of the Faculty, Michigan
College of Mining and Technology, Houghton, Mich |
| 1 | Professor Carl Kisslinger, St. Louis University, 3621 Olive
Street, St. Louis 8, Mo |
| 1 | Professor Frank E. Richart, Jr., School of Civil Engineering,
University of Michigan, Ann Arbor, Mich |
| 1 | Professor George A. Young, School of Civil Engineering,
University of New Mexico, Albuquerque, NM |
| 1 | Official Record Copy (WLRS, Lt Joe Johnson) |

<p>Air Force Weapons Laboratory, Kirtland AF Base, New Mexico</p> <p>Report No. AFWD TR-63-3021. INTERACTION OF PLANE ELASTIC WAVES WITH A CYLINDRICAL CAVITY. June, 1963. 121 p. incl illus, 13 refs.</p> <p>Unclassified Report</p> <p>A method is presented for computing stresses in the vicinity of a long cylindrical cavity in an infinite, elastic, isotropic, homogeneous medium when the cavity is enveloped by a plane stress wave traveling in a direction perpendicular to its axis. Loop stresses around the cavity boundary were computed for the passage of a wave of dilation and a wave of pure shear; the stresses in the medium away from the boundary were computed for a wave of dilation. Initially the stress behind the incident wave front was considered to be constant.</p>	<p>Fourier analysis</p> <p>Shelters -- effects of atomic explosions</p> <p>Shock waves</p> <p>Stress and strain</p> <p>Underground structures</p> <p>-- effects of atomic explosions</p> <p>AFSC Project 1000, Task 100001</p> <p>Contract AF 29(601)-5007</p> <p>Illinois, Univ., Urbana</p> <p>Stanley L. Paul</p> <p>DASA WEB No. 13,140</p> <p>In DDC collection</p>	<p>1. Fourier analysis</p> <p>2. Shelters -- effects of atomic explosions</p> <p>3. Shock waves</p> <p>4. Stress and strain</p> <p>5. Underground structures</p> <p>-- effects of atomic explosions</p> <p>AFSC Project 1000, Task 100001</p> <p>Contract AF 29(601)-5007</p> <p>Illinois, Univ., Urbana</p> <p>Stanley L. Paul</p> <p>DASA WEB No. 13,140</p> <p>In DDC collection</p>	<p>1. Fourier analysis</p> <p>2. Shelters -- effects of atomic explosions</p> <p>3. Shock waves</p> <p>4. Stress and strain</p> <p>5. Underground structures</p> <p>-- effects of atomic explosions</p> <p>AFSC Project 1000, Task 100001</p> <p>Contract AF 29(601)-5007</p> <p>Illinois, Univ., Urbana</p> <p>Stanley L. Paul</p> <p>DASA WEB No. 13,140</p> <p>In DDC collection</p>
<p>Air Force Weapons Laboratory, Kirtland AF Base, New Mexico</p> <p>Report No. AFWD TR-63-3021. INTERACTION OF PLANE ELASTIC WAVES WITH A CYLINDRICAL CAVITY. June, 1963. 121 p. incl illus, 13 refs.</p> <p>Unclassified Report</p> <p>A method is presented for computing stresses in the vicinity of a long cylindrical cavity in an infinite, elastic, isotropic, homogeneous medium when the cavity is enveloped by a plane stress wave traveling in a direction perpendicular to its axis. Loop stresses around the cavity boundary were computed for the passage of a wave of dilation and a wave of pure shear; the stresses in the medium away from the boundary were computed for a wave of dilation. Initially the stress behind the incident wave front was considered to be constant.</p>	<p>Fourier analysis</p> <p>Shelters -- effects of atomic explosions</p> <p>Shock waves</p> <p>Stress and strain</p> <p>Underground structures</p> <p>-- effects of atomic explosions</p> <p>AFSC Project 1000, Task 100001</p> <p>Contract AF 29(601)-5007</p> <p>Illinois, Univ., Urbana</p> <p>Stanley L. Paul</p> <p>DASA WEB No. 13,140</p> <p>In DDC collection</p>	<p>1. Fourier analysis</p> <p>2. Shelters -- effects of atomic explosions</p> <p>3. Shock waves</p> <p>4. Stress and strain</p> <p>5. Underground structures</p> <p>-- effects of atomic explosions</p> <p>AFSC Project 1000, Task 100001</p> <p>Contract AF 29(601)-5007</p> <p>Illinois, Univ., Urbana</p> <p>Stanley L. Paul</p> <p>DASA WEB No. 13,140</p> <p>In DDC collection</p>	<p>1. Fourier analysis</p> <p>2. Shelters -- effects of atomic explosions</p> <p>3. Shock waves</p> <p>4. Stress and strain</p> <p>5. Underground structures</p> <p>-- effects of atomic explosions</p> <p>AFSC Project 1000, Task 100001</p> <p>Contract AF 29(601)-5007</p> <p>Illinois, Univ., Urbana</p> <p>Stanley L. Paul</p> <p>DASA WEB No. 13,140</p> <p>In DDC collection</p>

<p>The effect of a stress decay behind the front was then computed by using the Duhamel integral for the case of an incident wave of dilation.</p> <p>The method of solution of the problem involves superposition of the stress field of an incoming plane step wave and a stress field corresponding to waves which diverge from a line source.</p>		<p>The effect of a stress decay behind the front was then computed by using the Duhamel integral for the case of an incident wave of dilation.</p> <p>The method of solution of the problem involves superposition of the stress field of an incoming plane step wave and a stress field corresponding to waves which diverge from a line source.</p>	
<p>The effect of a stress decay behind the front was then computed by using the Duhamel integral for the case of an incident wave of dilation.</p> <p>The method of solution of the problem involves superposition of the stress field of an incoming plane step wave and a stress field corresponding to waves which diverge from a line source.</p>		<p>The effect of a stress decay behind the front was then computed by using the Duhamel integral for the case of an incident wave of dilation.</p> <p>The method of solution of the problem involves superposition of the stress field of an incoming plane step wave and a stress field corresponding to waves which diverge from a line source.</p>	